The Roles of the Germination-Specific Lytic Enzymes CwlJ1, CwlJ2, and SleB in *Bacillus anthracis* Spores

Jared David Heffron

Dissertation submitted to the faculty of the Virginia Polytechnic Institute and State University in partial fulfillment of the requirements for the degree of

Doctor of Philosophy
In
Biological Sciences

David L. Popham, Chair
Timothy J. Larson
Steven B. Melville
Susan S. Sumner

March 26, 2010
Blacksburg, Virginia

Keywords: *Bacillus anthracis*, spore, germination, cortex, lytic enzyme, anthrax

Copyright 2010, Jared David Heffron

The Roles of the Germination-Specific Lytic Enzymes CwlJ1, CwlJ2, and SleB in *Bacillus anthracis* Spores

Jared David Heffron

ABSTRACT

The *Bacillus anthracis* spore is highly resistant to environmental stresses, but cannot cause anthrax until it successfully germinates. An essential step of germination, degradation of the cortex peptidoglycan layer, is carried out by germination-specific lytic enzymes (GSLEs). While the GSLEs of several other *Bacillus* species have been investigated, they have not been characterized in the pathogen *B. anthracis*. In this work three GSLEs, CwlJ1, CwlJ2, and SleB are identified in *B. anthracis* and are investigated in order to better understand their functions.

Genetic manipulation of *cwlJ1*, *cwlJ2*, and *sleB* was fundamental to this work. First, reporter gene fusions revealed that all three are expressed during spore formation and that CwlJ1 is likely the most abundant GSLE in the spore. Second, gene deletions eliminating each GSLE enabled the observation of mutant phenotypes during spore cortex degradation. CwlJ1 and SleB were identified as the most critical GSLEs for successful germination. High-performance liquid chromatography and mass spectroscopy revealed that SleB is required for lytic transglycosylase activity, but CwlJ1's mode of action was unclear. Multiple mutations of all of the GSLEs revealed that CwlJ2 is the least active GSLE, but that it participates in germination in response to Ca-Dipicolinic acid; a role it shares with the more dominant CwlJ1.

Purification of the CwlJ1 and SleB proteins permitted *in vitro* assays of enzymatic activity as measured by changes in substrate optical density, solubility, and product formation. While CwlJ1 was recalcitrant to these methods, it was observed to cause cortex hydrolysis independently. SleB was more amenable and it was discovered to contain a peptidoglycan-

binding domain that is primarily responsible for substrate binding, and a lytic transglycosylase domain that facilitates cortex-specific hydrolysis by recognizing muramic-δ-lactam.

Future research will include determining the structure of SleB through x-ray crystallography and the identification of CwlJ1 activity by refining the protein purification method. The results of this and future research into CwlJ1, CwlJ2, and SleB may lead to a means to initiate spore germination prior to host infection. This will greatly ease spore decontamination measures, lower risk of infection, and discourage the use of *B. anthracis* spores as a biological weapon.

DEDICATION

This dissertation is dedicated to my lovely wife Ashley for inspiring me to start this journey, and to our beloved first child, expected in July 2010, for motivating me to finish.

ACKNOWLEDGEMENTS

First, I must thank David Popham for his invaluable role as my advisor throughout my time at VA Tech. Your breathless depth of knowledge and skill at solving complicated problems has been essential for my progress and will always be something I will strive to emulate. In addition, your remarkable patience and calm demeanor has allowed me to learn from my mistakes instead of dread them. I know it will be impossible for me to address any challenges in my future scientific research without considering how Dave might handle the given situation, and most certainly I will be better off for that.

I would also like to thank my committee members Tim Larson, Steve Melville, and Susan Sumner. In looking back, my most memorable moments of the past five years are when I was standing in the hall during your deliberations at committee meetings. This was not so much due to anxiety, but instead to the exhilaration that each meeting kindled in my scientific heart. Your insights, advice, criticism, and guidance always motivated me to jump right back into the lab regardless of the challenge ahead. You have taught me that science is a collaborative process that benefits more from support than censure.

An enormous thank you is due to the many members of the Popham lab I have had the pleasure to know and work with. To Melissa for teaching me the ropes in lab, to Lin for soft-spoken insights, to Yong for making sure I was never working at night alone, to Ben for quick laughs and an opinion on any subject, to Michelle for the supportive attitude, to Pradeep for wisdom beyond your years, to Emily for showing me the paradigm of efficiency, to Jessica for unending optimism, to Casey for swapping teaching stories, to Yan for the thought-provoking questions, and to Sean for much-needed camaraderie. Of course I cannot forget to thank Nora,

who was patient enough to listen to my tangents and diatribes, smart enough to think on her own, and enthused enough to work more than I ever expected.

Lastly, but most importantly, I want to express my deepest appreciation to my family. Thanks to Mom and Dad for motivating me to do my best, and never giving up on me even when I was at my worst. Thanks to my sister, Meghan, for being equal parts competition and a best friend. Thanks to the in-laws, Sissy and Mike, for being supportive and trusting me with the most wonderful woman in the world. And thanks to the most wonderful woman in the world, Ashley Michelle Heffron, for getting me in grad in school in the first place, making every day a pleasure, and showing me what unlimited patience really is.

TABLE OF CONTENTS

ABSTRACT ii

DEDICATION iv

ACKNOWLEDGEMENTS v

LIST OF FIGURES x

LIST OF TABLES xi

CHAPTER 1: Introduction and Review of the Literature 1
- Bacterial Endospores and Resistance Properties. 2
- Spore Germination. 5
- Germination-Specific Lytic Enzymes. 7
- The value of understanding *Bacillus anthracis* spore germination. 9
- Objectives of this work. 10

CHAPTER 2: The Roles of Germination-Specific Lytic Enzymes CwlJ and SleB in *Bacillus anthracis* 16
- Author Contributions 17
- Abstract 18
- Introduction 19
- Materials and Methods 21
  - Bacterial strains and antibiotics. 21
  - Mutant construction. 21
  - β-galactosidase assay. 22
  - Germination assays. 23
  - HPLC analysis of PG. 23
- Results 25
  - GSLE Homologs in *B. anthracis*. 25
  - GSLE-encoding genes are transcribed during sporulation. 25
  - Effects of GSLE mutations on germination. 26
  - DPA, NAM, and Dpm release from spores. 29
  - Cortex hydrolysis is slowed in *cwlJ1* and *sleB* spores. 30
  - Muropeptides G7a and G7b contain anhydromuramic acid. 32
- Discussion 33
- Acknowledgements 50

CHAPTER 3: Contributions of Four Cortex Lytic Enzymes to Germination of *Bacillus anthracis* Spores 51
- Author Contributions 52
- Abstract 53
- Introduction 54
- Materials and Methods 57

Bacterial strains and growth conditions. 57
Spore preparation. 57
Spore germination assays. 58
Biochemical analyses of PG hydrolysis and release. 58
Results 59
Effects of GSLEs on nutrient-triggered germination. 59
Effects of GSLEs on Ca-DPA-triggered germination. 60
Release of cortex fragments from germinating spores. 61
GSLE effects on cortex hydrolysis. 62
Discussion 64
Acknowledgements 77

Chapter 4: *In Vitro* Studies of Peptidoglycan Binding and Hydrolysis by the *Bacillus anthracis* Germination-Specific Lytic Enzyme SleB 78
Author Contributions 79
Abstract 80
Introduction 81
Materials and Methods 83
Protein expression and purification. 83
Preparation of peptidoglycan substrates. 84
Enzymatic activity assays. 85
PG binding assay. 86
Results 87
Structural features of SleB, its overexpression, and purification. 87
SleB and $SleB_{125-253}$ hydrolyze intact and fragmented cortex. 88
The hydrolase domain of SleB is dependent on muramic-δ-lactam for activity. 91
Both the N and C terminal domains of SleB participate in binding cortex peptidoglycan. 91
Discussion 93
Acknowledgements 104

Chapter 5: The *Bacillus anthracis* Germination-Specific Lytic Enzyme CwlJ1 is Active *In Vitro* 105
Author Contributions 106
Abstract 107
Introduction 108
Materials and Methods 110
Protein expression and purification. 110
Enzymatic activity assays. 111
Results 113
Structural features of CwlJ1, its overexpression, and purification. 113
The solubility of His_6-MBP-CwlJ1 is improved with additives to the buffer. 113
The His_6-MBP-CwlJ1 fusion protein is recalcitrant to TEV protease digestion. 115

Hydrolysis of cortex by His_6-MBP-CwlJ1 after TEV protease digestion. 116
Cloning and overexpression of an improved His_6-MBP-CwlJ1 protein fusion. 116
Discussion 118
Acknowledgements 126

Chapter 6: Final Discussion 127

REFERENCES 134

APPENDIX A: Supplemental material for Chapter 2 143

LIST OF FIGURES

CHAPTER 1
Figure 1.1. The spore structure of *Bacillus anthracis*. 12
Figure 1.2. Spore germination. 13
Figure 1.3. Cortex degradation. 14

CHAPTER 2
Figure 2.1. Expression of *cwlJ1*, *cwlJ2*, and *sleB* during *B. anthracis* sporulation. 36
Figure 2.2. Germination and outgrowth of native and decoated spores in BHI. 37
Figure 2.3. Release of NAM and Dpm from germinating *B. anthracis* spores. 38
Figure 2.4. RP-HPLC separation of muropeptides from germinating *B. anthracis* spores. 39
Figure 2.5. Complementation of Δ*sleB*. 40
Figure 2.6. RP-HPLC separation of muropeptide exudates from decoated germinating *B. anthracis* spores. 41
Figure 2.7. Muropeptides G7a and G7b are anhydro-tetrasaccharides. 42
Figure 2.8. A model for cortex hydrolysis by GSLEs in *B. anthracis*. 43

CHAPTER 3
Figure 3.1. Spore PG structure and hydrolysis. 69
Figure 3.2. Germination and outgrowth of spores in BHI. 70
Figure 3.3. Germination of spores in response to Ca-DPA. 71
Figure 3.4. Release of cortex fragments from germinating spores. 72
Figure 3.5. RP-HPLC separation of muropeptides released from germinating spores. 73

CHAPTER 4
Figure 4.1. Domain architecture of SleB and overexpressed proteins. 97
Figure 4.2. Purification of SleB and $SleB_{125-253}$ from the His_6-MBP tag. 98
Figure 4.3. Action of SleB and $SleB_{125-253}$ on spore sacculi. 99
Figure 4.4. RP-HPLC separation of muropeptides released from spore sacculi digested with SleB or $SleB_{125-253}$. 100
Figure 4.5. Binding of SleB and $SleB_{125-253}$ to cortical fragments. 101

CHAPTER 5
Figure 5.1. Domain architecture of CwlJ1 and overexpressed proteins. 121
Figure 5.2. Purification of His_6-MBP-CwlJ1 fusion. 122
Figure 5.3. TEV protease digestions of CwlJ1 protein fusion. 123
Figure 5.4. CwlJ1 activity on spore sacculi after TEV protease treatment. 124

CHAPTER 6
Figure 6.1. Cortex degradation during nutrient and Ca-DPA triggered germination. 133

LIST OF TABLES

CHAPTER 1
Table 1.1. Homologs of *B. subtilis* proteins involved in cortex lysis. 15

CHAPTER 2
Table 2.1: *B. anthracis* strains and plasmids. 44
Table 2.2. Homologs of *B. subtilis* GSLEs. 45
Table 2.3. Germination of Spores in BHI. 46
Table 2.4. Muropeptide peak identification. 47
Table 2.5. Novel muropeptide identification. 49

CHAPTER 3
Table 3.1. *B. anthracis* strains and plasmids. 74
Table 3.2. Spore plating efficiency and lysozyme recovery. 75
Table 3.3. Muropeptide peak identification. 76

CHAPTER 4
Table 4.1. SleB and $SleB_{125-253}$ activity on spore sacculi PG. 102
Table 4.2. SleB and $SleB_{125-253}$ activity on cortex fragment PG. 103

CHAPTER 5
Table 5.1. His_6-MBP-CwlJ1 fusion protein solubility with various additives. 125

APPENDIX A
Table A.1. Oligonucleotide primers for plasmid construction. 144

CHAPTER 1

Introduction and Review of Literature

Bacterial Endospores and Resistance Properties. The *Bacillus* species are a ubiquitous group of bacteria that have a typical cell cycle involving growth, chromosomal replication, and division into two daughter cells; cells that are performing this cycle are termed vegetative. However, when conditions for growth are unfavorable, *Bacilli* are capable of making a detour in the cell cycle to form endospores (61). Spores are a metabolically dormant cell type that can survive in poor nutrient conditions and are resistant to a range of environmental insults (135). *Bacilli* form spores as a defensive mechanism when the environment starts to become too harsh; when the spore later finds itself in an improved situation it will germinate back into a vegetative cell and resume cellular division (136).

Structurally, the spore is composed of several distinct layers that contribute to its resistance (Fig. 1.1). The innermost layer is the core (135). The core is analogous to the vegetative cell cytoplasm since it contains DNA, ribosomes, tRNAs, and most of the spore enzymes (133, 136). Most notably the spore core has an extremely low hydration state that greatly restricts water movement (23, 38). A vegetative cell's wet weight is approximately 80% water, but in the spore core water is responsible for only 25% to 30% of the wet weight (23, 61). The low water content is considered to be the primary reason for spore dormancy because hydration levels are too low to allow sufficient macromolecular movement for metabolic activities (23, 135). Dehydration is also the main contributor to spore heat resistance, likely because the molecular targets in cells that are heat labile are inactive and stable inside the spore core (23, 38, 135). The core contains pyridine-2,6-dicarboxylic acid (DPA) where it is chelated with divalent cations. The most common chelate DPA forms is with Ca^{2+}, and results in calcium dipicolinate (Ca-DPA) (38, 109, 134, 142). Since Ca-DPA comprises 5-15% of the spore's dry weight it is largely insoluble inside the core, and subsequently helps maintain the spore core's

dehydration state (135). In addition, the DPA functions as a photosensitizer that protects spore DNA from ultraviolet (UV) light by promoting easy-to-repair DNA lesions (29, 107). However, the major factor in UV resistance is left to another group of spore core molecules called small, acid-soluble spore proteins (SASP) (132). SASPs bind the spore DNA and, when exposed to UV light, promote the formation of a spore photoproduct that is less damaging and easier to repair than the dimers typically found in irradiated DNA (37, 132).

Surrounding the core is the inner forespore membrane (IFM) whose composition is similar to the plasma membrane of vegetative cells (21-22). As a strong permeability barrier, the IFM affords protection in two ways: by preventing damaging chemicals from entering into the core; and by keeping solutes in the core from exiting, thus maintaining dehydration (22, 24).

Beyond the IFM is the germ cell wall. It is a layer of peptidoglycan (PG) which has a structure resembling that of the vegetative cell wall (90). Germ cell wall PG consists of a repeating disaccharides of β-1,4-linked N-acetylglucosamine (NAG) and N-acetylmuramic acid (NAM). Each NAM residue has a peptide side-chain extending from the lactyl group that are either involved in interstand cross-linking or cleaved to a single L-alanine side chain (144). When cross-linked, one peptide chain forms a bond with a peptide chain on another PG strand to result in a cross-linked network surrounding the entire cell (127). When a spore germinates and completes outgrowth the IFM and the germ cell wall will serve the new vegetative cell as the initial plasma membrane and cell wall respectively (7, 21-22, 24, 90).

Just above the germ cell wall is another layer of PG called the cortex (135). It composes >80% of the total spore peptidoglycan and it has a defining modification where as much as 50% of the NAM is converted to muramic-δ-lactam (ML) (6, 117). The synthesis of ML during sporulation requires two proteins: CwlD to cleave off the peptide side-chain; and PdaA in order

to carry out deacetylation and lactam cyclization (43). The conversion of NAM to ML results in the cortex having a significantly reduced level of cross-linking (90, 118-119). Interestingly, the amount of cross-linking in the cortex is in a gradient where the inner most layers are less cross-linked than the outermost regions (43, 90).

The cortex is essential for reduction of water content in the spore and by proxy has a major role in resistance, because any increase in core hydration in turn decreases resistance to heat and chemical agents (114-115, 118, 120, 135). The cortex is essential to maintain spore dormancy and durability since degradation with cortex-specific enzymes can cause a rapid loss of dehydration and premature germination without the presence of germinants (106). The loss of resistance that results is such that a germinated spore's susceptibility parallels that of a vegetative cell. Despite our knowledge of its structure and apparent role, it remains unclear exactly how the cortex facilitates dehydration maintenance (114, 118, 135).

Surrounding the cortex is the outer forespore membrane (OFM), which is a remnant of the mother cell that results during sporulation (126). It is not considered a significant permeability barrier, and its integrity in the dormant spore has been questioned (113, 135). The OFM makes no apparent contribution to any known spore resistances (102).

A complex structure called the spore coat exists just beyond the OFM. It contains more than 50 proteins, which together make up 30% of the total protein in the dormant spore (33-34, 44, 55, 78). Even though the function of most of these proteins is unknown, the coat has been demonstrated to be important in protecting the spore from damaging chemicals, exogenous lytic enzymes, and predation by protozoa (33, 74, 102, 135).

In the case of *B. subtilis* spores the coat is the outermost layer, but those species of the *B. cereus* group, including *B. anthracis*, have another loose-fitting structure making up their

outermost spore layer called the exosporium (78, 125, 135, 143). It has been postulated that the exosporium is an expanded portion of the outermost coat layer since many of the exosporium proteins in *B. anthracis* are homologous to coat proteins in *B. subtilis* (78, 125, 140). Regardless, the exosporium does contain proteins and glycoproteins that are not found in the coats of other spore-forming bacteria (26, 125, 140). There has not been any correlation discovered between the exosporium and spore resistance, however it has been implicated in the pathogenicity of *B. anthracis* (125).

Spore Germination. Although the spore is insensitive to environmental insults, it remains responsive to particular chemical germinants. Contact with these germinants can induce germination and outgrowth into a vegetative cell (35). Germinants can be nutritive or nonnutritive. In *B. subtilis* the nutrients L-alanine, L-asparagine, glucose, and fructose have been shown to initiate germination either individually or in combination with each other (96). In addition to L-alanine, *B. anthracis* and *B. cereus* also have shown a response to inosine and other purines; germination is maximal when these two classes of nutrients are used together (19, 147). The known nonnutritive germinants in *B. subtilis* are themselves spore-associated and may function to provide positive feedback to a germinating spore population; they include Ca-DPA (107), and germ cell wall fragments (137).

In order to initiate the signaling for germination the germinants must contact receptors on the IFM. The well-researched *B. subtilis* uses a tri-cistronic operon, *gerA,* to encode three membrane-associated proteins (GerAA, GerAB, and GerAC) that form one germinant receptor (59-60). *B. subtilis* also contains two more *gerA* homologs named *gerB* and *gerK*. Each receptor requires all three protein components from its particular operon to function properly (96). In *B. cereus,* homologous germination receptors also exist, with *gerQ* and *gerL* reacting to L-alanine

and inosine respectively while *gerI* contributes to germination via both molecules (19). *B. anthracis* contains two plasmids that are absent from *B. cereus*, and it is on the pXO1 plasmid that another *gerA* homolog, *gerX*, is located. *GerX* is the only germination operon found on the plasmid and is located in the large (40kb) toxin-encoding region of pXO1 (46). On the *B. anthracis* chromosome *gerA*-type operons (*gerS* and *gerH*) have been identified and proposed to act together towards host-mediated germination after being signaled by a variety of germinants (alanine, aromatic amino acids, proline and inosine) (63, 147). Microarray analyses suggest even more *gerA* homologs may participate in *B. anthracis* spore germination (27). When a germinant binds to one of these receptors the complex, in an unknown manner, initiates the events characterized with endospore germination.

Three major events occur once germination has been triggered by the germinant receptors (Fig 1.2): 1.The spore core starts to rehydrate as water moves in (106). 2. Ions are transported either actively or passively to levels seen in hydrated vegetative cells and Ca-DPA is released from the core (23, 96, 106). 3. Finally, the spore cortex peptidoglycan is degraded by germination specific lytic enzymes (GSLEs) and released into the surrounding environment (96). The released cortical fragments are called muropeptides. At this point, the spore core is now free to expand fully and proceed towards a vegetative cell cycle (95). In addition, the resistances that are associated with the spore are completely lost (95, 134, 136). This process is also of medical significance because released cortex PG is a likely ligand for NOD-like receptors and peptidoglycan recognition proteins in macrophages that normally stimulate the inflammatory response (45, 67).

It has been postulated that cortex degradation may occur first when the non-nutritive germinant Ca-DPA is added exogenously to a population of spores (106, 137). In this scenario a

GSLE is directly activated by the chelate and initiates germination by degrading cortex, thus facilitating core rehydration and expansion (108). A similar sequence of germination events occurs when sensitized spores are treated with the cell wall hydrolase lysozyme (109). A cationic detergent such as dodecylamine can trigger a nutritive-like germination response by causing DPA release before cortex hydrolysis, but similarly to exogenous DPA or lysozyme treatment this does not require germinant receptors (142).

Germination-Specific Lytic Enzymes. Germination specific lytic enzymes (GSLEs) have been shown to degrade only peptidoglycan with muramic-δ-lactam, thus explaining cortex-exclusive breakdown (118, 129) (Fig. 1.3). In *B. subtilis* two GSLEs, in particular, appear crucial to germination; CwlJ and SleB (5, 64). CwlJ is expressed under the control of the mother cell sporulation factor σ^E (64), is present in the dormant spore (8), and is required for spores to germinate in response to exogenous Ca-DPA (106). CwlJ localizes to the outer layers of the spore, most likely in the proteinaceous coat (8, 18, 64, 78). Proper localization, and hence function, requires another gene product from *gerQ* (*ywdL*) (124). A previous attempt to purify *B. subtilis* CwlJ indicated that the protein is largely insoluble (18), and that the protein may either oligomerize or associate with another spore component, thus creating a complex that is not fully dissociated during standard SDS-PAGE analysis. CwlJ is required for germination in response to Ca-DPA, however, its specific enzymatic activity on peptidoglycan remains unclear (95, 106). CwlJ shows 30% sequence identity to the proposed catalytic domain of *B. subtilis*'s other main GSLE, SleB.

SleB has an N-terminal putative cell-wall-binding domain and is thought to act as a lytic transglycosylase in *B. subtilis* (5). Mature SleB and its homologs have been observed in the cortex in *B. cereus* (99), *B. subtilis* (18, 89), and *B. anthracis* (83). Expression of *sleB* is

controlled by σ^G in the forespore (98). In *B. subtilis*, proper function of the protein is dependent on *ypeB*, which is encoded in a bicistronic operon with *sleB* (13). *YpeB* is located downstream of *sleB* and presumed to either aid in *sleB* localization or stabilization (18). In *B. anthracis sleB* is the first of a tricistronic operon. The second gene is a *ypeB* homolog (protein homology: 57% identity; 77% similarity) and the third protein is a homolog of the *B. subtilis ylaJ* (protein homology: 57% identity, 67% similarity). YlaJ is an uncharacterized putative lipoprotein in *B. subtilis* (84).

B. subtilis appears to encode yet another GSLE at the *yaaH* locus (64). *yaaH*, like *cwlJ*, is under the control of σ^E and YaaH is present in the spore coat (75, 78). Interestingly, YaaH appears to be required for an activity on cortex that does not actually hydrolyze the structure, but is instead an epimerase that targets the ML moieties (7, 18). With 48% identity the *B. cereus* homolog to *yaaH* is *sleL*, but SleL differs because it does hydrolyze cortex PG as an N-acetylglucosaminidase (16). In addition, SleL is a cortical fragment-lytic enzyme (CFLE), which can use cortex PG as a substrate only after it has been previously hydrolyzed by another GSLE such as CwlJ or SleB (16, 87). Recently it has been shown that the most evident GSLE activity in *B. anthracis* is that of an N-acetylglucosaminidase with no evidence of epimerase products (32). A focused analysis of *sleL* in *B. anthracis* indicates that the protein is more akin to the *B. cereus* homolog than to that of *B. subtilis*. In *B. anthracis*, spores lacking *sleL* lose the N-acetylglucosaminidase activity, but it is not yet known whether this activity is exclusive to cortex fragments (80). Similarities do exist between the *B. subtilis* and *B. anthracis* genes as they are expressed during midsporulation, likely under the control of σ^E, and the protein is apparently localized in the mature spore (12, 75, 80, 83).

B. subtilis and *B. anthracis* contain another coat-associated protein that is homologous to YaaH (78). Termed YdhD in *B. subtilis*, this protein has been shown to have a role in sporulation and/or germination; this function likely utilizes its YaaH-like putative peptidoglycan binding domain (77). There is no definitive evidence that this protein is a GSLE.

The GSLEs active during *B. anthracis* spore germination are the focuses of this research. BLAST analysis suggests *B. anthracis* contains GSLE homologs in its genome (Table 1.1). The most notable of these is one homolog of *sleB* and two homologs of *cwlJ*. A second homolog of *sleB* is also present in *B. anthracis*, but it appears to be more closely related to another *B. subtilis* cell wall hydrolase, *ykvT*, whose function is purported to involve vegetative cell autolysis (57).

The value of understanding *Bacillus anthracis* spore germination. The *B. anthracis* spore is the infectious agent of the disease anthrax. Inside a host, the highly resistant spore withstands many of the attacks carried out by the immune system, and once it gains entry to a suitable location, the endospore undergoes germination as the first event toward a potentially lethal disease course (25, 47, 96). Natural occurrences of anthrax in humans are rare, but past and potentially future uses of *B. anthracis* spores as a biological weapon have kept this organism and its dangers publically relevant (47, 61-62).

Disinfecting a location contaminated with anthrax spores is one critical issue, because typical antimicrobial methods are ineffective at killing the highly durable spores (135). As a result, the only efficacious methods of destroying spores in a "real-world" environment require the use of formaldehyde and/or chlorine dioxide. Unfortunately these treatments are not ideal because these chemicals are flammable, carcinogenic, toxic, and extremely costly to utilize in a safe manner (10, 62).

Spores also pose a threat when inside a host, not because they germinate, but in the cases in which they remain dormant. Superdormant spores can persist for several months inside a mammalian host and initiate disease long after the infection's original symptoms have manifested (14, 39, 52, 54). Consequently antibiotic treatments against anthrax, which are effective against vegetative cells but not spores, require a lengthy dosing schedule of 60 days (15, 62). Such a prolonged therapy raises corollary problems such as antibiotic resistance by the microorganism and incomplete adherence to the antibiotic regimen by the patient, which can lead to incomplete infection clearance (15).

The problems presented above could be addressed by prematurely triggering spore germination at a high efficiency either before decontamination or during antibiotic treatment as recently suggested (61). In both cases, the spores are coerced at one time into their vulnerable vegetative state allowing simple antimicrobial measures to be effective with less monetary and temporal costs. However, the current understanding of the initiation and events of spore germination are too incomplete to have developed a practical treatment that achieves this goal.

Objectives of this work. The purpose of this research is to uncover the role GSLEs play during *B. anthracis* spore germination. In Chapter 2 the individual roles of the GSLE homologs SleB, CwlJ1, and CwlJ2 are revealed by creating and observing mutant strains that lack each protein. It is discovered that all three proteins are likely present in the spore, and that SleB and CwlJ1 are particularly critical for cortex hydrolysis. The results of this study begin to uncover that cortex degradation is faster and more thorough when the functions of each protein are combined.

Chapter 3 further investigates the cooperative nature of GSLEs by using mutant strains containing multiple deletions of the *B. anthracis* GSLE homologs. This study, which includes

SleL along with SleB, CwlJ1, and CwlJ2, reveals that no single protein is responsible for the depolymerization of cortex. Instead, each GSLE specializes in a particular facet of the process in order to provide the spore with an efficient means to remove its cortical PG. It is also revealed that cortex degradation, despite its canonical role as the last event in germination, can initiate the other germination-related events of spore core hydration and ion release, which results in spores with lost resistances.

SleB is the focus of Chapter 4 because of its ability to independently manage enough cortex degradation to produce vulnerable spores. This aspect of the project utilizes protein purification and *in vitro* methods to conclusively demonstrate that SleB's specific hydrolytic activity does not require any other spore proteins. Additional analyses of the protein architecture establish what domains carryout substrate-binding versus enzymatic functions.

Chapter 5 details the purification of CwlJ1 for *in vitro* analyses similar to those described in Chapter 4. CwlJ1 proved to be highly challenging, but methods to improve and ease its manipulation are described. The chapter culminates with encouraging evidence of hydrolytic activity from CwlJ1, which is a first for any bacteria with a known CwlJ homolog.

The results of these studies culminate to provide a better understanding of how GSLEs function independently and cooperatively to facilitate cortex degradation. In the larger scheme of things, this body of work illustrates the roles of several components necessary for *B. anthracis* spore germination, an integral process to anthrax pathogenesis.

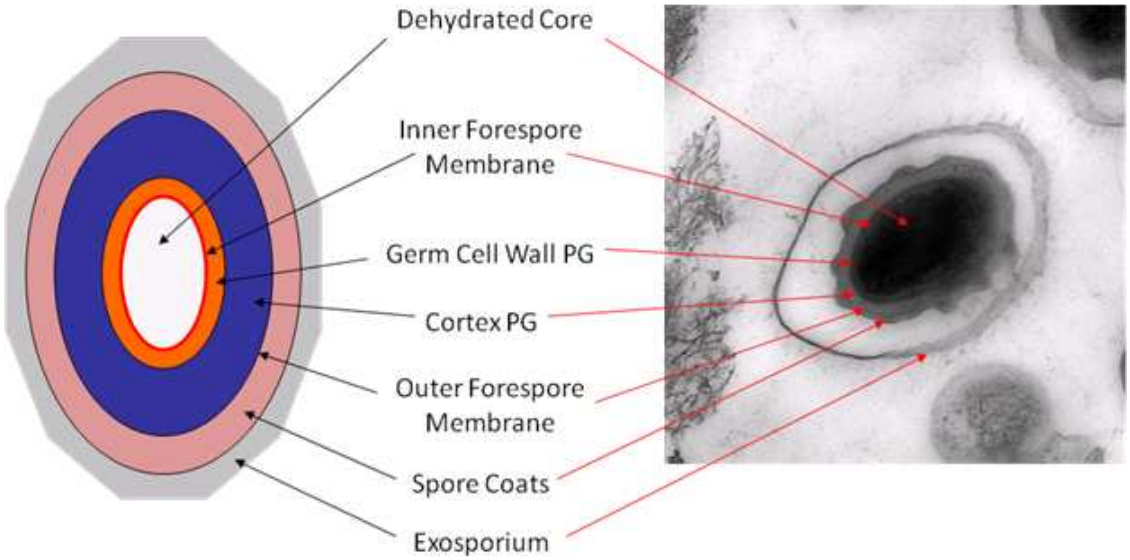

Figure 1.1. The spore structure of *Bacillus anthracis*. Major spore structures of *B. anthracis* are indicated in the illustration (left) and in the transmission electron microscopy image (right).

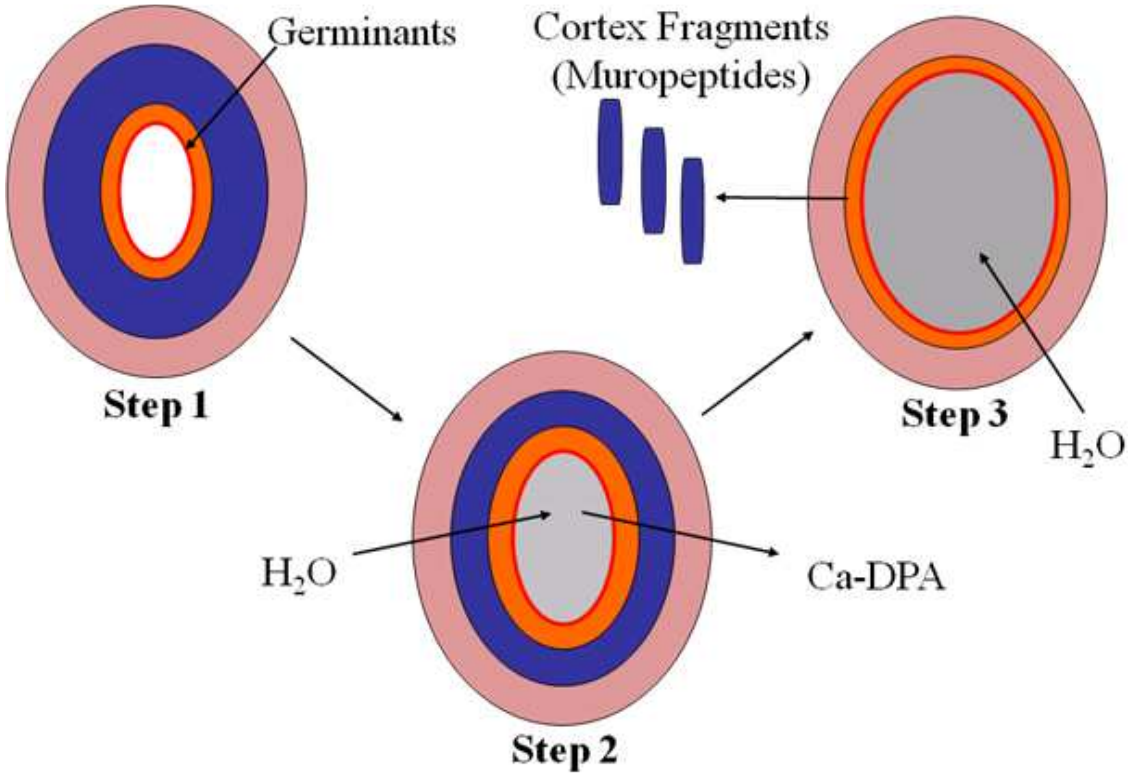

Figure 1.2. Spore germination. A simplified representation of spore germination is presented. Refer to Figure 1.1 for details of the spore's gross structural layers. The exosporium is not shown for simplicity, and it is not known to play any direct role in germination. Step 1: Germinants contact Ger receptors on the inner forespore membrane. Step 2: Ions and Ca-DPA are released from the spore core as partial rehydration occurs (as indicated by a darkening of the spore core). Step 3: GSLEs are activated and degrade cortex, which allows the core to fully rehydrate, expand, and resume cellular metabolism.

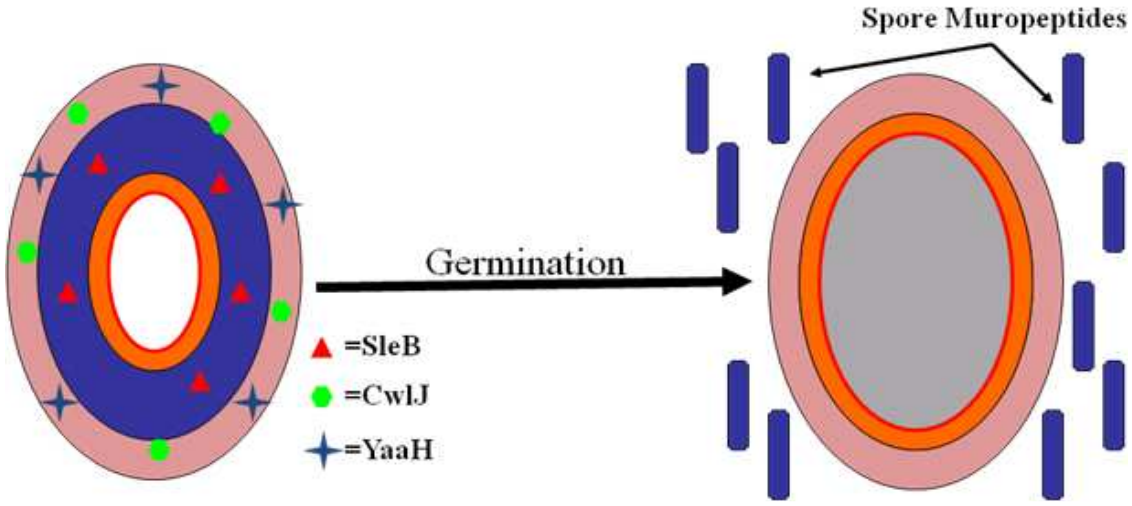

Figure 1.3. Cortex degradation. Step 3 from Figure 1.2 is illustrated in more detail. GLSEs, SleB (triangles), CwlJ (hexagons), and YaaH (stars), depolymerize spore cortex. Resulting fragments of cortex, called muropeptides, are released from the spore and out into the environment. The spore can now fully rehydrate (as indicated by a darkening of the spore core).

Table 1.1. Homologs of *B. subtilis* proteins involved in cortex lysis.

B. subtilis Protein	Locus	Size[a]	*B. anthracis* Homolog[b]	Locus	Size[a]	Identity (%)[c]	Similarity (%)[c]
SleB	CAB14209	305	SleB	AAT54872	253	47	59
CwlJ	CAB12054	142	CwlJ1	AAT57529	140	62	77
			CwlJ2	AAT54728	142	58	77
YaaH	CAB11792	427	SleL	AAT55709	430	48	70
YkvT	CAB13255	208	N/A	AAT55910	265	54	70

[a] Protein size is given in units of amino acids.

[b] Homolog names are based on those of homologous protein in *B. subtilis*, and are unique for the purposes of this research. N/A = Not Applicable.

[c] The percentage of amino acid identity and similarity to the respective *B. subtilis* homolog was determined by BLASTP 2.2.23 available from NCBI (2-3).

CHAPTER 2

The Roles of Germination-Specific Lytic Enzymes CwlJ and SleB in *Bacillus anthracis*

Jared D. Heffron, Benjamin Orsburn, and David L. Popham. 2009.

Journal of Bacteriology. 191:2237-2247.

AUTHOR CONTRIBUTIONS

Jared Heffron performed the research, data analysis, and writing of the material presented herein, as well as all of the experiments except mass spectrometry. Benjamin Orsburn operated the mass spectrometer. David Popham was the principal investigator.

ABSTRACT

The structural characteristics of a spore enable it to withstand stresses that typically kill a vegetative cell. Spores remain dormant until small molecule signals induce them to germinate into vegetative bacilli. Germination requires degradation of the thick cortical peptidoglycan by germination-specific lytic enzymes (GSLEs). *B. anthracis* has four putative GSLEs based upon sequence similarities with enzymes in other species: SleB, CwlJ1, CwlJ2, and SleL. In this study, the roles of SleB, CwlJ1, and CwlJ2 were examined. The expression of all three genes peaks 3.5 hours into sporulation. Genetic analysis revealed that, similar to other known GSLEs, none of these gene products are individually required for growth, sporulation, or triggering of germination. However, later germination events are affected in spores lacking CwlJ1 or SleB. Compared to wild type, germinating spores without CwlJ1 suffer a delay in optical density loss and cortex peptidoglycan release. The absence of SleB also causes a delay in cortex fragment release. A double mutant lacking both SleB and CwlJ1 is completely blocked in cortex hydrolysis and progresses through outgrowth to produce colonies at a frequency 1000-fold lower than the wild type strain. A null mutation eliminating CwlJ2 has no effect on germination. HPLC and mass spectroscopy analysis revealed that SleB is required for lytic transglycosylase activity. CwlJ1 also clearly participates in cortex hydrolysis, but its specific mode of action remains unclear. Understanding the lytic germination activities that naturally diminish spore resistance can lead to methods for prematurely inducing them, thus simplifying the process of treating contaminated sites.

INTRODUCTION

The spore of *Bacillus anthracis* is the infectious agent of the disease anthrax. Once entry to a suitable host has occurred, the endospore must undergo germination before it can produce any deadly toxins (47, 96). The bacterial endospore is a modified cell where the cytoplasm (spore core) is relatively dehydrated and surrounded by a thick peptidoglycan (PG) wall, called the cortex. As a result, the spore is metabolically dormant and strongly resistant to environmental insults (135). The cortex plays a major role in maintaining spore resistance by limiting the amount of water present in the core (135).

Although the spore is insensitive to environmental challenges, it remains responsive to particular chemical germinants. Contact with these germinants to a spore's germinant receptors can induce germination and outgrowth into a vegetative cell (35). There are three major events that occur once germination has been signaled. The first is that the spore core starts to rehydrate as water moves inward (106). The second event, likely coupled with the first, is transport of ions and dipicolinic acid (DPA) out of the core (23, 85, 96, 106). The third major step during germination includes the degradation of spore cortex PG by germination specific lytic enzymes (GSLEs), and the release of muropeptides into the surrounding environment (96). At this point, the spore core is now free to expand fully and proceed towards a vegetative cell cycle (95).

PG consists of a repeating disaccharide of β-1,4-linked N-acetylglucosamine (NAG) and N-acetylmuramic acid (NAM). The NAM residue has a peptide side-chain extending from the lactyl group, which is able to form a bond with a peptide chain on another PG strand to result in a cross-linked network surrounding the entire cell (127). This structure accurately describes the thin innermost layer of PG that encases an endospore. Termed germ cell wall, it may serve as the foundation for newly synthesized PG after germination. The second layer of PG around

endospores, referred to as cortex, composes >80% of the total spore PG (90). It has a defining modification where as much as 50% of the NAM is converted to muramic-δ-lactam (90). During germination the cortex, but not the germ cell wall, is broken down.

Germination specific lytic enzymes (GSLEs) have been shown to degrade only PG with muramic-δ-lactam thus explaining cortex-exclusive breakdown (118, 129). In *B. subtilis* two GSLEs, in particular, appear crucial to germination; *cwlJ* and *sleB* (5, 64). CwlJ is expressed under the control of the mother cell sporulation factor σ^E and evidence suggests that it ultimately localizes to the spore coat (8, 64). Proper localization, and hence function, is dependent on the product of *gerQ* (124). CwlJ is required for germination in response to Ca-DPA; however, its specific enzymatic activity on PG remains a mystery (95, 106). CwlJ shows 30% sequence identity to the proposed catalytic domain of *B. subtilis*' other main GSLE SleB. SleB has an N-terminal putative cell-wall-binding domain and is required for the appearance of lytic transglycosylase activity during germination of *B. subtilis* spores (5). Mature SleB and its homologs localize to the spore cortex and inner membrane in *B. cereus* (99), *B. subtilis* (18, 89), and *B. anthracis* (83). Expression of *sleB* is controlled by σ^G in the forespore (98). In *B. subtilis*, proper function of SleB is dependent on *ypeB*, which is encoded downstream of and in a bicistronic operon with *sleB* (13, 18).

This study investigated three putative *B. anthracis* GSLEs referred to as SleB, CwlJ1, and CwlJ2. Using null mutants, we show that SleB and CwlJ1 play significant roles in *B. anthracis* spore cortex hydrolysis. Both *sleB* and *cwlJ1* are expressed in a manner consistent with that observed in *B. subtilis*. We find that SleB is required for lytic transglycosylase activity. CwlJ2 is poorly expressed and plays no evident role in germination.

MATERIALS AND METHODS

Bacterial strains and antibiotics. All *B. anthracis* strains are derived from the Sterne strain 34F2 and are listed in Table 2.1. Electroporation of *B. anthracis* was performed as described previously (123). Transformants were selected on LB + 1% glucose plates containing the appropriate antibiotics: 5 µg/ml erythromycin (Fisher), 50 µg/ml kanamycin sulfate (Jersey Lab Supply) or 10 µg/ml tetracycline (Jersey Lab Supply). Vegetative growth of all strains was examined in brain heart infusion (BHI; Difco) medium with the corresponding antibiotic at 37°C for deletion mutants and 39°C for insertion mutants. Sporulation of insertion mutant strains was in Modified G medium (Mod G) without antibiotics (72) while shaking at 39°C for 3 days. Deletion mutants were similarly sporulated at 37°C except for strains used for complementation experiments, which were cultivated at room temperature in Mod G containing the appropriate antibiotic. All spores were harvested by centrifugation and vegetative cells were killed by incubation at 65°C for 25 minutes. Further spore purification was done with water washing and density centrifugation over 50% sodium diatrizoate (Sigma) as previously described (104).

Maintenance of pNFd13 containing the counter selectable marker *ccdB* was done in the One Shot® *ccdB* Survival™ strain of *E. coli* available from Invitrogen. Growth of *E. coli* was in LB media containing 10 µg/ml tetracycline hydrochloride (Jersey Lab Supply), 30 µg/ml chloramphenicol (Fisher), 50 µg/ml kanamycin sulfate (Jersey Lab Supply), or 500 µg/ml erythromycin (Fisher) as appropriate.

Mutant construction. All oligonucleotide sequences used in plasmid construction are in Table AI.1. In order to create plasmid-insertion mutations, truncated forms of each gene, containing the ribosome binding site but lacking a promoter, were generated using PCR as previously described (35). The truncated form of *sleB* contained 135 codons of the 305-codon

gene. The *cwlJ1* and *cwlJ2* truncations included 102 and 78 codons of their total 140 and 142 codons, respectively. The truncated gene fragments were recombined into pDONRtet and pNFd13 (35) using the Gateway cloning system (Invitrogen), and the resulting plasmids were inserted into the *B. anthracis* chromosome as described (35). PCR was used to confirm the gene disruptions. These plasmid insertions also created transcriptional fusions to *lacZ* (35).

In order to create in-frame deletions of each gene, PCR was used to amplify the entire target gene as well as several hundred bases up and downstream. Each fragment was cloned into pBKJ236 (65) using the corresponding endonucleases. Inverse PCR with appropriate primers produced deletion constructs with *BglI* sites at the deletion points, *Bgl*I digestion and subsequent ligation were used to create plasmids carrying in-frame deletions. The *sleB* deletion eliminated all but the first ten and last nine codons of the gene. The *cwlJ1* and *cwlJ2* deletions left only the first three and last two codons of each gene. Each mutation was introduced into *B. anthracis* via markerless gene replacement as previously described (65). Complementation of each mutation was achieved by the introduction of the pBKJ236 derivative with the corresponding full-length gene, while empty pBKJ236 served as a negative control. These complementing plasmids were maintained extrachromosomally at the permissive temperature of 27°C and under erythromycin selection.

β-Galactosidase assay. Strains carrying *lacZ* fusions were grown in Mod G medium, and samples were taken during sporulation concomitantly with optical density readings. Cell samples were permeabilized with 2% $CHCl_3$ and 0.001% SDS, and β-galactosidase activity was determined using the substrate *o*-nitrophenyl-β-D-galactopyranoside as previously described (91).

Germination assays. Spore germination and outgrowth was assayed by the change in optical density (OD_{600nm}) over time. Synchronous germination was achieved by heat activating spores at 70°C for 20 min and then suspending them in BHI broth to an OD_{600nm} of 0.2 at 39°C. Spore viability was determined using a simple plating assay, in which spores were first germinated in BHI. Germination and outgrowth to 100% of the initial OD_{600nm} was carried out to reduce spore aggregation, followed by serial dilution and plating. The colony forming units (cfu) per unit OD_{600nm} was calculated after incubation overnight at 39°C. Release of dipicolinic acid (DPA) and cortex fragments during germination in buffer was assayed as previously described (32). When required, the coats of *B. anthracis* spores were permeabilized (decoated) as previously described (106).

HPLC analysis of PG. Spores were germinated in buffer and used to prepare PG for reverse phase high-performance liquid chromatography (RP-HPLC) analysis as previously described (32). Briefly, the germinated spore suspension was separated into spore-associated (pellet) and released exudate (supernatant) fractions. Lytic enzymes were inactivated with heat (supernatant) or with heat and detergent (pellet), and PG was purified. The PG material from the pellets and half of each exudate fraction were then digested with the muramidase Mutanolysin (Sigma). All fractions were reduced with $NaBH_4$ prior to HPLC separation.

Amino acid and sugar analysis was used to characterize novel muropeptides eluted from the HPLC separation. The phosphate buffer from each collected muropeptide was removed by repeating the HPLC separation in 0.05% trifluoroacetic acid with a 0-20% acetonitrile gradient. The novel compounds were then hydrolyzed in HCL vapor and analyzed as previously described (32). Muropeptides of interest were identified by mass spectrometry using an Applied

Biosystems 3200 Q Trap MS/MS system. The total mass and fragmentation of each compound was determined in the negative ion mode as previously described (105).

RESULTS

GSLE Homologs in *B. anthracis*. Analysis of sequence similarities suggested that *B. anthracis* contains GSLE homologs in its genome (Table 2.2). The most notable of these are one homolog of SleB and two homologs of CwlJ. A second *B. anthracis* homolog of SleB is more closely related to another *B. subtilis* cell wall hydrolase, YkvT, which plays no role in spore metabolism (18, 57). For this reason, the second homolog of SleB was not analyzed. No homologs of the *Clostridium perfringens* SleC or SleM (17, 92) GSLEs were identified in the *B. anthracis* genome.

In *B. subtilis*, *sleB* is the first gene in a bicistronic operon with *ypeB*. Interestingly, the *sleB* homolog at locus BAS2562 in *B. anthracis* appears to be the first in a putative tricistronic operon. The second ORF, BAS2561, is homologous to *ypeB*. The product of the third ORF in this possible operon shares homology with the uncharacterized *B. subtilis* protein YlaJ (84).

In *B. subtilis*, *cwlJ* is the first gene in an operon with *gerQ*. The *B. anthracis cwlJ* homolog at locus BAS5241 is the first in a putative bicistronic operon with a *gerQ* homolog at BAS5242. The second *cwlJ* homolog at BAS2417 appears to be monocistronic. For the duration of this correspondence BAS5241 and BAS2417 will be referred to as *cwlJ1* and *cwlJ2* respectively, and the gene at BAS2562 will be called *sleB*.

GSLE-encoding genes are transcribed during sporulation. Plasmid insertion mutagenesis allowed the investigation of gene expression through the resulting genetic fusion of *lacZ* to the native promoter of each GSLE-encoding gene. Expression from these promoters was monitored by assaying β-galactosidase activity. The start of sporulation was defined as the transition from growth into stationary phase as observed by change in OD_{600nm} and is termed t_0. Wild type *B. anthracis*, without a *lacZ* fusion, exhibited the lowest levels of β-galactosidase

activity throughout the experiment (Fig. 2.1A and 2.1B). The highest level of activity was produced by the *cwlJ1* fusion, starting about one hour (t_1) after sporulation initiation. The transcription of *cwlJ1* peaked near $t_{3.5}$, which also coincided with the maximum activity from the *sleB* and *cwlJ2* fusions. However, expression from both the *cwlJ2* and *sleB* promoters was markedly less and was not detectable above the background prior to $t_{2.5}$ (Fig. 2.1B). Peak *cwlJ2* and *sleB* expression was 5- to 10-fold above background, similar to that observed for germinant receptors using the same type of *lacZ* fusion (35).

Our expression results agree with earlier microarray and proteome investigations of *B. anthracis* that suggest *cwlJ1* is expressed during an early wave of sporulation-associated transcription, and is then followed closely by another wave that includes *sleB* (12, 83). This is further supported by our observation of candidate promoter sequences for σ^E and σ^G (53) upstream of *cwlJ1* and *sleB* respectively (data not shown). The observed time of *cwlJ2* expression in this work more closely matches that of *sleB* than it does *cwlJ1*.

Effects of GSLE mutations on germination. None of the single and double mutant strains exhibited any significant deviations from the wild type with regard to doubling times during exponential growth, formation of heat-resistant spores, or spore morphology (data not shown).

Spores of strains lacking *cwlJ1*, *cwlJ2*, *sleB*, or both *cwlJ1* and *sleB* were germinated in BHI, and monitored through germination and outgrowth by measuring the change in $OD_{600nm.}$ As spores germinate they rapidly lose between 40% and 60% of their optical density within the first few minutes of contact with germinants. This is due to spore water uptake, Ca-DPA release, and cortex hydrolysis (104). As the spore population completes germination and enters outgrowth the OD_{600nm} increases, thus continuing into vegetative growth.

Native spores of wild type and all single mutant strains lost at least 58% of their initial OD, indicating that all were successful at synchronous germination (Fig. 2.2A). However, the precise kinetics for strains to finish germination and enter outgrowth was variable. The *cwlJ2* and *sleB* mutants mimicked wild type in their progress and lost 40% of their initial OD within one minute of each other. The entire curve for *cwlJ2* spores looked almost identical to that of the wild type, but the *sleB* spores appeared to undergo a slightly less efficient germination response coupled with a slower rate of outgrowth. Due to variability among spore preparations, this slow response of *sleB* spores was not statistically different from that of wild type spores, but it was reproducible in three independent spore preparations.

An overall delay by *cwlJ1* spores was evident by the rightward shift of the strain's germination curve. Compared to the wild type, *cwlJ1* spores were significantly delayed in OD loss from five to ten minutes after germination initiation, as well as during outgrowth for a span of forty minutes ($p \leq 0.05$ as determined by an unpaired Student's t-test) (Fig. 2.2A). These spores took at least twice as long as wild type spores to lose 40% of their starting optical density (Table 2.3), and the time it took to reach their minimal OD was also significantly delayed. The rate of outgrowth for the *cwlJ1* strain was normal; its starting point was simply delayed due to slowed germination. Identical effects on germination were obtained with plasmid-insertion and in-frame deletion mutations in each gene (data not shown), suggesting that if other genes in these operons play significant roles in germination, then they may be involved in the same GSLE functions. The *cwlJ1* slow germination phenotype was complemented with pDPV345, but not the empty vector control (Fig. 2.2C).

Spores produced by the *cwlJ1 sleB* double deletion strain were capable of losing OD only in the first five minutes after contact with germinants (Fig. 2.2A). Germination was arrested at

this point and a 40% loss in optical density was never reached (Table 2.3), nor was the OD ever observed to increase (Fig. 2.2A). This defect was complete enough to affect spore viability since the *ΔcwlJ1 ΔsleB* spores had a 1000-fold loss in colony forming ability (Table 2.3). Native spores lacking only one of the putative GSLEs had no change in viability.

Permeabilizing (decoating) the spore coats either removes or greatly disrupts proteins sequestered in that region of the spore (106). In *B. subtilis*, CwlJ and SleL have been shown to be located in or near the coat of dormant spores while SleB localizes to the cortex or membrane layers (18, 78, 124). As such, decoating spores offered a logical avenue to determine the effects of simultaneously losing the function of three putative GSLEs (CwlJ1, CwlJ2, and SleL) as shown in *B. subtilis* (106). The germination of decoated spores of all strains was substantially delayed compared to untreated spores (Table 2.3). Regardless, the stages of germination (loss of OD_{600nm}) and outgrowth (increase in OD_{600nm}) remained apparent and synchronous for wild type, *cwlJ1*, and *cwlJ2* strains (Fig 2.2B). The fact that decoated wild type and *cwlJ1* spores act indistinguishably suggests that this treatment inactivated CwlJ1.

The most profound result from investigating decoated spores was revealed by the *sleB* mutant. These spores responded to nutrients and engaged in early germination events indistinguishably from the wild type (Fig. 2.2B). However, that progress was arrested at a point just prior to losing 25% of the initial OD. From this point on, any loss of OD occurred at a significantly slower rate ($p \leq 0.05$). Decoated *sleB* spores never reached a 40% loss of OD nor exhibited any characteristics of outgrowth. Continued observation revealed no further loss in OD over 4.5 hours (data not shown). The decoating treatment did not prevent wild type, *cwlJ1*, or *cwlJ2* spores from germinating and forming colonies. However, the decoated *sleB* spores had a 1000-fold loss in colony forming ability. This was not simply a long germination delay;

continued observation of plates for three days revealed no new colony appearance. It should be noted that this phenotype is identical to what was observed for native *cwlJ1 sleB* double mutant spores.

DPA, NAM, and Dpm release from spores. One of the earliest events in spore germination is the release of Ca-DPA from the spore core into the surrounding medium (85). Despite observed changes in OD loss during germination, all of the mutant spores, including the *cwlJ1 sleB* double mutant, released as much DPA as the wild type during the earliest minutes following exposure to germinants (data not shown). In order to assay for the later steps in the germination process, one can analyze the ratio of the cortex-specific components NAM and Dpm found in the pellet versus the exudate fractions of germinating spores. Release of these compounds is rapid under the conditions used for this assay with measurable differences over the course of a few minutes (32). Assays revealed that both wild type and *cwlJ2* spores released ~50% of their NAM and Dpm within the first five minutes of contacting germinants, with maximum release occurring by ten minutes (Fig. 2.3A and 2.3B).

cwlJ1 spores were incapable of releasing cortex components as rapidly, hence after five minutes only 8% and 6% of NAM and Dpm, respectively, had been released (Fig. 2.3A and 2.3B). Still, the cortex was swiftly released from the *cwlJ1* spores in the following minutes and approached the wild type release by fifteen minutes. This result coincides with the delay in germination response revealed by OD changes (Fig. 2.2A). Complementation with pDPV345, but not with the vector control, restored both NAM and Dpm release to wild type levels (Figs. 2.3C and data not shown).

Spores without *sleB* were also delayed at discharging their cortex despite having no obvious changes in OD loss (Figs. 2.2A, 2.3A, and 2.3B). Initially, the delay was not as

dramatic as that exhibited by the *cwlJ1* spores, however, over the following minutes, the *sleB* mutant did not release cortex as speedily, thus resulting in the least total release among all strains. Fifteen minutes after the start of germination *sleB* spores had managed to release only 45% and 27% of their total NAM and Dpm, respectively. Complementation with pDPV346, but not with the vector control, restored both NAM and Dpm release to wild type levels (Figs. 2.3D and data not shown). Deleting both *cwlJ1* and *sleB* resulted in spores that released no NAM or Dpm during germination (Figs. 2.3A and 2.3B).

Cortex hydrolysis is slowed in *cwlJ1* and *sleB* spores. Previous HPLC analyses revealed that wild type *B. anthracis* spores released the majority of their cortex within the first ten minutes of germination with L-alanine and inosine (32). We obtained similar results, where after 5 minutes of germination, muropeptides derived from the spore pellet were predominantly germ cell wall associated (for example, peaks K and M) (Table 2.4, Fig. 2.4A), and all of the PG fragments found in germinating spore exudates were derived from the cortex (Table 2.4, Figs. 2.4E and 2.4I). When *cwlJ2* was disrupted, the chromatograms of pellet and exudate fractions were indistinguishable from those of the wild type (Figs. 2.4B, 2.4F, and 2.4J).

Spores lacking *cwlJ1* did not release muropeptides nearly as well. In fact, *cwlJ1* spores retained so much more spore PG during germination that cortex-derived muropeptides became the dominant peaks in the chromatogram of spore-associated material (for example peaks N and Q) (Fig. 2.4C). The average amount of muropeptide N retained increased by >350% when *cwlJ1* was disrupted. This retention of cortex was coupled with a decrease in cortex release as seen in exudates of germinating spores (Figs 2.4G and 2.4K). Cortex-derived muropeptides G6 and G7 diminished from levels seen in wild type spore exudates by an average of 48% and 50% respectively (Fig. 2.4E and 2.4G). The same change was observed when exudates were digested

with Mutanolysin except G4, the product of Mutanolysin activity on G6, was subject to a decrease (Fig 2.4I and 2.4K). A previous analysis of cortex hydrolysis by a *B. subtilis cwlJ* mutant revealed no change relative to the wild type (8). This difference is likely due to the very slow release of muropeptides by *B. subtilis*, relative to *B. anthracis* (32), making a difference in relative rate of release by *B. subtilis* strains difficult to detect.

Spores lacking SleB also exhibited a defect in muropeptide release. Much more cortex remained in the spore during germination, for instance, muropeptide N had an average increase of >350% compared to the wild type (Fig. 2.4D). This result is nearly identical to what was seen in *cwlJ1* spores, however, the associated change in released muropeptides was unique. The exudates of *sleB* spores did not contain any of muropeptides G7a or G7b (Fig. 2.4H). Exudate digested with Mutanolysin lacked the same two muropeptides (Fig. 2.4L), but no other muropeptides were altered from what was observed in wild type exudates. This phenotype was fully complemented by introducing *sleB* on a plasmid, but not by the empty vector (Fig. 2.5A-D). The requirement for SleB in the production of this class of anhydromuropeptide (see below) was also observed in *B. subtilis* (13). No muropeptides were released from spores containing both the *cwlJ1* and *sleB* deletions (data not shown). The germinated spore pellets contained cortex identical to that found in dormant *B. anthracis* spores during previous work (32).

Spores that had been decoated were also poor at digesting cortex. Pellet fractions of these spores contained the majority of total PG as N replaced K as the dominant peak (Data not shown). Very little material was released in the exudates (Fig. 2.6A-D). Decoated wild type, *cwlJ1*, and *cwlJ2* spores all generated similar exudate muropeptide profiles. Prior to Mutanolysin exposure the predominant muropeptides were G7a and G7b. After treatment with Mutanolysin, G7a and G7b remained, but N was the dominant muropeptide (data not shown), indicating that

the exudates contained large, not fully digested PG fragments. Decoated *sleB* spores, similarly to the *sleB cwlJ1* double mutant under native conditions, released little to no PG during germination, with or without Mutanolysin digestion (Fig. 2.6D and data not shown).

Muropeptides G7a and G7b contain anhydromuramic acid. Muropeptides G7a and G7b were identified through a combination of amino acid analysis and mass spectrometry (Fig. 2.7 and Table 2.5). The ratio of individual amino acids in G7a matched the expectations for a muropeptide containing a tetrapeptide side chain. The qualitative results of an amino sugar analysis revealed only NAM and NAG were present. No reduced sugars, muramitol (MOH) or glucosaminitol (GOH), were detected despite the fact that the sample was reduced prior to HPLC separation, indicating that the "reducing-end" sugar in this muropeptide is resistant to reduction. Mass spectrometry showed G7a to be 20 Da smaller than the tetrasaccharide-tetrapeptide muropeptide, N (Table 2.4). N releases MOH upon amino sugar analysis due to the reduction prior to HPLC separation (30). If G7a is similarly ordered as a TS-TP then the 20 Da mass discrepancy can be explained by the presence of an anhydro-muramic acid as the product of a lytic transglycosylase (7, 56). Mass spectrometry analysis of G7a fragmentation matches exactly to the expectations of anhydro-tetrasaccharide tetrapeptide (Table 2.5 and Fig. 2.7). Amino acid analysis, mass spectrometry, and fragmentation analysis of muropeptide G7b (Table 2.5 and data not shown) revealed that it is anhydro-tetrasaccharide alanine.

DISCUSSION

The GSLE mechanism of *B. anthracis* spores appears to function similarly to that of *B. subtilis*, with some minor but potentially important differences. *B. anthracis* strains with mutations affecting *cwlJ1*, *cwlJ2*, *sleB*, or *cwlJ1* and *sleB* grow, divide, and sporulate without difficulty, and their spores initially respond normally to nutrient germinants. In *B. subtilis*, the germination muropeptide profiles of wild type and *cwlJ* spores are indistinguishable (18), but in *B. anthracis* we were able to observe significantly less cortex-derived muropeptides being released from spores within ten minutes after contacting germinants. The structures of the released muropeptides did not differ from those produced by the wild type strain, leaving the bond specificity of any CwlJ1 enzymatic activity unresolved. SleB, like CwlJ1, is required for timely cortex degradation, but its mode of action is unique. Two cortex fragments that are entirely dependent on SleB are the result of lytic transglycosylase activity. This activity was associated with SleB using similar methods in *B. subtilis*, but was not previously detected in *B. anthracis* (13, 32). In response to germinants, the *cwlJ1 sleB* double mutant spores initiate but are incapable of completing germination, similarly to *cwlJ sleB B. subtilis* spores (64). However, unlike the situation in *B. subtilis*, we did not observe any delay in DPA release. The first five to ten minutes of *B. anthracis* germination (~25% loss in OD) is independent of GSLE activity and includes the release of nearly all of the DPA. Very rapid DPA release, like quicker cortex fragment release (13, 30), may be a function of thinner, more permeable *B. anthracis* spore coat layers.

The highest rate of cortex degradation requires both *cwlJ1* and *sleB*, yet they do not cause release of cortex fragments in exactly the same manner (Figs. 2.3A and 2.3B). This suggests that SleB and CwlJ1 provide alternate pathways for cortex depolymerization (Fig. 2.8). We propose

that this difference is best explained in context with SleL, which shares 98% identity with its *B. cereus* homolog, and functions as an N-acetylglucosaminidase in both *B.* anthracis (80) and *B. cereus* (16). In *B. cereus*, SleL has been further defined as a cortex-fragment-lytic-enzyme (CFLE) that recognizes only cortex substrate that has undergone previous digestion by another GSLE (16). In this model the initial depolymerization of the cortex would be the responsibility of SleB and CwlJ1. The NAM release from a *cwlJ1* spore indicated that 6-fold less cortex was digested and released than from wild type spores in the first five minutes of germination (Fig. 2.3A). In addition, this was more than 3-fold less NAM than the *sleB* spores could discharge. These initial differences are likely due to a large disparity in protein available for depolymerization as suggested by the higher level of *cwlJ1* transcription (Fig. 2.1A). However, this situation rapidly reverses as germination continues. Within ten minutes, germinating *cwlJ1* and *sleB* spores have the same amount of NAM released, and by fifteen minutes *cwlJ1* spores have surpassed *sleB* spores to achieve NAM release near wild type levels (Fig. 2.3A). It is our suggestion that the rapid acceleration of NAM release by *cwlJ1* spores is due to SleL action, which would have ample substrate available after several minutes of SleB-initiated cortex digestion. Meanwhile, *sleB* spores release cortex fragments early during germination due to naturally high levels of CwlJ1, but are unable to maintain this rapid release. Perhaps the population of cortex fragments that CwlJ1 yields does not provide the best substrate for SleL. Patterns of Dpm release support the same conclusions. Sequential digestion of spore PG by SleB and SleL has previously been suggested for *B. cereus* (87). Our model does not rule out the possibility that some amount of CwlJ1-created muropeptides are acted on by SleL, indeed, SleL products are produced by *sleB* mutant spores. SleL may simply have a higher affinity for cortex fragments resulting from SleB action.

The responsibilities of *cwlJ1* and *sleB* are clearly redundant due the partial effects on cortex lysis they each have and the complete lysis defect that results when both are disrupted. Further study of multiple mutant strains might provide novel muropeptide HPLC profiles that offer better insight into a specific lytic activity associated with *cwlJ1*. These studies should include *sleL* to provide a comprehensive analysis of the events during cortex degradation. Understanding the lytic germination activities that naturally diminish spore resistance can lead to methods that prematurely activate cortex degradation, thus greatly simplifying the process of cleaning *B. anthracis* contaminated sites.

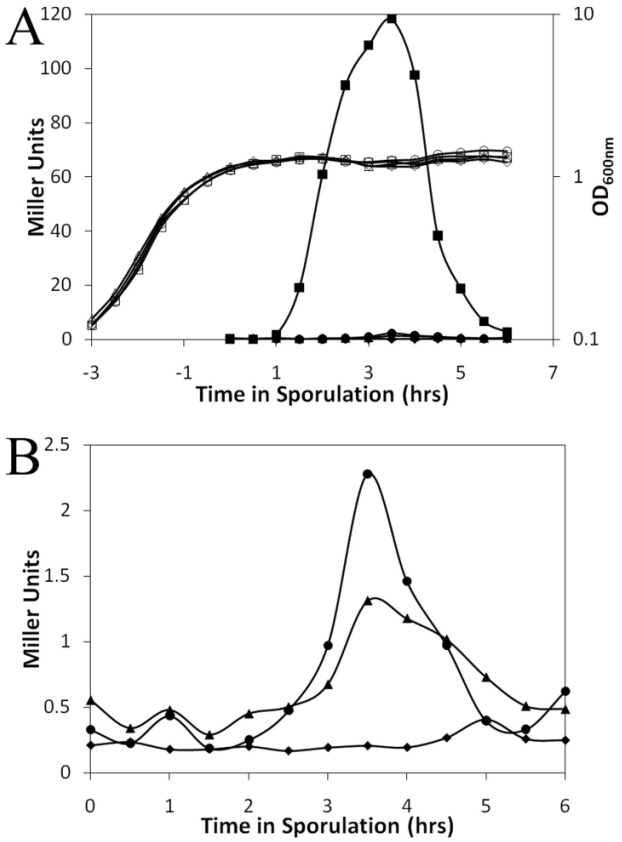

Figure 2.1. Expression of *cwlJ1*, *cwlJ2*, and *sleB* during *B. anthracis* sporulation. Strains carrying each promoter-*lacZ* fusion were shaken in Mod G medium at 39°C and were assayed for β-galactosidase activity. (A) Optical density (open symbols) and β-galactosidase activity (filled symbols) are for a wild type strain lacking *lacZ* (♦), and for strains with *lacZ* fused to *cwlJ1* (■), *cwlJ2* (▲), and *sleB* (●). (B) β-galactosidase activity for the wild type, *cwlJ2-lacZ*, and *sleB-lacZ* are shown on an expanded y-axis for clarity. Both panels show representative data for one of three independent experiments.

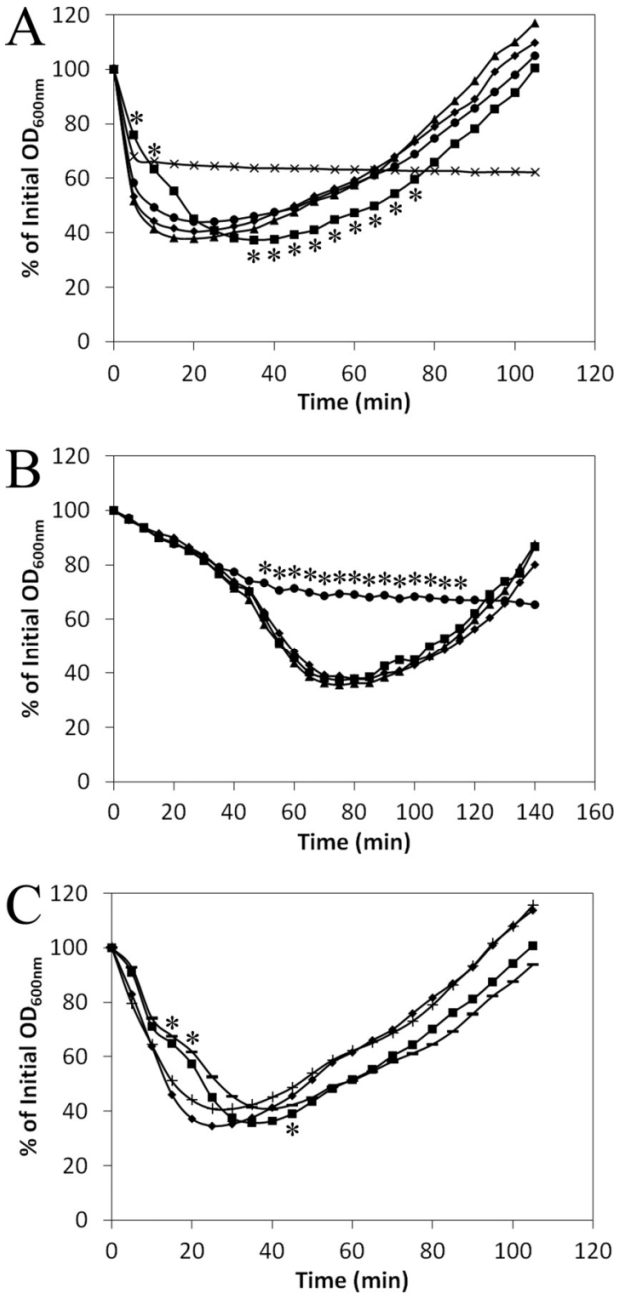

Figure 2.2. Germination and outgrowth of native and decoated spores in BHI. Wild type (♦), *cwlJ1*and *ΔcwlJ1* (■), *cwlJ2* (▲), *sleB* (●), *ΔcwlJ1 ΔsleB* (×), *ΔcwlJ1*+pBKJ236 (—), and *ΔcwlJ1*+pDPV345 (+) spores were heat activated and germinated in BHI at 39°C. (A) Germination of native spores. (B) Germination of decoated spores. (C) Complementation of the *ΔcwlJ1* phenotype. Data shown are an average of three independent experiments; error bars are not shown for clarity. Asterisks indicate those time points when *cwlJ1* (A) *sleB* (B), or *ΔcwlJ1* and *ΔcwlJ1*+pBKJ236 (C) spores were significantly different ($p \leq 0.05$) from wild type spores. The *ΔcwlJ1 ΔsleB* spores (A) were significantly different from those of the wild type at all time points except 60-70 min, where the lines cross.

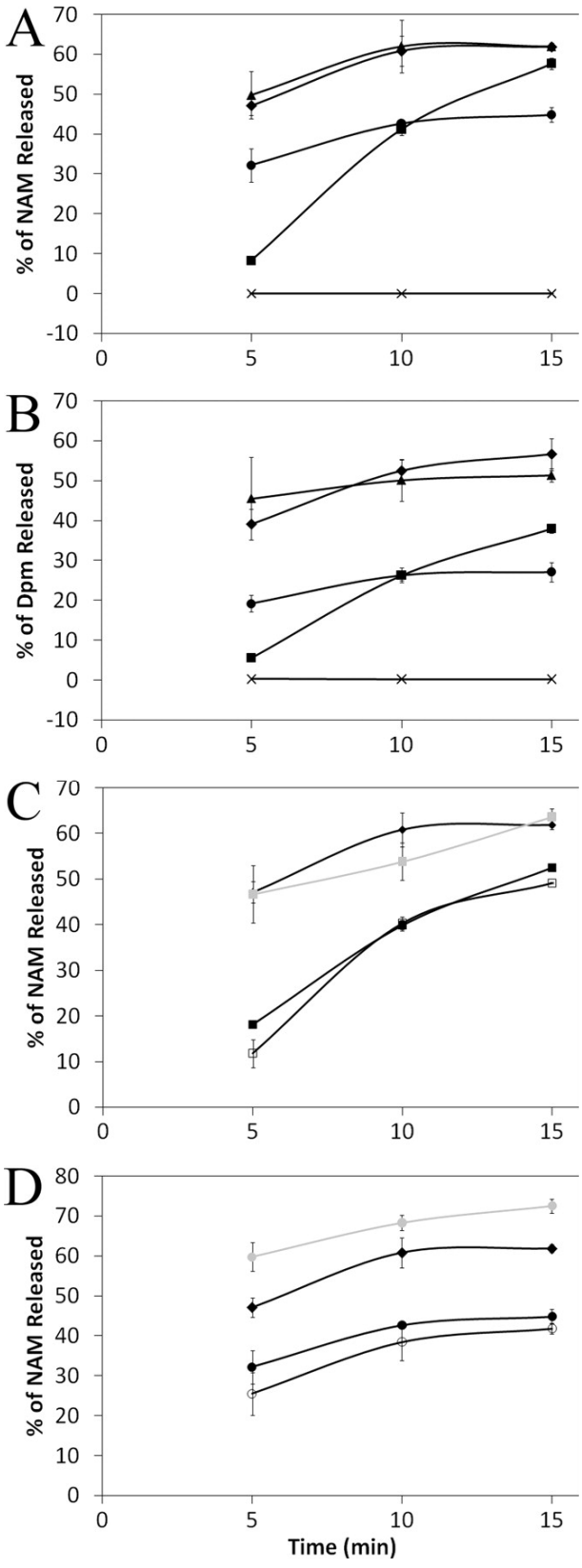

Figure 2.3. Release of NAM and Dpm from germinating *B. anthracis* spores. Dormant wild type (♦), *cwlJ1* (■), *cwlJ2* (▲), *sleB* (●), and *ΔcwlJ1 ΔsleB* (×) spores in buffer were germinated with L-alanine and inosine and were sampled for the release of NAM (A) and Dpm (B) at five minute intervals after contact with germinants. (C) Complementation of *ΔcwlJ1* (■) NAM release was tested with *ΔcwlJ1*+pDPV345 (■) and *ΔcwlJ1*+pBKJ236 (□) spores. (D) Complementation of *ΔsleB* (●) NAM release was tested with *ΔsleB*+pDPV346 (●) and *ΔsleB*+pBKJ236 (○) spores. All error bars represent 1 standard deviation of the mean of three (A, B, and D) or two (C) independent experiments. All points have error bars, but in some cases these are too small to be visible.

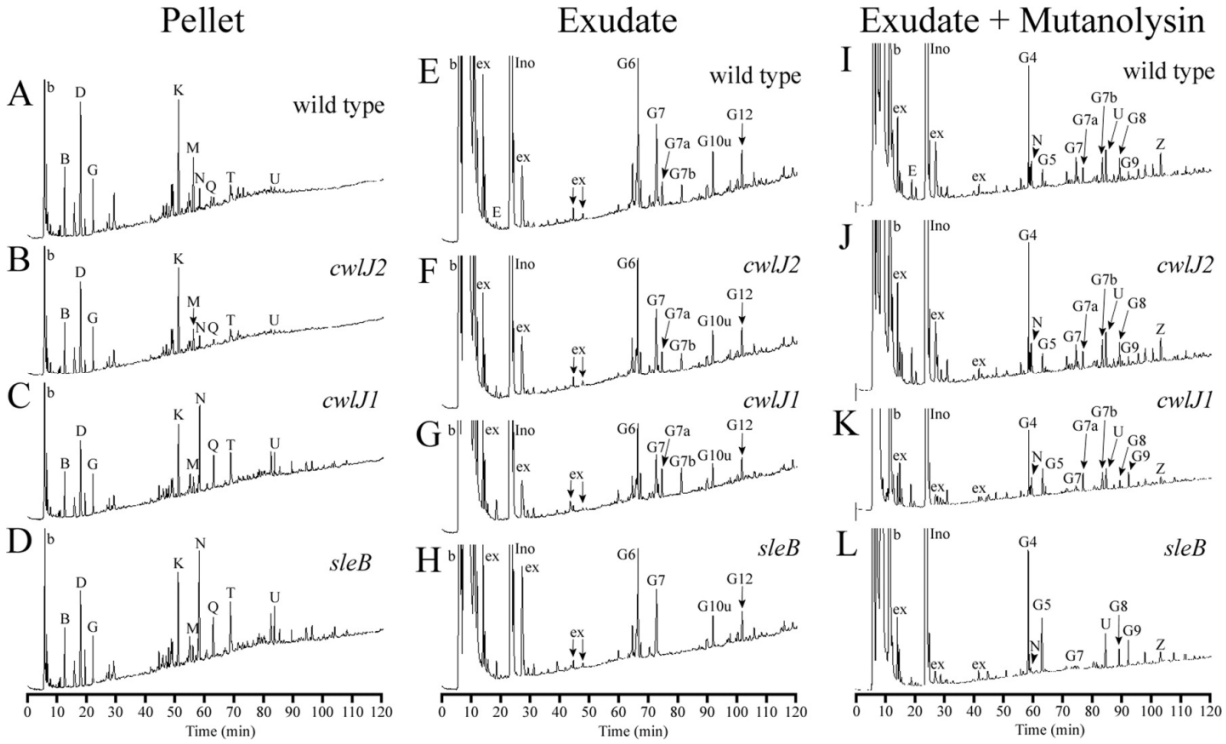

Figure 2.4. RP-HPLC separation of muropeptides from germinating *B. anthracis* spores. PG was prepared from germinating spore suspensions as described. Samples were collected after spore suspensions had lost 40% of their initial OD; approximately 5 minutes for wild type and *cwlJ2* spores and 10 minutes for *cwlJ1* and *sleB* spores. PG from germinating spore pellets (A-D) and from 50% of the exudate (I-L) preparations were digested with muramidase, reduced, and separated as previously described (90). The other 50% of the exudates (E-H) were reduced and separated without muramidase digestion. Peaks are numbered as in (32) and in Table 2.4, but the initial "a" in the germination-specific peaks names were omitted for space considerations. Early-eluting peaks labeled "b" are buffer components present in blank samples. Peaks labeled "ex" are spore exudate components that, based upon amino acid analysis, are not derived from PG. Peaks labeled as "Ino" are from the inosine used to germinate spores.

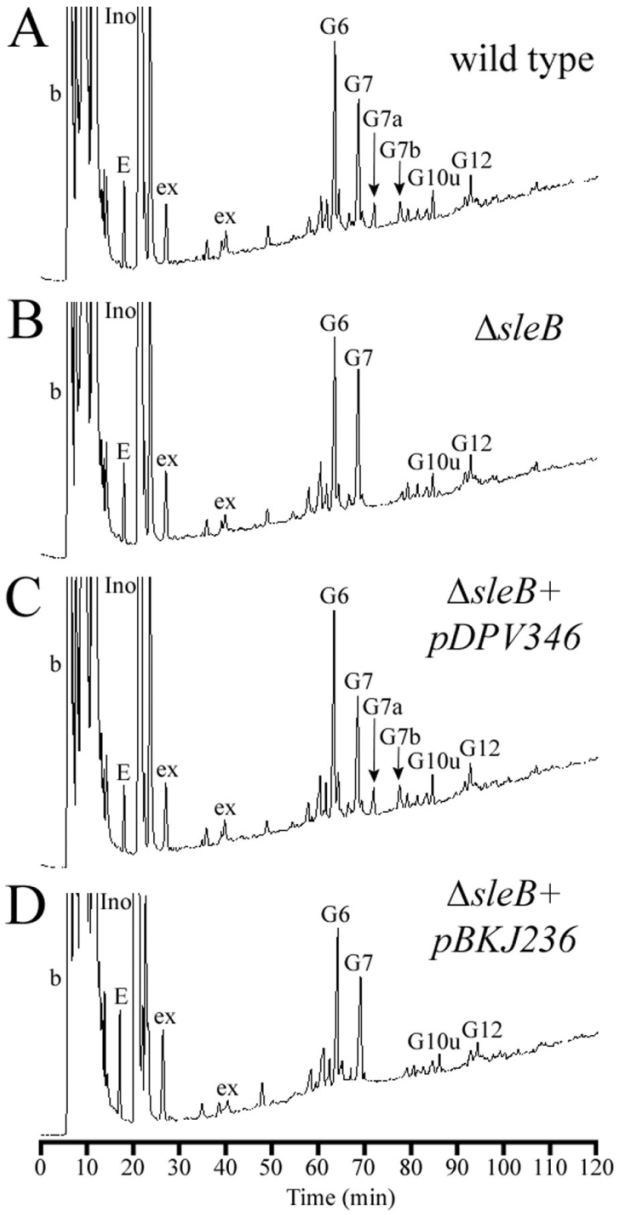

Figure 2.5. Complementation of Δ*sleB*. Samples were prepared and analyzed, and peaks are labeled, as in Fig. 2.4. (A) Muropeptides released from wild type spores. (B) Muropeptides released from *ΔsleB* spores. (C) Muropeptides released from spores with *ΔsleB* plus the complementing plasmid pDPV346. (D) Muropeptides released from spores with *ΔsleB* plus the control vector pBKJ236.

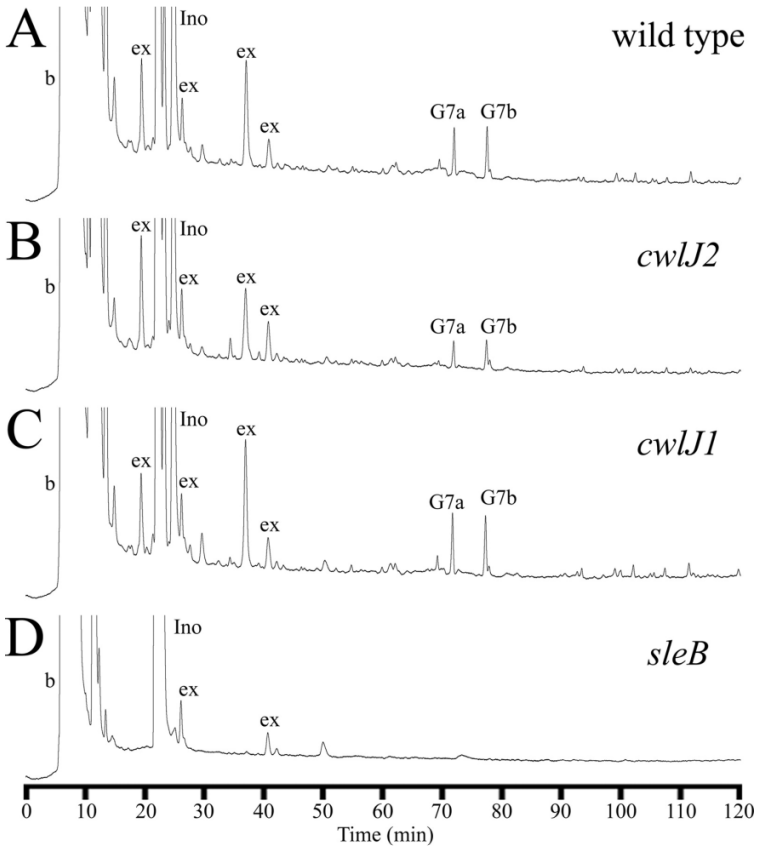

Figure 2.6. RP-HPLC separation of muropeptide exudates from decoated germinating *B. anthracis* spores. Spores were permeabilized as previously described (106). Samples were prepared and analyzed, and peaks are labeled, as in Fig. 2.4. All samples were harvested after spores lost 40% of their initial OD (~45min.). (A) Muropeptides released from wild type spores. (B) Muropeptides released from *cwlJ2* spores. (C) Muropeptides released from *cwlJ1* spores. (D) Muropeptides released from *sleB* spores.

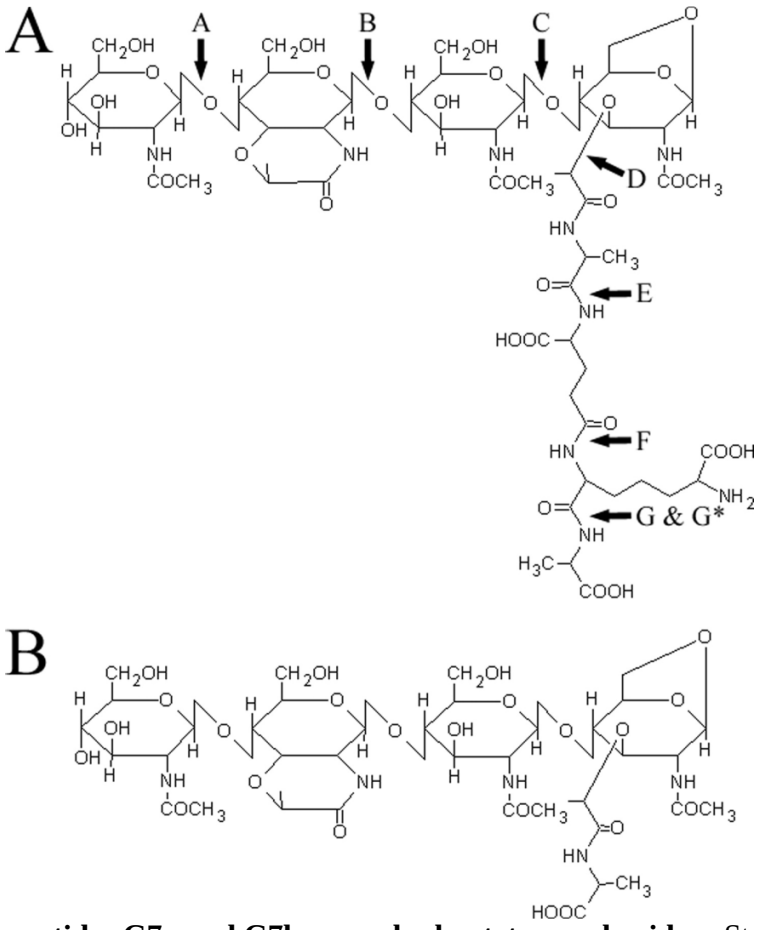

Figure 2.7. Muropeptides G7a and G7b are anhydro-tetrasaccharides. Structures were determined with a combination of HPLC amino acid/sugar analysis and ESI-MS. (A, B) Sugar residues are (from left to right) NAG, muramic-δ-lactam, NAG, anhydro-NAM. (A) Amino acid residues are, in order from lactyl linkage, L-alanine, D-glutamate, meso-diaminopimelic acid, and D-alanine. Arrows indicate sites of fragmentation during ESI-MS as identified in Table 2.5. (B) The single amino acid side chain is L-alanine.

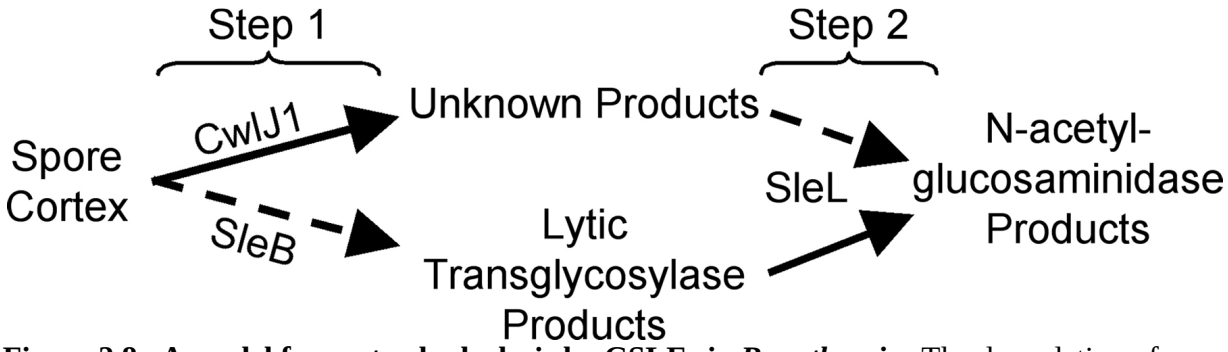

Figure 2.8. A model for cortex hydrolysis by GSLEs in *B. anthracis*. The degradation of spore cortex is illustrated as two steps. Solid arrows indicate the reaction that is responsible for the majority of activity at that given step. Dashed arrows indicate those reactions that compose the minority of enzymatic activity. SleB and CwlJ1 are both capable of depolymerizing intact cortex, with more initial digestion due to CwlJ1. SleL, as a CFLE, is capable of degrading only partially digested cortex. SleL prefers substrate provided by SleB, or the positioning of SleB results in production of a greater amount of SleL substrate. Fully digested cortex contains a mixed muropeptide population of all the shown substrates and products.

Table 2.1. *B. anthracis* strains and plasmids.

Strain	Relevant Genotype[a]	Construction[b]	Source
B. anthracis			
Sterne 34F2	pX01$^+$ pX02$^-$		P. Hanna
DPBa18	*cwlJ2*::pDPV331 (*cwlJ2'-lacZ* Kan^R *lacI* Pspac-*cwlJ2*)	pDPV331→34F2	This work
DPBa22	*cwlJ1*::pDPV330 (*cwlJ1'-lacZ* Kan^R *lacI* Pspac-*cwlJ1*)	pDPV330→34F2	This work
DPBa24	*sleB*::pDPV329 (*sleB'-lacZ* Kan^R *lacI* Pspac-*sleB*)	pDPV329→34F2	This work
DPBa38	*ΔsleB*	pDPV383→ 34F2	This work
DPBa57	*ΔsleB*, pDPV346 (*sleB*$^+$ Er^R)	pDPV346→ DPBa38	This work
DPBa59	*ΔsleB*, pBKJ236 (Er^R)	pBKJ236→ DPBa38	This work
DPBa61	*ΔcwlJ1*	pDPV347→ 34F2	This work
DPBa62	*ΔcwlJ1*, pBKJ236 (Er^R)	pBKJ236→ DPBa61	This work
DPBa63	*ΔcwlJ1*, pDPV345 (*cwlJ1*$^+$ Er^R)	pDPV345→ DPBa61	This work

Plasmid	Relevant Genotype[a]	Construction[b]	Source
pDONRtet	Tet^R		(35)
pNFd13	Kan^R, pE194 ori^{ts}, P$_{spac}$, *lacZ*		(35)
pBKJ223	Tet^R, P$_{amy}$-ISceI		(65)
pBKJ236	Er^R, ori^{ts}		(65)
pDPV329	Pspac-*sleB'-lacZ* Kan^R *lacI*	pNFd13::*sleB'*	This study
pDPV330	Pspac-*cwlJ1'-lacZ* Kan^R *lacI*	pNFd13::*cwlJ1'*	This study
pDPV331	Pspac-*cwlJ2'-lacZ* Kan^R *lacI*	pNFd13::*cwlJ2'*	This study
pDPV345	*cwlJ1*$^+$	pBKJ236::*cwlJ1*	This study
pDPV347	*ΔcwlJ1*	pBKJ236:: *ΔcwlJ1*	This study
pDPV346	*sleB*$^+$	pBKJ236::*sleB*	This study
pDPV383	*ΔsleB*	pBKJ236::*ΔsleB*	This study

[a] Abbreviations for antibiotic resistance genes: Kan, kanamycin; Er, erythromycin; Tet, tetracycline.

[b] Strains were constructed by electroporation or conjugation. The designation preceding the arrow is the plasmid and the designation following the arrow is the recipient strain.

Table 2.2. Homologs of *B. subtilis* GSLEs.

B. subtilis Protein	SleB	CwlJ		SleL (YaaH)
Size (amino acids)	305	142		427
B. anthracis Homolog[a]	SleB	CwlJ1	CwlJ2	SleL
Locus	BAS2562	BAS5241	BAS2417	BAS3402
Size (amino acids)	253	140	142	430
Identity (%)[b]	53	62	58	48
Similarity (%)[b]	67	76	76	70

[a] Homolog names are based off of homologous protein in *B. subtilis*, and are unique for the purposes of this research. N/A = Not Applicable.

[b] The percentage of amino acid identity and similarity was determined using BLASTP 2.2.18 (97, 148).

Table 2.3. Germination of Spores in BHI.

	Native spores		Decoated Spores	
Genotype	Time for 40% loss of OD[a,b] (m)	Cfu/OD[a]	Time for 40% loss of OD[a,b] (m)	Cfu/OD[a]
Wild type	4 ± 1	1×10^8	54 ± 10	1×10^8
cwlJ1	14 ± 5*	1×10^8	54 ± 5	1×10^8
cwlJ2	4 ± 1	1×10^8	53 ± 8	1×10^8
sleB	5 ± 2	9×10^7	N/A	1×10^5*
cwlJ1 sleB	N/A	1×10^5*	not tested	not tested

[a] Averages were determined from three independent experiments.
[b] Values are rounded to the nearest minute. Error is one standard deviation of the mean.
N/A = Not Applicable, sample never reached a 40% loss.
* Indicates a value that is significantly different from similarly treated wild type spores with a $p \leq 0.01$ as determined by an unpaired two-tailed Student's t-test.

Table 2.4. Muropeptide peak identification.

Name[a]	Structure[b]	Source[c]
Muropeptides produced from dormant spore peptidoglycan		
A	DS-TriP	
B	DS-Ac-TriP	Germ Cell Wall
C	DS-TriP+Am	Germ Cell Wall
D	DS-Ac-TriP+Am	Germ Cell Wall
E	DS-Ala	
F	DS-TP	
G	DS-Ac-TP	
H	TS-TP open lactam	Cortex
I	TS Red-TP	Cortex
J	TS Red-Ala	Cortex
K	DS-Ac-TP x TriP+Am-DS-Ac	Germ Cell Wall
L	TS-TP-Ac	Cortex
M	DS-Ac-TP+Am x TriP+Am-DS-Ac	Germ Cell Wall
N	TS-TP	Cortex
O	TS-TP x TP	Cortex
P	DS-TP x TP-TS Red	Cortex
Q	TS-Ala	Cortex
R	HS Red-Ac-TP (right lactam reduced)	Cortex
S	HS Red-Ac-TP (left lactam reduced)	Cortex
T	DS-TP x TP-TS	Cortex
U	HS-TP-Ac	Cortex
V	TS-TP x TP-TS	Cortex
W	HS-Ala-Ac	Cortex
X	HS-Ala-Ac	Cortex
Y	HS-TP	Cortex
Z	HS-Ala	Cortex
AA	TS-TP x TP-HS	Cortex
Muropeptides produced from germinated spore exudate following Mutanolysin digestion		
aG1	TriS-TP Red	Cortex, N-acetylglucosaminidase
aG4	TriS-TP	Cortex, N-acetylglucosaminidase
aG5	TriS-Ala	Cortex, N-acetylglucosaminidase
aG8	PS-TP-Ac	Cortex, N-acetylglucosaminidase
Muropeptides produced from germinated spore exudate with no Mutanolysin digestion		
aG2	TS-TP NAGr Red	Cortex, N-acetylglucosaminidase
aG3	TS-Ala NAGr Red	Cortex, N-acetylglucosaminidase
aG6	TS-TP NAGr	Cortex, N-acetylglucosaminidase
aG7	TS-Ala NAGr	Cortex, N-acetylglucosaminidase
aG7a	TS-TP anhydro	Cortex, lytic transglycosylase
aG7b	TS-Ala anhydro	Cortex, lytic transglycosylase
aG10u	HS-TP-Ac NAGr	Cortex, N-acetylglucosaminidase
aG12	HS-Ala-Ac NAGr	Cortex, N-acetylglucosaminidase

[a] Muropeptide names are determined by their order of elution during RP-HPLC. Muropeptide names preceded by "a" indicate those generated by *B. anthracis* in order to differentiate from those of other species.

[b] Abbreviations: DS, disaccharide (NAG-NAM); TS, tetrasaccharide (NAG-lactam-NAG-NAM); HS, hexasaccharide (NAG-lactam-NAG-lactam-NAG-NAM); TriS, trisaccharide (lactam-NAG-NAM); PS, pentasaccharide (lactam-NAG-lactam-NAG-NAM); TriP, tripeptide (Ala-Glu-Dpm); TP, tetrapeptide (Ala-Glu-Dpm-Ala); -Ac, deacetylated glucosamine; +Am, amidated Dpm; Red, reduced lactam (an artifact of sample preparation (146); NAGr, NAG at the reducing end; x, crosslink between two peptides; anhydro, the NAM at the reducing end is in the anhydro form**.**

[c] Indicates the structure of origin for each muropeptide under the assumption that muramic-δ-lactam is unique to cortex and tripeptide is exclusive to the germ cell wall. Entries that are blank cannot be attributed to a single source. For muropeptides released during germination the enzymatic activity responsible is indicated.

Table 2.5. Novel muropeptide identification.

Name	Structure[a]	m/z[b] predicted	m/z[b] observed	Amino acid/amino sugar analysis[c] M	G	MOH	GOH	Ala	Glu	Dpm
aG7a	TS-TP anhydro	1338.5	1338.4	+	+	-	-	2	1	1
aG7b	TS-Ala anhydro	966.4	966.3	+	+	-	-	1	0	0
Fragments of aG7a[d]										
A	TriS-TP anhydro	1135.5	1135.2							
B	DS-TP anhydro	920.4	920.3							
C	MS-TP anhydro	717.3	717.2							
D	TS anhydro	823.3	823.1							
E	Glu-Dpm-Ala	389.2	389.2							
F	Dpm-Ala	260.1	260.2							
G	Ala	88.0	88.1							
G*	TS-TriP anhydro	1251.6	1251.2							

Abbreviations: M, N-acetylmuramic acid; G, N-acetyl glucosamine; MOH, muramitol; GOH, glucosaminitol; TS, tetrasaccharide (NAG-ML-NAG-NAM); TriS, trisaccharide (ML-NAG-NAM); DS, disaccharide (NAG-NAM); MS, monosaccharide (NAM); TP, tetrapeptide (Ala-Glu-Dpm-Ala); TriP, tripeptide (Ala-Glu-Dpm); Ala, alanine; Glu, glutamate; Dpm, meso-diaminopimelic acid

[a] Anhydro structures have a 1,6-anhydro linkage in the terminal NAM.

[b] Mass to charge ratio for the deprotonated ion of the predicted or expected muropeptide as determined by ESI-MS.

[c] The analysis method does not allow reliable quantitative results for amino sugars. + indicates that this compound was clearly detected. – indicates that this compound was not clearly detected. For amino acids, the molar ratios are rounded to the nearest whole number.

[d] Fragment names refer to the muropeptide fragmentation indicated by arrows in Figure 2.7.

ACKNOWLEDGMENTS

This research was supported by Public Health Service grant AI060726 from the National Institute of Allergy and Infectious Disease. ABI mass spectrometers were donated to Virginia Tech by PPD, Inc., Richmond, VA.

CHAPTER 3

Contributions of Four Cortex Lytic Enzymes to Germination of *Bacillus anthracis* Spores

Jared D. Heffron, Emily A. Lambert, Nora Sherry, and David L. Popham. 2010.

Journal of Bacteriology. 192:763-770.

AUTHOR CONTRIBUTIONS

Jared Heffron and Emily Lambert contributed equally to the research, data analysis, and writing of the material presented herein, as well as the creation of multi-deletion mutant strains. Jared conducted spore germination assays in response to nutrient and non-nutrient stimuli, and muropeptide analyses. Emily prepared spores, conducted colony formation assays, and cortex fragment release tests. Nora Sherry assisted in the creation of the multi-deletion mutant strains used in the study. David Popham was the principal investigator.

ABSTRACT

Bacterial spores remain dormant and highly resistant to environmental stress until they germinate. Completion of germination requires the degradation of spore cortex peptidoglycan by germination-specific lytic enzymes (GSLEs). *Bacillus anthracis* has four GSLEs: CwlJ1, CwlJ2, SleB, and SleL. In this study the cooperative action of all four GSLEs *in vivo* was investigated by combining in-frame deletion mutations to generate all possible double, triple, and quadruple GSLE mutant strains. Analyses of mutant strains during spore germination and outgrowth combined observations of optical density loss, colony-producing ability, and quantitative identification of spore cortex fragments. The lytic transglycosylase SleB alone can facilitate enough digestion to allow full spore viability and generates a variety of small and large cortex fragments. CwlJ1 is also sufficient to allow completion of nutrient-triggered germination independently and is a major factor in Ca-DPA-triggered germination, but its enzymatic activity remains unidentified because its products are large and not readily released from the spore's integuments. CwlJ2 contributes the least to overall cortex digestion, but plays a subsidiary role in Ca-DPA-induced germination. SleL is an N-acetylglucosaminidase that plays the major role in hydrolyzing the large products of other GSLEs into small, rapidly released muropeptides. As the roles of these enzymes in cortex degradation become clearer, they will be targets for methods to stimulate premature germination of *B. anthracis* spores, greatly simplifying decontamination measures.

INTRODUCTION

The gram-positive bacterium *Bacillus anthracis* is the etiologic agent of cutaneous, gastrointestinal, and inhalational anthrax (94). An anthrax infection begins when the host is infected with highly resistant, quiescent *B. anthracis* spores (1, 94). Within the host, the spore's sensory mechanism recognizes chemical signals, known as germinants, and triggers germination which leads to the resumption of metabolism (134). Spores that have differentiated into vegetative cells produce a protective capsule and deadly toxins. These virulence factors allow the bacteria to evade the host's immune system and establish an infection resulting in septicemia, toxemia and frequently death (94). Although vegetative cells produce virulence factors that are potentially fatal, these cells cannot initiate infections and are much more susceptible to antimicrobial treatments than spores (94). Therefore, efficient triggering of spore germination may enhance current decontamination methods.

Spores are highly resistant to many environmental insults because the spore core (cytoplasm) is dehydrated, dormant, and surrounded by multiple protective layers including a modified layer of peptidoglycan (PG) known as the cortex (134). The cortex functions to maintain dormancy and heat resistance by preventing core rehydration (38). It is composed of alternating N-acetylglucosamine (NAG) and N-acetylmuramic acid (NAM) sugars (Fig. 3.1). Peptide side chains on the NAM residues are either involved in interstrand cross-linking, cleaved to a single L-alanine side chain, or are fully removed with accompanying formation of muramic-δ-lactam (6, 116, 145). After germination is initiated by either nutrient or non-nutrient germinants, the cortex is depolymerized resulting in complete core rehydration, resumption of metabolic activity, and outgrowth (129, 134).

Cortex hydrolysis is driven by autolysins called germination-specific cortex-lytic enzymes (GSLEs) that recognize the cortex-specific muramic-δ-lactam residues (6, 16, 88, 118). GSLEs fall into two classes; spore cortex lytic enzymes (SCLEs) are thought to depolymerize intact cortical PG, and cortical fragment lytic enzymes (CFLEs) which further degrade partially hydrolyzed cortex (88). Both SCLEs and CFLEs have been identified in a variety of spore forming species including *B. anthracis* (50, 81-82), *Bacillus cereus* (16, 86, 101), *Bacillus megaterium* (36, 130), *Bacillus subtilis* (64, 76, 100), *Bacillus thuringiensis* (58), and *Clostridium perfringens* (17, 92). Of the four GSLEs identified in *B. anthracis* CwlJ1, CwlJ2 and SleB are predicted to be SCLEs (50) whereas SleL is thought to be a CFLE (81).

Recently, independent studies showed that CwlJ1 and the lytic transglycosylase SleB (Fig. 3.1) play partially redundant roles and that either is sufficient for spore germination and outgrowth (41, 50). However, these same studies report conflicting results concerning the role of CwlJ2 during germination. Heffron *et al.* found no effect of CwlJ2 on the biochemistry of cortex hydrolysis or on colony forming efficiency of spores (50). Giebel *et al.* reported that loss of CwlJ2 caused a minor defect in germination kinetics and that in the absence of SleB and CwlJ1, further loss of CwlJ2 had a major effect on colony forming efficiency (41). SleL in *Bacillus anthracis* is proposed to be an N-acetylglucosaminidase (Fig. 3.1) whose role is to further degrade cortex fragments resulting from SCLE hydrolysis (81). SleL is not essential for the completion of germination but does promote the release of small muropeptides to the spore's surrounding environment (81).

This study reports the effects of multiple deletion mutations affecting GSLEs on spore germination efficiency and kinetics of cortex hydrolysis. The data confirm the dominant roles played by CwlJ1 and SleB in initiation of cortex hydrolysis and the major role of SleL in release

of small cortex fragments. A minor role of CwlJ2 in nutrient-triggered germination and the contributions of CwlJ1 and CwlJ2 to Ca^{2+}-dipicolinic acid (DPA) triggered germination were revealed.

MATERIALS AND METHODS

Bacterial strains and growth conditions. *B. anthracis* strains and plasmids used are listed in Table 3.1. *Escherichia coli* strains used to propagate plasmids were grown in LB with 500 μg/ml erythromycin (Fisher) or 100 μg/ml ampicillin (Jersey Lab Supply) and incubated at 37°C. *B. anthracis* strains were grown in brain heart infusion (BHI, Difco) containing 5 μg/ml erythromycin or 10 μg/ml tetracycline (Jersey Lab Supply) and incubated at 22°C prior to allelic exchange or 37°C afterwards.

In-frame deletion mutagenesis of *cwlJ1*, *cwlJ2*, *sleB*, and *sleL* has previously been published (50, 81). Each deletion encoded only 6-9 codons of the original gene. In-frame deletions were integrated into the *B. anthracis* chromosome using markerless gene replacement as previously described (66). The deletion mutations were verified in each new strain by PCR amplification of each locus and sequencing the regions including >250 base pairs both up and downstream.

Spore preparation. *B. anthracis* strains were incubated at 37°C with shaking in Modified G broth (73) for 3 days. Spores were harvested by repeated centrifugation and water washing. Vegetative cells were heat killed at 65°C for 30 minutes. Spores were purified by centrifugation through 50% sodium diatrizoate (Sigma) (103). Purified spores were ~99% free of vegetative cells and were stored in deionized water at 4°C until analysis.

Spores at an optical density at 600nm (OD) = 2 were decoated at 70°C for 30 minutes in 0.1 N NaOH, 0.1 M NaCl, 1% (wt/vol) sodium dodecyl sulfate, and 0.1 M dithiothreitol. After decoating, spores were washed 5 times in sterile deionized water. To evaluate the effects of decoating on viability, decoated and intact spores were serially diluted and plated on BHI.

Spore germination assays. To evaluate colony formation efficiency, intact or decoated spores were resuspended at an OD = 0.2. After heat activation at 70°C for 30 minutes, the suspensions were serially diluted, spotted on BHI with or without 1 μg/ml lysozyme (Sigma), and incubated at 30°C overnight.

Spore germination and outgrowth in liquid BHI was assayed by monitoring OD as previously described except incubation was done at 37°C (50, 81). Ca-DPA treatment to trigger germination was carried out essentially as previously described (106). Spores were suspended at an OD = 1 in water or 50 mM Ca-DPA solution and incubated at 25°C for 60 minutes. Spore suspensions were then heated at 70°C for 20 minutes, serially diluted in water, spotted on BHI plates, and incubated at 37°C overnight to determine heat-resistant titers.

Biochemical analyses of PG hydrolysis and release. After heat activation, spores were induced to germinate in a buffered solution containing 10 mM L-alanine and 1 mM inosine as previously described (81). Spore-associated (pellet) and exudate (supernatant) fractions collected throughout germination were assayed for muramic acid and diaminopimelic acid (Dpm) content as described previously (90). PG was purified and prepared for reverse-phase high-pressure liquid chromatography (RP-HPLC) analysis as previously described (31). Briefly, the germinated spore suspension was separated into pellet and supernatant fractions. Lytic enzymes were inactivated with heat (supernatant) or with heat and detergent (pellet), and PG was purified. The PG material from the pellets and half of each exudate fraction was then digested with the muramidase Mutanolysin (Sigma). All fractions were reduced with $NaBH_4$ prior to HPLC separation.

RESULTS

Effects of GSLEs on nutrient-triggered germination. Wild-type and mutant spores were allowed to germinate and produce colonies on BHI plates overnight. All strains containing either CwlJ1 or SleB produced an equivalent number of colonies per OD unit as the wild-type strain (Table 3.2 and data not shown). However, all strains lacking both CwlJ1 and SleB exhibited a $>10^3$ fold decrease in colony formation. There was no further decrease in colony formation when other GSLEs, CwlJ2 and/or SleL, were also absent. Colony formation efficiency was restored to near wild-type levels in strains lacking both CwlJ1 and SleB when decoated spores were plated on BHI supplemented with 1 μg/ml of lysozyme (Table 3.2). Spores were decoated to facilitate the penetration of lysozyme to the cortex, but this treatment did not affect colony formation, and lysozyme did not affect colony formation by non-decoated spores (data not shown).

Spores lacking GSLEs in various combinations were germinated in liquid BHI and monitored by measuring the change in OD. Germinating spores rapidly lose approximately 50% of their OD in the first few minutes, and the OD then increases as the population continues into vegetative growth. As previously demonstrated (50, 81), spores of the wild-type strain and strains lacking any single GSLE were successful at synchronous germination, and those strains without functional CwlJ1, SleB, or SleL had delays in loss of OD during germination, though these did not always translate to a delay in the initiation of outgrowth (Fig. 3.2A and 3.2B). When both *cwlJ1* and *sleB* were deleted, spores were capable of initiating germination and lost OD for only ten minutes, but at that point germination was arrested and no further changes were observed (Fig. 3.2A and (50)). This was the most dramatic phenotype, and adding any number of additional GSLE-eliminating mutations to the *ΔcwlJ1 ΔsleB* background did not produce

further significant changes ($P > 0.05$, as determined by a Tukey-Kramer HSD analysis) (Fig. 3.2A and data not shown).

Adding a *ΔsleL* mutation to *ΔcwlJ1*, *ΔsleB*, *ΔcwlJ1 ΔcwlJ2*, and *ΔsleB ΔcwlJ2* strains generated spores with increased delays in OD loss during germination that were evidenced by shallower curves (Fig. 3.2A and 3.2B and data not shown). Despite this consistent trend, these differences were not statistically significant ($P > 0.05$, as determined by a Tukey-Kramer HSD analysis) which is likely the result of variability inherent in assay of multiple independent spore preparations. Placing a *ΔcwlJ2* deletion into any other GSLE mutant strains, whether single, double, or triple, did not impact the preexisting germination phenotypes except in the case of *ΔcwlJ1 ΔcwlJ2* spores. This strain exhibited a slowed OD increase compared to *ΔcwlJ1* spores with statistically significant delays from 60 minutes onward ($P \leq 0.01$, as determined by a Tukey-Kramer HSD analysis) (Fig. 3.2B).

Effects of GSLEs on Ca-DPA-triggered germination. It was previously demonstrated that *B. subtilis* and *B. megaterium* spores that lack CwlJ are extremely unresponsive to the non-nutrient germinant Ca-DPA (106, 130). Spores that germinate in response to Ca-DPA become heat sensitive. For example, after treatment with Ca-DPA, our control wild-type *B. subtilis* spores lost a significant level of heat resistance indicating that 99% of the spores had germinated while *B. subtilis* spores carrying a *cwlJ* mutation were not affected (Fig. 3.3).

Wild-type *B. anthracis* spores incubated with exogenous Ca-DPA exhibited a 99% decrease in heat-resistant colony forming units (Fig. 3.3). Surprisingly, *ΔcwlJ1* spores were also significantly heat sensitive after Ca-DPA exposure, suffering a 79% lowered titer. While *ΔcwlJ2* spores performed similarly to those of the wild-type strain, spores lacking both *cwlJ1* and *cwlJ2* had no significant change in heat resistance after Ca-DPA treatment (Fig. 3.3). Phase-contrast

microscopy of spores during their Ca-DPA incubation was also carried out since germinating spores transition from phase bright to phase dark. Consistent with the heat resistance assay, 98% of wild-type and *ΔcwlJ2* spores became phase dark after 60 minutes, 60% of *ΔcwlJ1* spores transitioned, but only 6% of spores carrying both *cwlJ1* and *cwlJ2* deletions became phase dark (data not shown). Together these observations show that, in *B. anthracis* spores, both CwlJ1 and CwlJ2 independently contribute to a Ca-DPA germination response, and that CwlJ1 is responsible for the majority of the activity. Deletions of either *sleB* or *sleL* had no impact on the spore response to Ca-DPA (data not shown).

Release of cortex fragments from germinating spores. During germination, spores release cortex fragments that can be quantified based upon muramic acid and Dpm content. Data is presented only for muramic acid release, but in all cases Dpm release was analyzed and paralleled the release of muramic acid (data not shown). Wild-type *B. anthracis* spores released nearly 90% of their muramic acid within 15 minutes of germination initiation (Fig. 3.4). The *ΔcwlJ1* spores had an early delay in muramic acid release, but these spores still released nearly as much muramic acid as those of the wild-type strain after 15 minutes (Fig. 3.4 and (50)). While the *ΔcwlJ2* mutant was indistinguishable from the wild-type strain (data not shown and (50)), *ΔcwlJ1 ΔcwlJ2* spores exhibited an additive decrease in muramic acid release which was significant during the first 15 minutes of germination in comparison to both the wild-type and *ΔcwlJ1* strains (Fig. 3.4). However, by 30 minutes the double mutant was still able to release a normal amount of cortex fragments.

The Δ*sleL* mutation caused dramatic effects on muramic acid release (Fig. 3.4 and (81)). These spores released ≤40% of their muramic acid within 15 minutes, and even after 90 minutes expelled a maximum of only 65% of this cortex component. The Δ*sleL* Δ*cwlJ1* double mutant

spores displayed kinetics similar to the Δ*sleL* single mutant over the course of the assay. However, Δ*sleB* Δ*sleL* spores were more severely impaired at discharging cortical fragments. While Δ*sleB* spores have only a minor delay in cortex release (50), Δ*sleB* Δ*sleL* double mutant spores released considerably less muramic acid throughout the assay than did those of the single mutants (Fig. 3.4 and (50)). In fact, the Δ*sleB* Δ*sleL* spores released muramic acid with kinetic similar to the quadruple mutant lacking all four GSLEs. These two strains released a maximum ~30% of their muramic acid, however, the Δ*sleB* Δ*sleL* spore accomplished this within 15 minutes whereas the quadruple mutant required 60 minutes (Fig. 3.4).

GSLE effects on cortex hydrolysis. Cortex structural changes during germination of spores lacking multiple GSLEs were analyzed using a RP-HPLC technique that was previously employed to identify the cortex lytic activities of SleB and SleL in *B. anthracis* spores (50, 81). In these earlier studies, spores lacking CwlJ2 were indistinguishable from those of the wild-type. Spores of strains carrying mutations in *cwlJ1, sleB,* or *sleL* released lower amounts of muropeptides, and in the cases of *sleB* and *sleL* specific muropeptides indicative of those gene products' activities were lacking. It was shown that Δ*cwlJ1* Δ*sleB* spores released essentially no measurable muropeptides, consistent with their germination block. For the present study, spores with a combination of *cwlJ1* and *sleB* deletions were not investigated for muropeptide release due to this severe phenotype.

The muropeptides released from *ΔcwlJ1 ΔsleL* spores were anticipated to be the consequence of SleB's lytic transglycosylase activity. After germinating for two hours this strain released more than 60% of cortex PG into the exudate and, as expected, generated the lytic transglycosylase products aG7a and aG7b (Fig. 3.1 and 3.5B, Table 3.3, and (50)). Further digestion of the exudate with the muramidase Mutanolysin increased the relative amounts of

aG7a and aG7b by 44% and 114% respectively, and generated a large amount of muropeptide N (Fig. 3.1 and 3.5E). Muropeptide N is a tetrasaccharide that is the predominant product produced by muramidase digestion of intact cortex strands (Table 3.3 and (31)). Based on the sizes of peaks aG7a, aG7b, and N released from *ΔcwlJ1 ΔsleL* spores, we calculate that 42% of SleB products are anhydrotetrasaccharides (aG7a and aG7b) and that the remaining 58% are larger fragments. Also after muramidase digestion, the increase of anhydrotetrasaccharides compared to muropeptide N is in a ratio of nearly 1:1, which suggests the average large muropeptide after SleB digestion is eight sugars in length (Fig 3.1). Muramidase digestion of the PG retained in the germinated *ΔcwlJ1 ΔsleL* spore pellet released a small amount of aG7a and aG7b, demonstrating that a few SleB products remained too large to be released from the spore (data not shown).

The chromatograms of spore germination exudates from *ΔsleB ΔsleL* (Fig. 3.5C) and *ΔcwlJ2 ΔsleB ΔsleL* strains (data not shown) were indistinguishable; any cortex fragments released from these strains are expected to be products of CwlJ1 activity. These spores released no detectable small muropeptides (Fig. 3.5C), however, treatment of the exudates with muramidase produced a small quantity of muropeptide N (Fig. 3.5F). This suggests that depolymerization of cortex catalyzed by CwlJ1 alone produced large muropeptides that are not resolved with this method. In fact, assays of released cortex fragments (Fig. 3.4) and of cortex released from the germinated spore pellet by muramidase (data not shown) indicate that ≥75% of CwlJ1-generated cortex fragments are too large to be released from the spore.

DISCUSSION

In the simplest measure of spore germination kinetics, tracking of OD loss, slight delays in germination are observed in single mutants lacking *cwlJ1*, *sleB*, or *sleL*, and combinations of these mutations result in additive effects. In the cases of *sleB* and *sleL* mutants, germination is indistinguishable from that of the wild-type strain during the first 10 minutes, and delays are obvious only after that time. A *cwlJ1* mutation affects OD loss even earlier, though it has the least effect on the overall kinetics of cortex hydrolysis and release, suggesting that this mutation has an additional effect on some other aspect of the germination process. A combination of *cwlJ1* and *sleB* mutations renders spores essentially incapable of completing germination (41, 50); cortex hydrolysis is completely blocked and OD decrease ceases after 10 minutes. This indicates that OD decrease during the first 10 minutes of germination is primarily associated with release of spore solutes and uptake of water, with accompanying loss of spore refractility and decrease in spore core density. Studies in other species demonstrated that *cwlJ* mutations slowed the process of Ca-DPA release (64, 112, 130), and we suggest that the early delay in OD loss in a *cwlJ1* mutant is due to a slowed process of spore solute exchange. How might a cortex lytic enzyme affect solute movement into and out of the spore? We propose that CwlJ1 (and CwlJ2) acts initially on the outer layers of the cortex, due to their apparent location at or near the cortex/coat interface (9, 18, 50, 78). Outer cortex layers are more highly cross-linked than the inner layers (90) and thus may produce a slightly greater diffusion barrier and/or might exert a greater influence on the ability of the spore core to expand and take up water in the first moments of germination. Such water uptake may be critical for solubilization and movement of Ca-DPA, for dissociation of SASP proteins from the spore DNA, and for activation of a germination-specific protease in the core (131, 134).

Giebel et al. found that spores of a *cwlJ2* mutant lost OD slightly more slowly than those of the wild-type strain during germination, but with an overall effect less dramatic than those of *cwlJ1* and *sleB* mutants (41). While our analyses with single mutants have never demonstrated a significant phenotypic change due to a single *cwlJ2* mutation (50), we and Giebel *et al*. (41) did observe that a *cwlJ2* mutation had additive effects to those of a *cwlJ1* mutation. In particular, we find that *cwlJ1 cwlJ2* spores exhibit a delay in outgrowth that is significantly greater than might be expected based on the relative delays in OD loss and cortex fragment release among all the mutant strains analyzed. We also found that *cwlJ2* plays a role in Ca-DPA-stimulated germination. Studies in other species have demonstrated roles of CwlJ proteins in response to this non-nutrient germinant, and release of Ca-DPA from the germinating spore is apparently the mechanism by which this lytic enzyme is normally activated (106). In *B. anthracis*, Ca-DPA-triggered germination utilizes CwlJ1 and CwlJ2 working independently and with partial redundancy, since loss of both enzymes is required to completely eliminate the response. Low expression of *cwlJ2* (50) may produce spores with an insufficient amount of CwlJ2 to respond to Ca-DPA in the absence of CwlJ1. We assert that CwlJ1 and CwlJ2 carry out identical functions given: 1) the high level of sequence identity (58%) between the proteins, 2) that deletion of the former is needed in order to demonstrate activity for the latter, and 3) the requirement of both enzymes for maximum response to Ca-DPA.

Colony formation is unaffected in *B. anthracis* spores that contain at least SleB or CwlJ1 (41, 50), supporting the idea that either one of these SCLEs is sufficient to degrade the cortex to a great enough degree that metabolic activity resumes and the cell can grow out of its integuments. When both SleB and CwlJ1 are absent from spores, in strains with or without other GSLEs present, we observe a 1000-fold decrease in colony-forming efficiency (Table 3.2 and

(50)). In each case, colony forming ability can be rescued by the addition of lysozyme, indicating that the block to germination is due to incomplete cortex hydrolysis. Contrary to our results, a recent report indicated that the additional loss of CwlJ2 from a *ΔcwlJ1ΔsleB* double mutant resulted in a much more profound loss of colony-forming efficiency (41). To explain this difference, we must ask why 0.1% percent of spores that lack all known GSLEs are able to produce colonies in our studies, but not in those of Giebel *et al*. One potential explanation is that some vegetative cell-derived lytic enzyme copurified with our spores and might be hydrolyzing the cortex PG enough to allow a small percentage of spores to complete germination. A contribution of vegetative lytic activities to germination of defective *C. perfringens* spores has been postulated (110). However, our decoating procedure, which should inactivate spore surface-associated enzymes, did not significantly reduce the colony forming ability of *ΔcwlJ1 ΔsleB* spores (data not shown). An alternative explanation is that small amounts of exogenous lytic enzymes in our growth media might be hydrolyzing the cortex PG, despite the fact that we have used BHI medium from the same manufacturer as Giebel *et al*. (41). The potential for exogenous lytic enzymes to allow germination of GSLE-deficient spores was also cited as an explanation for the virulence of these spores at a level greater than would be expected from their colony forming efficiency on laboratory medium (41).

Cortex fragment release from germinating *B. anthracis* spores follows three different kinetic paths depending on which proteins are actively digesting the cortex PG. Maximum total release occurs when both SleB and SleL are functional, and CwlJ1 and CwlJ2 only affect the initial rate of release. SleB digests the PG into fragments of varying sizes, some of which are released, but the majority of which are initially retained within the spore. SleL then acts on these fragments, thus increasing the proportion that is small enough for rapid release. In the absence

of SleL, muropeptides found in the exudates are significantly reduced in quantity. Given enough time, SleB alone can digest the PG to fragments small enough, primarily tetra- and octa-saccharides, for release of >50% of the cortex from the spore. In the absence of both SleB and SleL, cortex degradation can still be accomplished by CwlJ1 and CwlJ2 to allow outgrowth. However, the cortex fragments are apparently so large that they are not released, and muramic acid release by *sleB sleL* spores is indistinguishable from that of spores lacking all four GSLEs.

The fact that the products of CwlJ1 activity are so large has prevented determination of the site of PG cleavage by this enzyme. Muramidase digestion of germinated *cwlJ2 sleB sleL* spore PG, which presumably has been cleaved only by CwlJ1, has yielded only muramidase products (data not shown). This suggests that CwlJ1 is either a muramidase or that its cleavage sites are so few as to be undetectable by our current methods. The possibility of CwlJ1 muramidase activity is consistent with the significant sequence homology between CwlJ and SleB lytic transglycosylase proteins. Lytic transglycosylases and muramidases cleave the same bond in PG, but differ in the chemistry of their products, the former producing anhydro-N-acetylmuramic acid and the latter producing N-acetylmuramic acid. Similar protein folds can result in these two enzymatic activities (139). Ongoing efforts to produce significant CwlJ1 activity *in vitro* may allow cleavage of a purified substrate to an extent sufficient to directly identify the enzymatic products.

While the roles played by the *B. anthracis* GSLEs and their requirements for germination both in and out of the host (41, 50, 81) are becoming clear, many questions remain concerning the mechanisms by which they are held inactive in the dormant spore and activated during germination. Future studies of the localization, processing, and interaction partners of these enzymes may answer these questions. A strategy for efficient external activation of GSLEs, and

therefore initiation of germination, will allow the development of simpler methods for decontamination of sites of spore release.

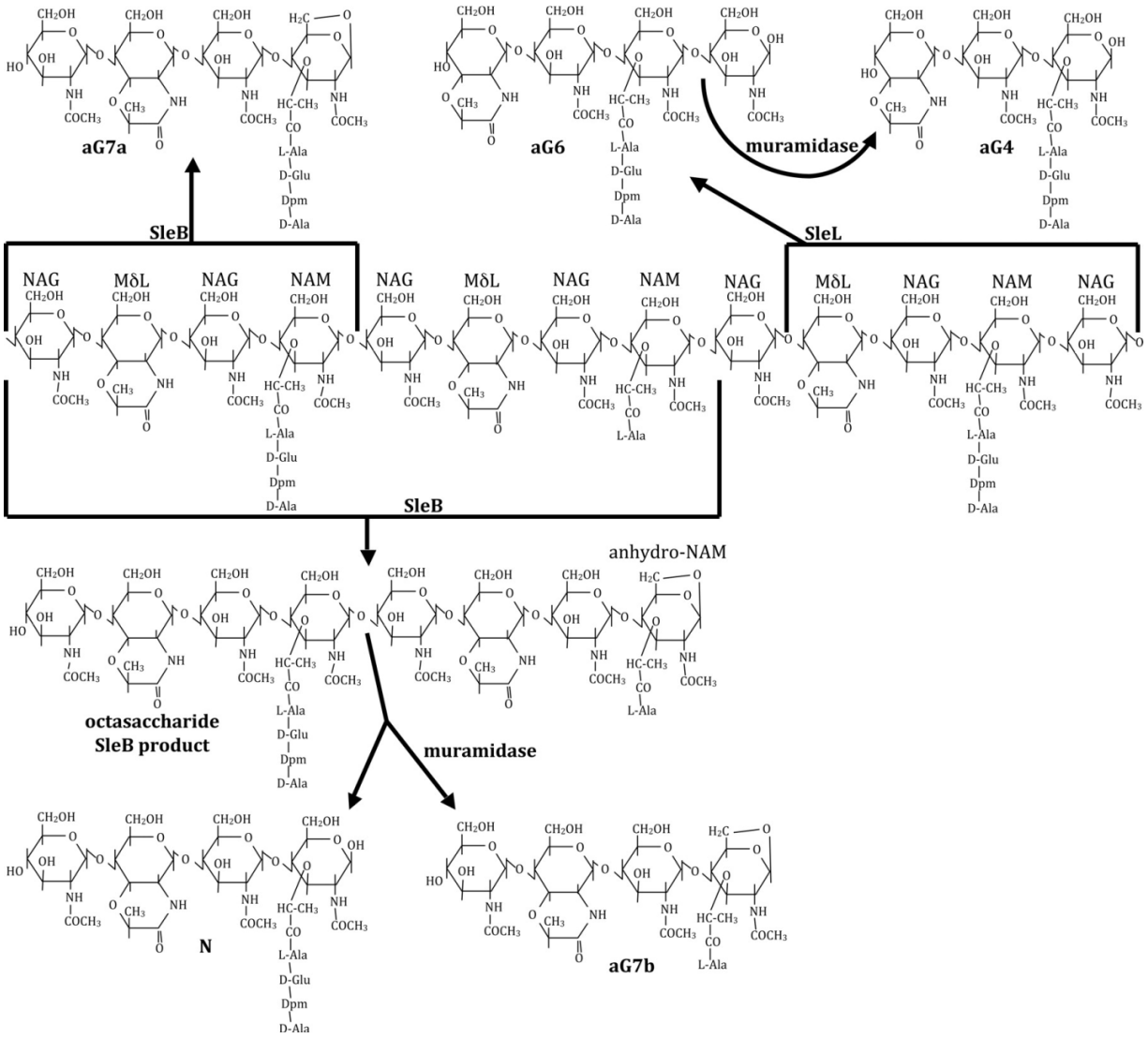

Figure 3.1. Spore PG structure and hydrolysis. The central structure shows a representative spore PG strand with alternating NAG and NAM or muramic-δ-lactam (MδL) residues, and with tetrapeptide or L-ala side chains on the NAM residues. Forked arrows originate at sites of hydrolysis by the indicated enzymes and point to muropeptide products. The indicated "aG" muropeptide names are as previously published (31, 50). SleB lytic transglycosylase activity produces muropeptide terminating in anhydro-NAM. Cleavage at adjacent NAM residues produces the tetrasaccharides aG7a or aG7b, while cleavage further apart can produce octasaccharides or larger fragments. These can be further cleaved by muramidase treatment, resulting in the production of tetrasaccharide N, which terminates in NAM. The N-acetylglucosaminidase activity of SleL produces tetrasaccharides terminating in NAG, which can be further cleaved by muramidase to trisaccharides terminating in NAM.

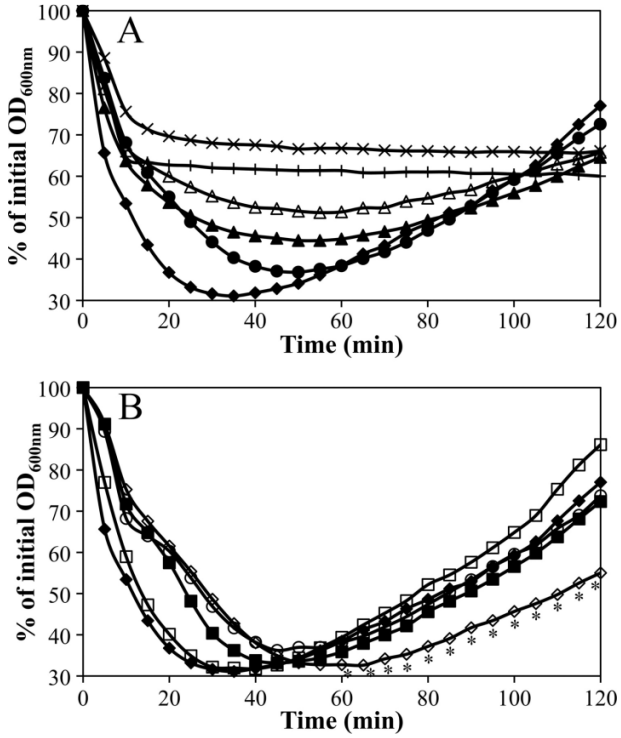

Figure 3.2. Germination and outgrowth of spores in BHI. Spores were heat activated in water and germinated in BHI at 37°C, and OD was monitored. Data shown are averages for three independent spore preparations; error bars are omitted for clarity. A) Germination of wild-type (♦), *ΔsleB* (▲), *ΔsleL* (●), *ΔsleB ΔsleL* (Δ), *ΔcwlJ1 ΔsleB* (+), and *ΔcwlJ1 ΔcwlJ2 ΔsleB ΔsleL* (×) spores. B) Germination of wild-type (♦), *ΔcwlJ1* (■), *ΔcwlJ2* (□), *ΔcwlJ1 ΔcwlJ2* (◇), and *ΔcwlJ1 ΔsleL* (○) spores. Asterisks indicate those time points when *ΔcwlJ1 ΔcwlJ2* spores were significantly different ($P \leq 0.01$) from *ΔcwlJ1* spores.

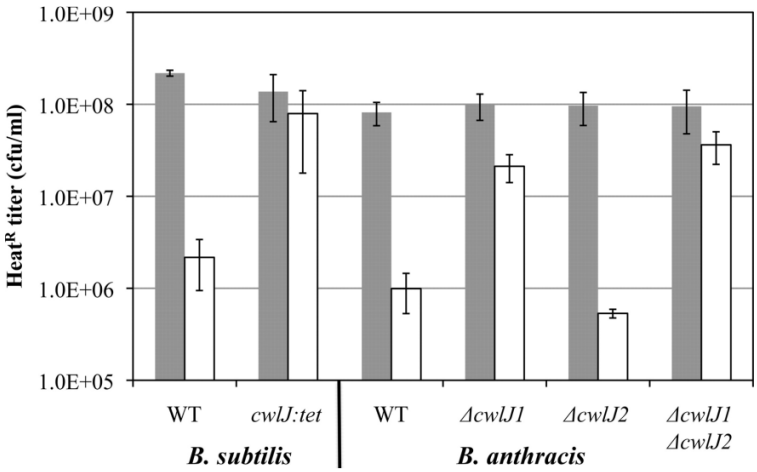

Figure 3.3. Germination of spores in response to Ca-DPA. Spores from *B. subtilis* strains PS832 (wild-type) and FB111 (*ΔcwlJ::tet*) (106), and *B. anthracis* strains DPBa2 (wild-type), DPBa61 (*ΔcwlJ1*), DPBa60 (*ΔcwlJ2*), and DPBa78 (*ΔcwlJ1 ΔcwlJ2*) were incubated in water (gray bars) or 50 mM Ca-DPA pH 8.0 (white bars) for 60 minutes at 25°C before being heated at 70°C for 20 min, serially diluted, and plated on BHI. Values are averages of at least three independent spore preparations. Error bars represent one standard deviation of the mean.

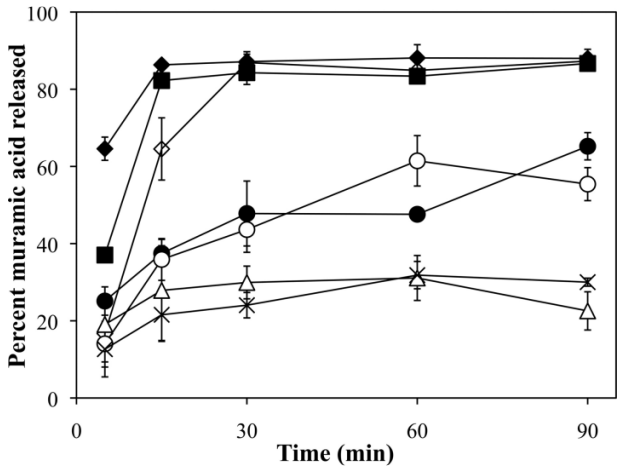

Figure 3.4. Release of cortex fragments from germinating spores. Dormant wild-type (♦), *ΔcwlJ1* (■), *ΔsleL* (●), *ΔcwlJ1 ΔsleL* (○), *ΔsleB ΔsleL* (Δ), *ΔcwlJ1 ΔcwlJ2* (◇), and *ΔcwlJ1 ΔcwlJ2 ΔsleB ΔsleL* (×) spores in buffer were sampled for assay of the release of muramic acid following exposure to the germinants L-alanine and inosine. Error bars represent one standard deviation of the mean for three independent spore preparations. All points have error bars, but in some cases, these are too small to be visible.

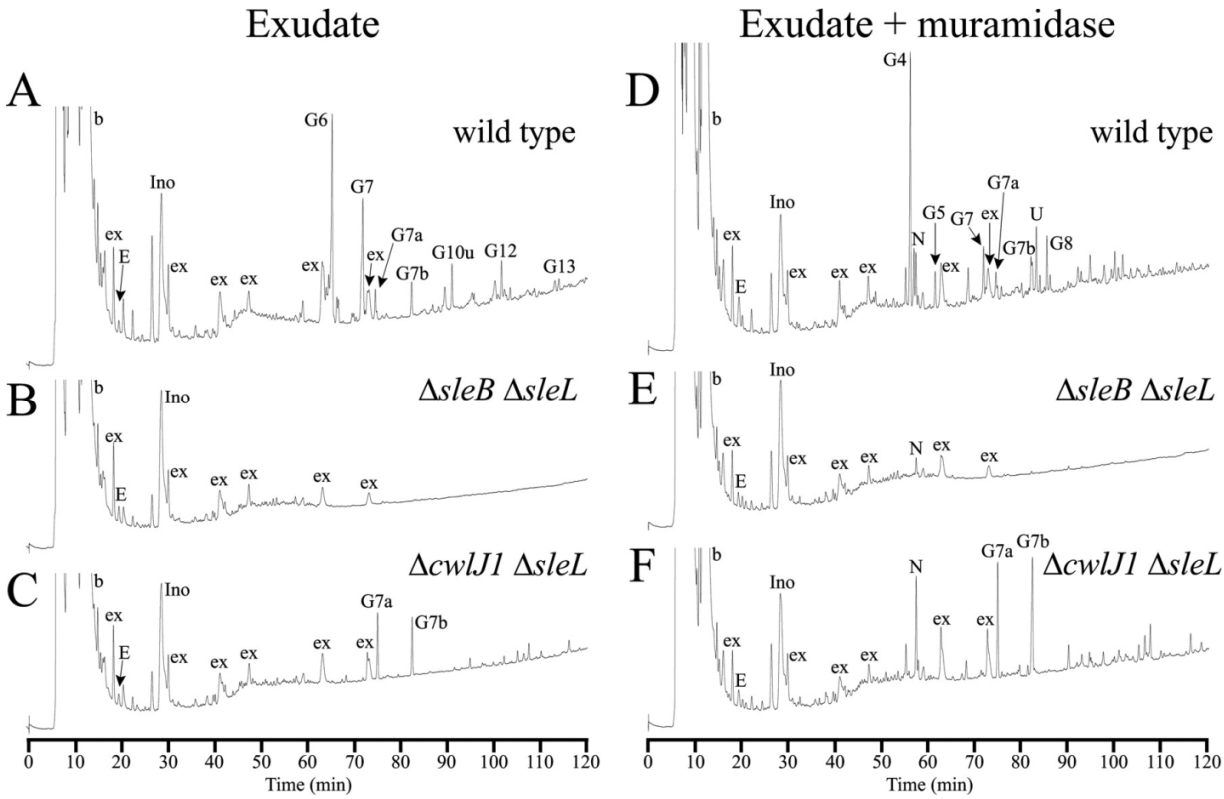

Figure 3.5. RP-HPLC separation of muropeptides released from germinating spores. PG was prepared from germinating spore suspensions as described in Materials and Methods. Samples were collected after spores were allowed to germinate for 120 minutes. 50% of each exudate (D-F) sample was digested with muramidase, reduced, and separated as previously described (90). The other 50% of each exudate (A-C) was reduced and separated without muramidase digestion. Peaks are numbered as in (50) and Table 3.3, but the initial "a" in the germination-specific-peak names were omitted for space considerations. Early-eluting peaks labeled "b" are buffer components present in blank samples. Peaks labeled "ex" are spore exudate components that are not derived from PG. Peaks labeled "Ino" are from the inosine used as germinant.

Table 3.1. *B. anthracis* strains and plasmids.

Strain or plasmid	Relevant genotype[a]	Construction[b]	Source or reference
Strains			
Sterne 34F2	pXO1^{+}, pXO2^{-}		P. Hanna
DPBa35	*ΔsleL*	pDPV351→34F2	(81)
DPBa38	*ΔsleB*	pDPV383→34F2	(50)
DPBa55	*ΔsleB ΔsleL*	pDPV383→DPBa35	This study
DPBa60	*ΔcwlJ2*	pDPV344→34F2	This study
DPBa61	*ΔcwlJ1*	pDPV347→34F2	(50)
DPBa66	*ΔcwlJ2 ΔsleL*	pDPV344→DPBa35	This study
DPBa69	*ΔcwlJ1 ΔsleL*	pDPV347→DPBa35	This study
DPBa72	*ΔcwlJ1 ΔsleB ΔsleL*	pDPV347→DPBa55	This study
DPBa73	*ΔcwlJ2 ΔsleB*	pDPV383→DPBa60	This study
DPBa74	*ΔcwlJ1 ΔsleB*	pDPV383→DPBa61	This study
DPBa78	*ΔcwlJ1 ΔcwlJ2*	pDPV347→DPBa60	This study
DPBa82	*ΔcwlJ2 ΔsleB ΔsleL*	pDPV344→DPBa55	This study
DPBa83	*ΔcwlJ1 ΔcwlJ2 ΔsleL*	pDPV344→DPBa69	This study
DPBa84	*ΔcwlJ1 ΔcwlJ2 ΔsleB ΔsleL*	pDPV344→DPBa72	This study
DPBa85	*ΔcwlJ1 ΔcwlJ2 ΔsleB*	pDPV347→DPBa73	This study
Plasmids			
pBKJ223	Tet^{R}, P$_{amy}$-*I-SceI*		(66)
pBKJ236	Er^{R}, ori^{ts}		(66)
pDPV344	*ΔcwlJ2*	pBKJ236	This study
pDPV347	*ΔcwlJ1*	pBKJ236	(50)
pDPV351	*ΔsleL*	pBKJ236	(81)
pDPV383	*ΔsleB*	pBKJ236	(50)

[a] Abbreviations: Tet^{R}, tetracycline resistance; Er^{R}, erythromycin resistance; ori^{ts}, temperature-sensitive origin of replication.

[b] Strains were constructed by conjugation followed by the published series of steps required for recombination of the deletion mutation into the chromosome. The designation preceding the arrow is the plasmid and the designation following the arrow is the recipient strain. Single plasmid designations indicate the vector in which the deletion construct was created.

Table 3.2. Spore plating efficiency and lysozyme recovery.

		CFU/ml/OD on[a]	
Strain	Genotype	BHI	BHI+Lyso[b]
34F2	Wild-type	$1.5x10^8$	$1.1x10^8$
DPBa72	*ΔcwlJ1, ΔsleB, ΔsleL*	$3.7x10^4$*	$1.2x10^8$
DPBa74	*ΔcwlJ1, ΔsleB*	$4.3x10^4$*	$1.5x10^8$
DPBa82	*ΔcwlJ2, ΔsleB, ΔsleL*	$9.9x10^7$	ND
DPBa83	*ΔcwlJ1, ΔcwlJ2, ΔsleL*	$9.3x10^7$	ND
DPBa84	*ΔcwlJ1, ΔcwlJ2, ΔsleB, ΔsleL*	$2.9x10^4$*	$7.9x10^7$
DPBa85	*ΔcwlJ1, ΔcwlJ2, ΔsleB*	$1.3x10^5$*	$6.1x10^7$

[a] Values are averages for three independent spore preparations.

[b] Spores were decoated and plated on BHI containing 1 μg/ml of lysozyme. ND, not determined.

* Indicates a value that is significantly different from that for wild type spores with a $p \leq 0.01$ as determined by an unpaired two-tailed Student's t-test.

Table 3.3. Muropeptide peak identification.

Name[a]	Structure[b]	Enzymatic origin
N	TS-TP	muramidase
U	HS-TP-Ac	muramidase
aG4	TriS-TP	N-acetylglucosaminidase + muramidase
aG5	TriS-Ala	N-acetylglucosaminidase + muramidase
aG6	TS-TP NAGr	N-acetylglucosaminidase
aG7	TS-Ala NAGr	N-acetylglucosaminidase
aG7a	TS-TP anhydro	Lytic transglycosylase
aG7b	TS-Ala anhydro	Lytic transglycosylase
aG8	PS-TP-Ac	N-acetylglucosaminidase + muramidase
aG10u	HS-TP-Ac NAGr	N-acetylglucosaminidase
aG12	HS-Ala-Ac NAGr	N-acetylglucosaminidase
aG13	HS-TP NAGr	Cortex, N-acetylglucosaminidase

[a] Muropeptide names are as previously published (31, 50). Muropeptide names preceded by "a" indicate those generated by *B. anthracis* in order to differentiate them from those generated by other species.

[b] Abbreviations: TS, tetrasaccharide (NAG-MδL-NAG-NAM); HS, hexasaccharide (NAG-MδL-NAG-MδL-NAG-NAM); TriS, trisaccharide (MδL-NAG-NAM); PS, pentasaccharide (MδL-NAG-MδL-NAG-NAM); TP, tetrapeptide (Ala-Glu-Dpm-Ala); -Ac, deacetylated glucosamine; NAGr, NAG at the reducing end. "Anhydro" indicates that the NAM at the reducing end is in the anhydro form.

ACKNOWLEDGMENTS

This research was supported by Public Health Service grant AI060726 from the National Institute of Allergy and Infectious Disease. We thank P. Setlow for providing strains. We thank Mark Seiss and Chongrui Yu at the VT Laboratory for Interdisciplinary Statistical Analysis for their advice.

CHAPTER 4

In Vitro Studies of Peptidoglycan Binding and Hydrolysis by the *Bacillus anthracis* Germination-Specific Lytic Enzyme SleB

Jared D. Heffron, Nora Sherry, and David L. Popham

Manuscript in Preparation

AUTHOR CONTRIBUTIONS

Jared Heffron performed the research, experimentation, data analysis, and writing of the material presented herein. Nora Sherry prepared spore sacculi and cortical fragment substrates. David Popham was the principal investigator.

ABSTRACT

The *Bacillus anthracis* endospore loses resistance properties during germination when its cortex peptidoglycan is degraded by germination-specific lytic enzymes (GSLEs). Although this event normally employs several GSLEs for complete cortex removal, the SleB protein alone can facilitate enough cortex hydrolysis to produce vulnerable spores. In order to better understand its enzymatic function, SleB was overexpressed, purified, and tested *in vitro* for depolymerization of cortex by measuring optical density loss and the solubilization of substrate. Its ability to bind peptidoglycan was also investigated. SleB functions independently as a lytic transglycosylase on both intact and fragmented cortex. Most of the muropeptide products that SleB generates are large, and are potential substrates for other GSLEs present in the spore. Study of a truncated protein revealed that SleB has two domains. The N-terminal domain is required for stable peptidoglycan binding, while the C-terminal domain is the region of peptidoglycan hydrolytic activity. The C-terminal domain also exhibits dependence for cortex with muramic-δ-lactam in order to carry-out hydrolysis. As the conditions and limitations for SleB activity are further elucidated they will enable the development of treatments that stimulate premature germination of *B. anthracis* spores, greatly simplifying decontamination measures.

INTRODUCTION

The bacterial endospore contains several integument layers that contribute to make a structure that is dehydrated, dormant, and highly resistant to environmental insults (135). One of these layers is a modified stratum of peptidoglycan (PG) termed the cortex, which comprises >80% of the total spore PG and is responsible for maintaining spore dehydration, dormancy, and wet heat resistance (90, 135). Like PG from vegetative cells, the cortex consists of repeating disaccharide units of β-1,4-linked *N*-acetylglucosamine (NAG) and *N*-acetylmuramic acid (NAM). The NAM residues have peptide side chains which become covalently bonded with peptide chains from neighboring strands, resulting in a cross-linked network surrounding the entire spore (144) . Cortex differs from vegetative PG by a modification where as much as 50% of the NAM is converted to muramic-δ-lactam, which contributes to a ~75% reduction in cross-linking (90, 121, 144). In order for the spore to complete germination, this thick, constraining layer of PG must be degraded by germination-specific lytic enzymes (GSLEs), which recognize the cortex-specific muramic-δ-lactam residues (87, 95, 118).

A typical germination response begins when spores detect nutrient germinant compounds in the environment through the use of receptors located on the inner spore membrane (35, 108). Three major events then transpire. The first is that the spore core starts to rehydrate as water moves inward (106). The second event, likely coupled with the first, is transport of ions and dipicolinic acid (DPA) out of the core (23, 85, 96, 106). The third major step is the depolymerization of cortex by GSLEs and the release of muropeptides into the surrounding environment (96). At this point the spore core is free to fully rehydrate, resume metabolism, and proceed toward a vegetative cell cycle; consequently, the spore has now lost its resistance properties (134-135). Exactly how GSLEs are held inactive in the dormant spore and later

activated during germination is not fully understood, but it is clear that cortex hydrolysis by a GSLE is capable of causing germination without nutrients or the prior steps of water movement and ion release (95, 106, 124).

The endospore of *Bacillus anthracis* is known to be the infectious agent of all forms of the disease anthrax (93), and as a result, the destruction of spores is the most direct means to prevent infection. However, since dormant spores are so highly resistant, current methods of decontamination require the use of highly toxic and/or destructive compounds that have undesirable consequences (10, 71, 138). A recent U.S. Army sponsored workshop proposed that a potential strategy toward eliminating the threat of spores would be to trigger germination at a high efficiency and then use typical antibacterial procedures to inactivate the resulting vulnerable cells (61). GSLEs may be a suitable target for manipulation in order to instigate premature spore germination.

B. anthracis has four GSLEs that participate in cortex degradation during spore germination, SleB, CwlJ1, CwlJ2, and SleL (40, 49). However, none of these proteins have been investigated *in vitro* to conclusively define their roles and limitations during germination. SleB is a prime candidate for investigation because genetic analyses have shown it facilitates complete spore germination independently of the other known GSLEs (40, 51). This study conclusively demonstrates that purified recombinant SleB is a GSLE with lytic transglycosylase activity. The roles of its predicted domains in protein-substrate interactions and in cortex lysis are also reported.

MATERIALS AND METHODS

Protein expression and purification. The *sleB* ORF lacking the first 32 codons was amplified from *B. anthracis* Sterne 34F2 genomic DNA using a forward primer with a 5' end complementary to the TEV protease cleavage site region of pDEST-HisMBP (5'-GTGGAGAAC CTGTACTTCCAGGGTTTTTCTAATCAAGTCATTCAAAGGG-3') and a reverse primer with a 5' end complementary to the *att*R2.1 region of pDEST-HisMBP (5'-CCACTTTGTACAAGA AAGTTGCATTGCTCTATTTACAGAAAATATGTTTC-3'). The *sleB* ORF lacking the first 124 codons was similarly amplified with a different forward primer (5'-GTGGAGAACCTGTA CTTCCAGGGTTCTCAAAATAAAGGGACAAATGTTC-3'). Each PCR amplicon was inserted into pDEST-HisMBP (F. Schubot) using a restriction-free (RF) cloning method previously described (141) in order to construct the His_6-MBP-SleB (pDPV385) and His_6-MBP-$SleB_{125-253}$ (pDPV386) fusion vectors for protein overexpression.

The fusion proteins were overproduced in *Escherichia coli* BL21 (λDE3 $pLys^S$ Cm^R) (Novagen) grown in LB with 30 μg/mL chloramphenicol (Fisher) and 50 μg/mL ampicillin (Jersey Lab Supply). These cultures were grown by shaking (250 rpm) to saturation overnight at 37°C and then diluted 100-fold into 2 L of fresh medium. When the cells reached an optical density at 600 nm (OD_{600}) ~1.0, the temperature was reduced to 10°C and isopropyl-β-D-thiogalactopyranoside was added to a final concentration of 1 mM. Fifteen hours later, the cells were recovered by centrifugation at 10,000 × g for 10 min at 4°C and stored at -80°C.

E. coli cell paste was suspended in ice-cold 50 mM NaCl, 50 mM Tris-HCl, 5% glycerol, and 30 mM imidazole (pH 7.5) (buffer A). The cells were lysed with a French Press (Thermo Electron Corp.) at 1000 psi and centrifuged at 10,000 × g for 10 min at 4°C. The supernatant was further centrifuged at 40,000 × g for 1 hour at 4°C, the resulting supernatant was loaded onto

a 5 mL Ni Sepharose™ HisTrap™ HP affinity column (GE Healthcare) equilibrated with buffer A. The column was washed with twenty column volumes of buffer A and then eluted with a linear gradient from 30 to 500 mM imidazole in buffer A. Fractions containing either recombinant His_6-MBP-SleB or His_6-MBP-$SleB_{125-253}$ were pooled and dialyzed in buffer A. The sample was then digested overnight with 1 mg of His_6-tagged TEV (S219V) protease (68) per 100 mg of fusion protein at 15°C. The resulting soluble tag-free protein, either SleB or $SleB_{125-253}$, was next applied to a SP Sepharose™ HiTrap™ SP XL column (GE Healthcare) equilibrated with buffer A containing no imidazole (buffer B). The sample was eluted with a linear gradient from 50 to 500 mM NaCl in buffer B. The peak fractions containing either SleB or $SleB_{125-253}$ were pooled and dialyzed in buffer B. Aliquots were frozen and stored at -80°C.

Preparation of peptidoglycan substrates. Vegetative cell wall PG from *B. subtilis* PS832 (wild type) was prepared as previously described (4). Briefly, insoluble cell wall was recovered from cell cultures by boiling in sodium dodecyl sulfate (SDS) and then extensively washed. Covalently attached proteins were removed by protease treatment and the vegetative cell wall was again washed before storage at a neutral pH.

Bacillus subtilis strain 168 derivatives PS832 and VB19 (*cwlD::Sp*) (118) were grown in 2xSG sporulation medium at 37°C without or with 100 μg/mL spectinomycin (Sigma) respectively. Sporulation, spore harvesting, and purification was performed as previously described (118). Spore sacculi were prepared as previously described (32). Briefly, spores were first permeabilized by suspending at an OD_{600} of 30 in 1 mL of 50 mM Tris-HCl (pH 7.5), 1% SDS, 50 mM dithiothreitol (DTT), boiled for 20 min, and then stored at 4°C after warm water washes had removed all detectable SDS. Nucleic acids were removed by incubation in 1 mL 100 mM Tris-HCl (pH 7.5), 20 mM $MgSO_4$, 10 μg DNase I (Sigma), and 50 μg RNase A (Sigma) at

37°C for two hours. Residual protein was degraded overnight with 100 μg trypsin (Worthington TRTPCK) in 10 mM $CaCl_2$ at 37°C. Enzymatic digestion was ceased by boiling in 1% SDS and the resulting spore sacculi were stored at 4°C after warm water washes had removed all detectable SDS (48).

Cortex fragments were prepared by breaking spore sacculi suspended at OD_{600} = 10 in 0.5 mL 50 mM Tris-HCl (pH 8.0), with 0.1 mm glass beads in a Wig-L-Bug® amalgamator (Dentsply) at 3800 rpm using ten 30 sec. pulses. Glass beads were allowed to settle and spore fragments were recovered from the supernatant and in washes of the glass. Hydrophobic coat layer fragments were removed from the PG fragments by $CHCl_3$ extraction. Extracted PG fragments were washed three times with water before storage at 4°C.

Enzymatic activity assays. Hydrolysis of spore sacculi and cortex fragments by 10 nM SleB or $SleB_{125-253}$ was assayed by monitoring OD_{600} as previously described except 1 mM DTT and 0.1% Triton X-100 were used in place of sodium thioglycollate and $C_{12}E_9$ (86). A Tukey-Kramer honestly significant difference (HSD) analysis was used to compare OD_{600} loss curves and rates of maximum hydrolysis of all tested reactions.

The PG from SleB and $SleB_{125-253}$ hydrolysis reactions was separated into pellet and supernatant fractions and assayed for muramic acid content as described previously (90). The muropeptide products of SleB and $SleB_{125-253}$ hydrolysis were prepared for reverse-phase high-pressure liquid chromatography (RP-HPLC) analysis as previously described (32). Briefly, the hydrolyzed substrates were separated into pellet and supernatant fractions. Lytic enzymes were inactivated with heat (supernatant) or with heat and detergent (pellet), and PG was purified. The PG material from the pellets and half of each supernatant fraction was then digested with the

muramidase Mutanolysin (Sigma). All fractions were reduced with $NaBH_4$ prior to HPLC separation.

PG binding assay. SleB binding to PG was quantified following incubation of 8 μM protein with cortex fragments at OD_{600} = 40 in 15 μL 30 mM $NaPO_4$ (pH 7.0), 1 mM EDTA, and 1 mM DTT at 25°C for 1 min. Mixtures were separated by centrifugation into bound (pellet) and unbound (supernatant) fractions and analyzed on a 15% SDS-PAGE gel. Gels were stained with Sypro Ruby Protein Gel Stain (Sigma) and imaged with a Typhoon TRIO variable mode imager (GE Healthcare). Band density was measured with the ImageQuant TL version 2005 (GE Healthcare) software.

RESULTS

Structural features of SleB, its overexpression, and purification. BAS2562 encodes SleB during sporulation (51), which is a 253 amino acid protein with a signal sequence and two putative domains (Fig. 4.1). The SignalP 3.0 Server indicates SleB has a 99% likelihood of being a secretory protein with 95% probability of signal peptide cleavage between amino acid residues Ala-32 and Phe-33 (11). This region has 100% identity to the SleB signal sequence present in *B. cereus*, which was shown to be cleaved at the same position (101). The putative PG-binding domain (pfam01471), beginning at Gly-41 and ending at Leu-99, contains a tandem repeat sequence that is also observed in SleB from *B. subtilis* and *B. cereus* as well as a GSLE from *C. perfringens* (SleC) (89, 92, 101). This repeat sequence is also observed in other peptidoglycan hydrolases that have a variety of substrate specificities (101). The C-terminal domain, encompassing Lys-128 to Lys-253, belongs to a family of hydrolases (pfam07486). It is homologous to the sole putative domain of two other GSLEs in *B. anthracis*, CwlJ1 and CwlJ2, the former of which is capable of facilitating cortex hydrolysis independently (40, 49).

Full-length SleB was overexpressed in *E. coli* without a signal sequence to ease purification and mimic the mature protein's active structure (Fig. 4.1). A truncated version of SleB containing only the C-terminal hydrolase domain was also overexpressed and named $SleB_{125\text{-}253}$. Truncation between amino acids Pro-124 and Ser-125 was chosen because of this region's low probability to contain secondary structure and a high surface probability as determined using Protean 7.2.1 from the DNASTAR Lasergene software package. Both constructs were expressed as protein fusions with a combined histidine and maltose-binding protein tag (His_6-MBP) on the amino terminus. After purification with Ni-affinity and cation exchange chromatography, the tags were removed by TEV protease treatment; this left a single

additional glycine residue on the amino terminus of each protein. When observed on an SDS-PAGE gel, both SleB and $SleB_{125-253}$ matched their expected masses of 24 kDa and 14 kDa, respectively (Fig. 4.2). After further purification with cation exchange chromatography, both proteins were judged to be free of the His_6-MBP tags and >95% pure (Fig. 4.2).

SleB and $SleB_{125-253}$ hydrolyze intact and fragmented cortex. *B. anthracis* and *B. subtilis* spore PG are virtually identical (32), so *B. subtilis* spores were used as a source for cortex due to their ease of purification. Spore sacculi were prepared by chemical and enzymatic treatments, but still contained significant amounts of core and coat proteins (121). Spore sacculi appeared smaller and less phase-bright than dormant spores when observed with phase-contrast microscopy (data not shown). In addition, the spore sacculi did not lose OD_{600} when exogenously treated with a cortex-fragment lytic enzyme, SleL (data not shown), indicating that the peptidoglycan layers were still intact (80). In order to generate cortex fragments, spore sacculi were broken with glass beads and $CHCl_3$ extracted. Amino acid analyses indicated that the extraction was effective at removing 75% of residual protein from the fragmented PG preparation (data not shown), and consequently the cortex fragment preparation was enriched for PG. Since the spore sacculi preparation is estimated to be 43% PG and 57% protein (121), then the total enrichment of PG within the cortex fragments was 2-fold compared to spore sacculi.

SleB and $SleB_{125-253}$ were able to decrease the OD_{600} of permeabilized spores, spore sacculi, and cortex fragments (Fig. 4.3 and data not shown), although the OD_{600} loss from fragments was less rapid than that experienced by spore sacculi. On average, SleB decreased the OD_{600} of cortical fragments 4-fold slower than spore sacculi (Table 4.1 and 4.2), however when taking into account the PG enrichment of cortical fragments this difference is expected to be 2-fold. In support of this estimate the same assay was performed with half the cortical fragment

substrate, in order to negate the effects of PG enrichment, and the rate of OD_{600} loss by SleB was 1.8-fold slower than that on spore sacculi (data not shown). Furthermore, when the cortex fragments were not enriched by $CHCl_3$ extraction, the decrease in SleB action on the substrate was 5-fold less than that observed on spore sacculi (data not shown).

Using either spore sacculi or cortex fragments, SleB caused an OD_{600} loss rate that was significantly faster than that caused by $SleB_{125\text{-}253}$ ($p < 0.0001$) (Fig 4.3A, B, and Table 4.1). Neither protein caused any change in optical density when vegetative cell wall from PS832 cells was used as substrate (data not shown). Although SleB decreased OD_{600} of spore sacculi by as much as 60%, no reactions were ever observed to cause a complete loss in OD_{600}. This is not unexpected because the substrates also contained germ cell wall PG as well as remnants of spore core and coat protein structures (121).

Pellet and supernatant samples were collected from spore sacculi after treatment with either SleB or $SleB_{125\text{-}253}$ in order to determine if OD_{600} loss corresponded with cortex hydrolysis and hence muropeptide release into the supernatant. Pellets contained insoluble cortex that required muramidase treatment in order to resolve by RP-HPLC, and as a result, muramidase products were detected in all treatment groups (Fig. 4.4A-C). However, after SleB treatment the amount of insoluble cortex was dramatically reduced. As expected, the decrease of insoluble cortex by SleB coincided with an increase in soluble muropeptides in the reaction supernatant with (Fig. 4.4G and H) or without (Fig. 4.4D and E) muramidase treatment. Ultimately, SleB resulted in an average release of 96% of spore sacculi cortex into the supernatant (Table 4.1). The only muropeptides detected in supernatant untreated by muramidase were the anhydromuropeptides aG7a and aG7b, which were the only two products previously found to depend on *in vivo* SleB action (13, 18, 49, 51). Exposure to $SleB_{125\text{-}253}$ led to an almost

imperceptible decrease of insoluble cortex (Fig. 4.4A and C), but a small amount of lytic transglycosylase products, was evident in the pellet (Fig. 4.4A and C) and supernatants with (Fig. 4.4G and I) and without (Fig. 4.4D and F) muramidase. Only 14% of spore sacculi cortex was solubilized by $SleB_{125\text{-}253}$ (Table 4.1). The decrease in hydrolysis by $SleB_{125\text{-}253}$ is consistent with the reduced OD_{600} loss shown in Figure 4.3 when compared to that produced by SleB.

When cortex is degraded by GSLEs during spore germination a variety of PG fragments are generated (7, 49). Many of these fragments are small enough to remain soluble during centrifugation, but they are too large, and presumably heterogeneous, to clearly resolve on the HPLC. Muramidase treatment during this analysis is used to break cortex down into fragments that are small enough to be resolved (≤eight sugars). Hence in this analysis, it is reasonable to assume that most of the SleB cortex products are larger than eight sugars in length, because the majority of muropeptides were resolved only after muramidase digestion. When SleB lytic transglycosylase activity results in large muropeptides they contain potentially numerous sites for muramidase hydrolysis, and thus one SleB product can be cleaved into several different products (49). When this occurs the result is one SleB product for one or more muramidase products, and the ratio of these is calculable from the RP-HPLC chromatograms. The results of these calculations are in Table 4.1, and it is clear that *in vitro* SleB cleaved an available NAM-NAG glycosidic bond twice as often as $SleB_{125\text{-}253}$. This again is consistent with SleB-induced OD_{600} loss occurring significantly more efficiently than by $SleB_{125\text{-}253}$ (Fig. 4.3), and suggests the reason why lytic transglycosylase products appear in $SleB_{125\text{-}253}$ reaction pellets is because many of these products are too large to be soluble (Fig. 4.4C).

To conduct a similar analysis on cortex fragment hydrolysis, pellet and supernatant samples were collected from cortex fragments after treatment with either SleB or $SleB_{125\text{-}253}$. In

this instance muropeptides were not analyzed, but the total amount of NAM solubilized was used as a consistent measure (Table 4.2). Only SleB was capable of solubilizing a significant amount of cortex fragments, but at a reduced efficiency to that calculated for spore sacculi (compare Table 4.1 and 4.2). $SleB_{125-253}$ did not solubilize any detectable amount of the fragments despite lowering their OD_{600}.

The hydrolase domain of SleB is dependent on muramic-δ-lactam for activity. *B. subtilis* VB19 is a *cwlD* mutant that generates spore cortex without muramic-δ-lactam; instead, this strain's cortex is more similar to vegetative cell wall PG (118). Despite the fact that SleB was unable to change the OD_{600} of vegetative cell wall (data not shown), it was capable of significantly decreasing the OD_{600} of both spore sacculi ($p < 0.0001$) and cortex fragments ($p < 0.0001$) from the VB19 strain (Fig. 4.3A and B). $SleB_{125-253}$ had no effect on the OD_{600} of any VB19 PG substrate (Fig. 4.3A and B). No muropeptide production or NAM solubilization was detected when either SleB or $SleB_{125-253}$ were mixed with VB19 substrates (Fig. 4.5, Table 4.2, and data not shown).

Both the N and C terminal domains of SleB participate in binding cortex peptidoglycan. A simple peptidoglycan binding assay was used to investigate whether one of SleB's two domains is responsible for substrate binding, or if they function cooperatively. When both domains were present, at least 94% of SleB was able to bind cortical fragments both with and without muramic-δ-lactam (Fig. 4.5 and Table 4.2). $SleB_{125-253}$, with only 52% binding, was less capable of attaching to PS832 cortical fragments than the full-length protein. In addition, $SleB_{125-253}$ showed a preference for cortex that contained muramic-δ-lactam, since its average binding to VB19 PG dropped to 34%. Less than 10% of a negative control protein,

bovine serum albumin (BSA) (New England Biolabs), was associated with the cortical fragment PG pellet.

DISCUSSION

In this study, the *B. anthracis* SleB protein was overexpressed in *E. coli* and purified in two forms: as the native protein with both of its N and C terminal domains that are putative PG-binding and hydrolytic domains respectively, and as a truncated form that contained only the hydrolase domain. *In vitro* analyses of both proteins conclusively show that, as suggested by earlier genetics-based investigations (18, 51, 89), SleB independently binds cortex PG and functions as a GSLE with lytic transglycosylase activity. SleB carries out this function independently, since no other protein was required to facilitate PG binding, generation of anhydromuropeptide products, or solubilization of cortex. These results also indicate that SleB can depolymerize both intact and fragmented cortex. Nonetheless, neither of these substrates exhibited more than a 60% loss in OD_{600}. To explain this, we postulate that the spore sacculi preparation contains a significant amount of germ cell wall that is not degraded by SleB, as well as remaining core and coat molecules to cause a background level of light scattering. Consequently, one would expect that a better purified substrate containing an even greater accessibility to sites for enzymatic activity, such as cortical fragments, would potentially reach OD_{600} losses near 100%. One likely explanation that this was not the case is that cortical fragments are not the ideal substrates for SleB or $SleB_{125\text{-}253}$. In previous work, SleB homologs from *B. cereus* (86) and the spore-cortex lytic enzyme in *C. perfringens* (92) did not exhibit any activity toward cortical fragment substrate. It is a possibility that our slightly different reaction conditions coupled with a different substrate source has provided evidence for previously undetectable activity; it is also probable that purification from *E. coli* rather than from spore exudates generated not only more SleB, but also protein with a higher specific activity. However, in agreement with those earlier studies, our results do suggest that the SleB enzyme is

better at hydrolyzing intact cortex, which is a substrate SleB is more likely to encounter during the initial stages of germination where its role seems more critical (49, 51).

Muramic-δ-lactam has been implicated as the structural determinant that delineates spore cortex from germ cell wall and thus dictates substrate specificity by GSLEs (6, 118, 128). It was therefore surprising to observe SleB cause a significant decrease in the OD_{600} of VB19 spore sacculi and cortex fragments. Despite this loss in optical density, SleB treatment of VB19 substrates did not release identifiable muropeptides or solubilize any measurable cortex. One possible explanation for these results is that the VB19 substrate is aggregating prior to the assay, and that SleB binding (Fig. 4.5) is causing dissociation of aggregates; thus a loss in OD. Another alternative explanation that we feel is more likely is that SleB is hydrolyzing VB19 PG, but at such poor efficiency that no detectable amount of cortex is released. SleB may cleave this substrate that lacks muramic-δ-lactam so infrequently that very long muropeptide chains result, similar to the apparent action of $SleB_{125\text{-}253}$ on PS832 substrate (Table 4.1), which itself is only barely detectable with HPLC (Fig. 4.4F and I). In addition, the higher level of cross-linking in VB19 cortex compared to PS832 cortex (118) may keep these large strands covalently linked. The ultimate result then is a loosened spore sacculus that, due to reduced mass density, altered thickness, altered shape, or a combination of all three, exhibits a loss in light scattering properties but does not disassemble. Neither SleB nor $SleB_{125\text{-}253}$ caused any changes in optical density or muropeptide generation when vegetative cell wall from PS832 cells was used as a substrate. It is quite possible our *in vitro* assay is using such an excessive amount of SleB that a minimal amount of activity on VB19 PG is occurring that is not observable *in vivo*. We do not intend to suggest that this observation contradicts the *in vivo* evidence that muramic-δ-lactam is the structural determinant for cortex recognition by GSLEs and ultimately prevents germ cell wall

degradation (118). Instead, we suspect the *in vitro* conditions for this analysis afforded us an opportunity to observe activity by SleB that, while present, is inconsequential to a germinating spore.

SleB's C-terminal domain is most certainly the hydrolase domain as predicted, because it carries out lytic transglycosylase activity without the protein's N-terminus. This hydrolase domain is capable of maintaining a significant level of interaction with PG substrate, however this is not without precedent since CwlJ1 and CwlJ2, two other GSLEs active in *B. anthracis* spores, consist solely of this putative hydrolase domain. The C-terminus' dependence on muramic-δ-lactam is clear due to the significantly decreased levels of interaction of $SleB_{125\text{-}253}$ with VB19 substrate, in comparison to interaction with PS832 substrate, that results in a total loss of detectable hydrolytic activity.

SleB's N-terminal domain, as predicted, is the protein region primarily responsible for binding PG. The N-terminal domain's dominance for this role is asserted, because its presence completely masks the C-terminus' dependence on muramic-δ-lactam during the PG-binding assay. In fact, the PG-binding domain appears to function regardless of muramic-δ-lactam. Although the N-terminus does not likely carry out any direct hydrolytic activity, it does contribute greatly to SleB's overall capability as a lytic enzyme. This is most apparent since the presence of the N-terminus affords the C-terminus the ability to reduce the OD_{600} of cortex when muramic-δ-lactam is not present.

The mechanism that activates SleB in the dormant spore has remained an unresolved issue despite several investigations (18, 86). It has been proposed that SleB is triggered to degrade cortex once the PG is in a stressed conformation (36, 134). This theory proposes that the stress on the cortex becomes altered as the spore progresses from the dormant to the

germinated state and core rehydration takes place. Our data argues against this theory since SleB was able to hydrolyze the intact cortex of coat permeabilized spores, spore sacculi, and fragmented cortex. In coat permeabilized spores the dehydration and heat resistance are unaffected (33), which suggests the stress on the cortex is the same as in a dormant spore. Sacculi are presumably less stressed because no core is present, instead, only stress inherent to the cortex structure is expected. Fragments are then likely the least stressed substrate, because some of the inherent structural stress is relieved as, the PG is no longer in a spore superstructure. Our results suggest that SleB activation may be due to a more direct process involving Ger receptor activation, core rehydration, or the return of membrane fluidity.

Future research into SleB should focus on understanding how the protein is held inactive in the dormant spore. Additionally, SleB's ease of purification lends itself to structural analysis, which may reveal the first structural visualization of a GSLE either with or without substrate. Ultimately, these investigations may uncover a means to prematurely trigger SleB action in the dormant spore, reducing its resistance properties before causing infection, and greatly simplifying efforts of *B. anthracis* decontamination.

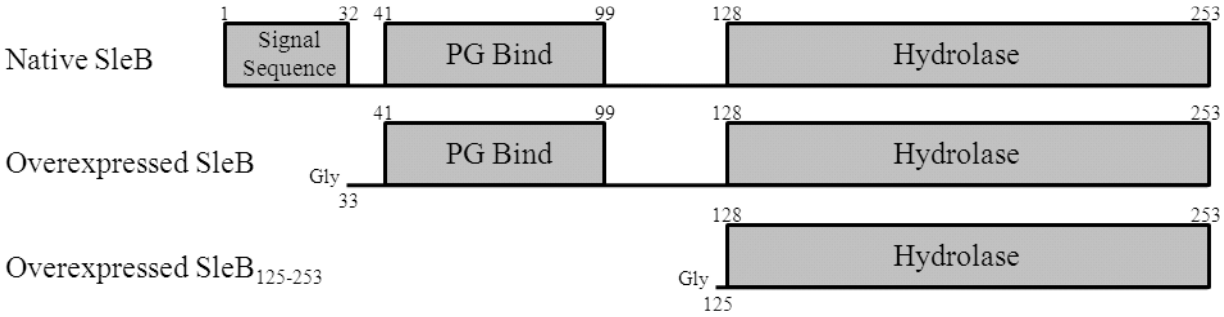

Figure 4.1. Domain architecture of SleB and overexpressed proteins. Predicted domains are illustrated as gray boxes with residue numbers indicating the amino acids at either end of each putative domain. Overexpressed proteins were truncated from the native protein at amino acid Phe-33 for SleB or Ser-125 for $SleB_{125\text{-}253}$. The amino-termini of both overexpressed proteins are glycine residues resulting from successful affinity tag removal by TEV protease.

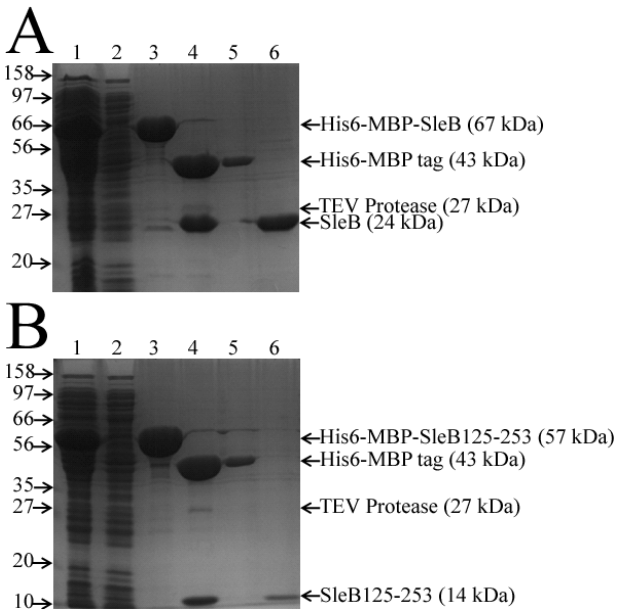

Figure 4.2. Purification of SleB and SleB$_{125-253}$ from the His$_6$-MBP tag. Gel electrophoresis (SDS-PAGE) of soluble fractions taken during SleB (A) and SleB$_{125-253}$ (B) protein purification as described in Materials and Methods. Lanes: 1, cell lysate; 2, Ni-affinity flowthrough; 3, Ni-affinity elute; 4, TEV protease digestion; 5, cation exchange flowthrough; 6, cation exchange eluate. The positions and masses (kDa) of molecular mass standards are indicated on the left. The positions and predicted masses of proteins are indicated at right.

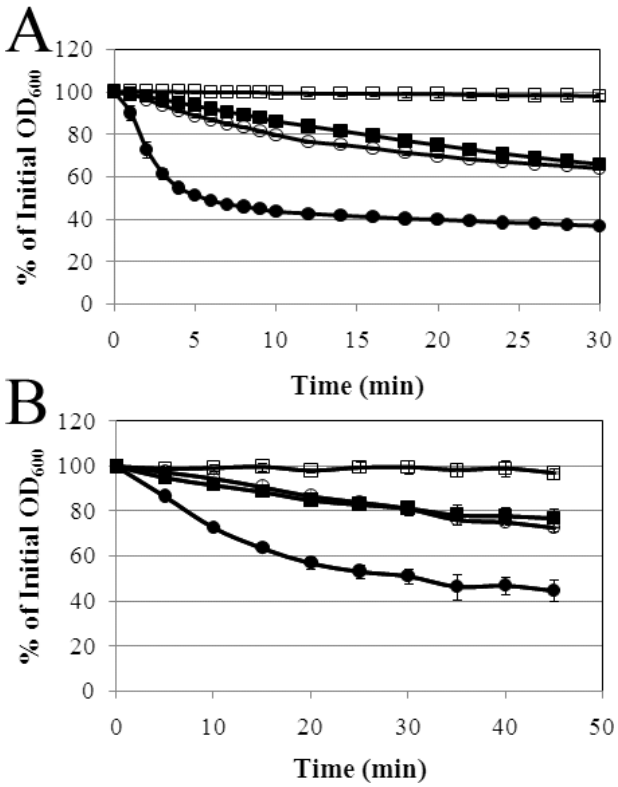

Figure 4.3. Action of SleB and SleB$_{125-253}$ on spore sacculi. Spore sacculi (A) or cortex fragments (B) were prepared from PS832 (filled symbols) or VB19 (open symbols) spores. These were then incubated at OD_{600} = 0.2 with 10 nM of SleB (circles) or SleB$_{125-253}$ (squares) at 25°C in a final volume of 1 mL 30 mM sodium phosphate buffer, pH 7.0, 1 mM EDTA, 1 mM DTT, and 0.1% Triton X-100. OD_{600} was monitored regularly with mixing between measurements. Data shown are averages for three independent reactions. Error bars represent 1 standard deviation of the mean of the results for three independent preparations; in most cases the error bars are too small to be visible. Control reactions where substrate was left untreated never experienced a loss in OD_{600}, and are not shown for clarity.

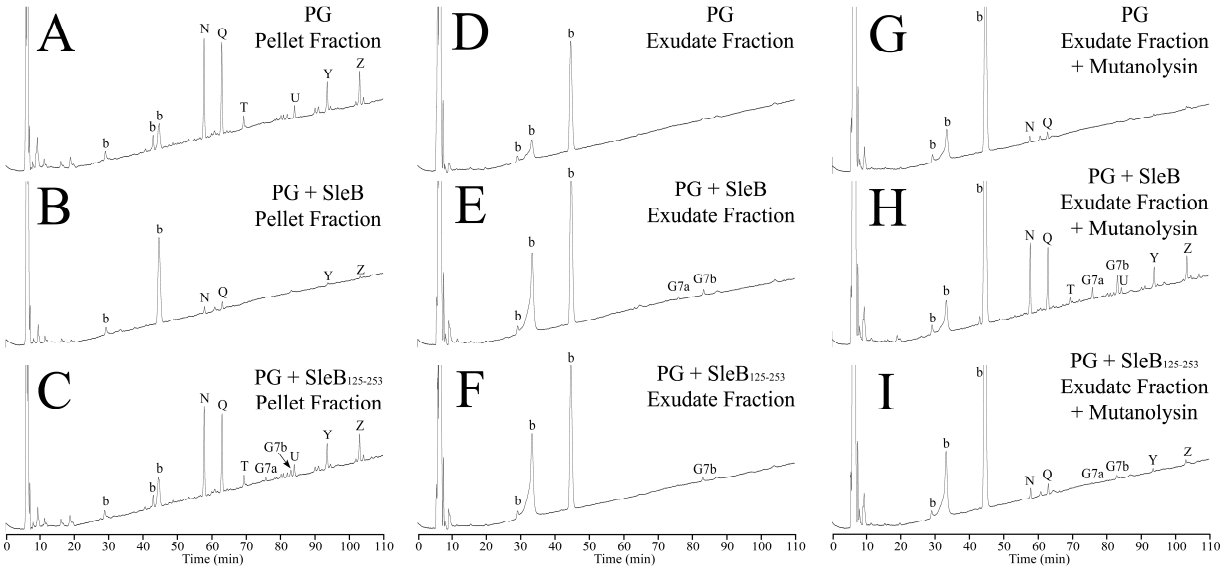

Figure 4.4. RP-HPLC separation of muropeptides released from spore sacculi digested with SleB or SleB$_{125-253}$. Spore sacculi were incubated with no enzyme (A, D, and G), SleB (B, E, and H), or SleB$_{125-253}$ (C, F, and I) as described in Figure 4.3. After incubation for 30 minutes the reactions were separated into pellet and supernatant fractions and prepared for analysis as described in Materials and Methods. Pellet (A-C) fractions and 50% of each supernatant (G-I) sample were digested with muramidase, reduced, and separated as previously described (90). The other 50% of each supernatant (D-F) was reduced and separated without muramidase digestion. Only 50% of the pellet fractions were analyzed. Peaks are numbered as in (49), but the initial "a" in the germination-specific peak names were omitted. Shown are representatives of one analysis; all samples were replicated in triplicate.

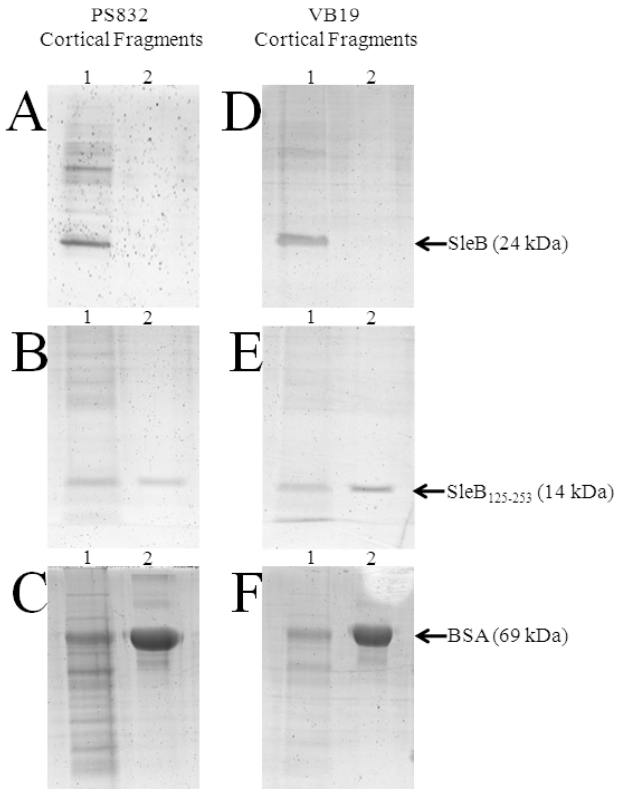

Figure 4.5. Binding of SleB and $SleB_{125-253}$ to cortical fragments. Cortical fragments from either PS832 (A-C) or VB19 (D-F) spores at OD_{600} = 40 were incubated at 25°C with 8 μM (A, D), $SleB_{125-253}$ (B,E), or BSA (C, F) in a final volume of 15 μL 30 mM sodium phosphate buffer, pH 7.0, 1 mM EDTA, and 1 mM DTT. After 1 minute of incubation the mixtures were separated into pellets, containing bound enzyme (Lane 1), and supernatants, containing unbound protein (Lane 2). All protein from each fraction was loaded onto a 15% SDS-PAGE gel after solubilization with sample loading buffer and boiling. Gels were stained with Sypro Ruby Protein Gel Stain prior to imaging. Unlabeled protein bands are derived from residual protein in the cortical fragment substrate.

Table 4.1. SleB and SleB$_{125-253}$ activity on spore sacculi PG.

Substrate	Enzyme	Ave. OD_{600} loss/min. (%)[a,b]	Ave. PG Solubilized in 30 min. (%)[a,b,c]	Detected Muropeptides	NAM-NAG linkages cleaved (%)	Ave. Muropeptide Length
PS832	None	0.1 ± 0.1	N/A	N/A	N/A	N/A
PS832	SleB	13.2 ± 0.4	96 ± 1	aG7a, aG7b	19	20-24 Sugars
PS832	SleB$_{125-253}$	1.4 ± 0.1	14 ± 6	aG7a, aG7b	10	40 Sugars
VB19	None	0.1 ± 0.1	N/A	N/A	N/A	N/A
VB19	SleB	2.1 ± 0.1	N/A	N/A	N/A	N/A
VB19	SleB$_{125-253}$	0.1 ± 0.1	N/A	N/A	N/A	N/A

[a] 0.2 OD_{600}/mL of spore sacculi and 10 nM of protein per reaction.
[b] Averages were determined from three independent experiments. Error is one standard deviation of the mean.
[c] Solubilized PG was calculated from the relative peak areas of muropeptides found in reaction pellets and supernatants after enzymatic treatment.
N/A = Not Applicable, sample never produced a detectable result.

Table 4.2. SleB and SleB$_{125-253}$ activity on cortex fragment PG.

Substrate	Enzyme	Ave. OD_{600} loss/min. (%)[a,b]	Ave. PG Solubilized in 90 min. (%)[a,b]	Enzyme Binding (%)[a,b,c]
PS832	None	0.1 ± 0.1	3 ± 2	ND
PS832	SleB	2.9 ± 0.2	70 ± 12	95 ± 4
PS832	SleB$_{125-253}$	0.6 ± 0.1	5 ± 1	52 ± 7
VB19	None	0.2 ± 0.1	2 ± 1	ND
VB19	SleB	0.6 ± 0.1	3 ± 1	94 ± 3
VB19	SleB$_{125-253}$	0.1 ± 0.1	1 ± 2	34 ± 3

[a] 0.2 OD_{600}/mL of spore sacculi and 10 nM of protein per reaction.
[b] Averages were determined from three independent experiments. Error is one standard deviation of the mean.
[c] Solubilized PG was calculated from the relative peak areas of NAM found in reaction pellets and supernatants after enzymatic treatment.
ND = Not Determined.

ACKNOWLEDGEMENTS

This research was supported by Public Health Service grant AI060726 from the National Institute of Allergy and Infectious Disease. We thank F. Schubot for the gift of pDEST-HisMBP and His_6-tagged TEV (S219V) protease.

CHAPTER 5

The *Bacillus anthracis* Germination-Specific Lytic Enzyme CwlJ1 is Active *In Vitro*

Jared D. Heffron and David L. Popham

AUTHOR CONTRIBUTIONS

Jared Heffron performed the research, experimentation, data analysis, and writing of the material presented herein. David Popham was the principal investigator.

ABSTRACT

The *Bacillus anthracis* endospore loses resistance properties during germination when its cortex layer of peptidoglycan is degraded by germination-specific lytic enzymes (GSLEs). Although this event requires several GSLEs for complete cortex removal, the CwlJ1 protein is involved in the earliest stage of cortex hydrolysis and can facilitate enough depolymerization to result in vulnerable spores. Homologs of CwlJ1 have been investigated in several spore-forming bacteria, but the precise enzymatic activity of this GSLE has remained unidentified. In order to better understand its function, a CwlJ1 fusion protein was overexpressed and purified for use in *in vitro* assays with cortex substrates. The marked insolubility of the CwlJ1 fusion protein is improved with the addition of zwitterionic, reducing, and cryoprotectant compounds. Once the fusion tag is removed, recombinant CwlJ1 is capable of reducing the optical density of decoated spore substrate and transitioning spores from a phase-bright to a phase-dark state, suggesting it alone can hydrolyze cortex *in vitro*. Current issues with inefficient fusion tag removal and unstable CwlJ1 have been addressed with the addition of a glycine linker between the tag and CwlJ1. Future assays with this improved recombinant protein will include high-performance liquid chromatography analysis of products from hydrolyzed cortex, thus revealing the concealed enzymatic role of CwlJ1.

INTRODUCTION

The infectious agent of anthrax is the *Bacillus anthracis* endospore. Once the spore has gained access to a nutritively rich environment, such as host tissue, it will germinate into a vegetatively growing cell that is capable of producing toxins and thus lead to disease symptoms (35, 93, 108). The spore contains several structural properties that contribute to make a cell that is dehydrated, dormant, and highly resistant to environmental insults (135). These combined properties of longevity and durability make the *B. anthracis* spore an ideal bioweapon that can be stockpiled and difficult to eradicate once administered to a target location (138). In fact, spore decontamination is considered a primary hurdle in preventing anthrax infections (10). It is notable however, that resistance properties are eliminated once a spore germinates (135).

Once germination is triggered, three major events then transpire. The first is that the spore core starts to rehydrate as water moves inward (106). The second event, likely coupled with the first, is transport of ions and dipicolinic acid (DPA) out of the core (23, 85, 96, 106). The third major step is the depolymerization of cortex by GSLEs and the release of muropeptides into the surrounding environment (96). It is at this point that the spore has now lost its resistances (134-135). Exactly how GSLEs are held inactive in the dormant spore and later initiated is not understood, but it has been demonstrated that cortex hydrolysis triggered by a GSLE is capable of stimulating germination without nutrients, water movement, or ion release (95, 106, 124). It therefore seems obvious that premature activation of cortex hydrolysis by triggering GSLEs may be a suitable treatment for reducing the natural resistances of spores and potentially improving the efficacy of decontamination procedures (61).

B. anthracis has four GSLE homologs that have all been implicated in the process of cortex degradation during spore germination, SleB, CwlJ1, CwlJ2, and SleL (40, 49). Of these

four, both SleB and CwlJ1 have been shown capable of independently facilitating enough cortex hydrolysis to result in the loss of spore resistance (49). Of these two proteins CwlJ1 is a prime candidate for investigation for several reasons: it may be more abundant in the spore because its ORF is transcribed at a level >100-fold higher than SleB; it is required for initial cortex depolymerization; and it already has a proven "trigger molecule", calcium dipicolinic acid (Ca-DPA), that induces CwlJ1-facilitated cortex hydrolysis, and thus may be the ideal protein to force premature spore germination (49, 51).

However, the CwlJ proteins in *B. anthracis* and other spore-forming organisms are arguably the most misunderstood GSLEs, because their enzymatic function has remained unknown despite several investigations (49, 51, 95, 106). We propose that CwlJ1 is an endo-muramidase whose enzymatic nature has remained elusive, because previous *in vivo* attempts to identify its activity required treating the hydrolyzed cortex (muropeptides) with commercially-prepared muramidase (Mutanolysin) to generate products small enough to be resolved with reverse-phase high-pressure liquid chromatography (RP-HPLC). As a result the Mutanolysin likely masks observation of the CwlJ1 activity. The aims of this study are to overexpress and purify CwlJ1 in an active conformation for use in *in vitro* analyses to better characterize its requirements for activity, substrate preferences, and enzymatic function.

MATERIALS AND METHODS

Protein expression and purification. The CwlJ1 ORF lacking the first codon was amplified from *B. anthracis* Sterne 34F2 genomic DNA using a forward primer with a 5' end complementary to the TEV protease region of pDEST-HisMBP (5'-GTGGAGAACCTGTACTT CCAGGGTGGCGTTATCGCGTATAACGAAGCAG-3') and a reverse primer with a 5' end complementary to the *att*R2.1 region of pDEST-HisMBP (5'-CCACTTTGTACAAGAAAGTTG CATTATTATCAATCCTTAATATACGCTAG -3'). The PCR amplicon was inserted into pDEST-HisMBP (F. Schubot) using a restriction-free (RF) cloning method previously described (141) in order to construct the His_6-MBP-CwlJ1 (pDPV384) fusion vector for protein overexpression.

The fusion protein was overproduced in *Escherichia coli* BL21 (λDE3 $pLys^S$ Cm^R) (Novagen) grown in LB with 30 μg/mL chloramphenicol (Fisher) and 50 μg/mL ampicillin (Jersey Lab Supply). The culture was grown by shaking (250 rpm) to saturation overnight at 37°C and then diluted 100-fold into 2 L of fresh medium. When the cells reached an optical density at 600 nm (OD_{600}) ~1.0, the temperature was reduced to 10°C and isopropyl-β-D-thiogalactopyranoside (IPTG) was added to a final concentration of 1 mM. Fifteen hours later, the cells were recovered by centrifugation at 10,000 g for 10 min at 4°C and stored at -80°C.

E. coli cell paste was suspended in ice-cold 50 mM NaCl, 50 mM Tris-HCl, 5% glycerol, and 30 mM imidazole (pH 7.5) (buffer A). The cells were lysed with a French Press (Thermo Electron Corp.) at 1000 psi and centrifuged at 10,000 g for 10 min at 4°C. The supernatant was further centrifuged at 40,000 g for 1 hour at 4°C, and the resulting supernatant was loaded onto a 5 mL Ni Sepharose™ HisTrap™ HP affinity column (GE Healthcare) equilibrated with buffer A. The column was washed with twenty column volumes of buffer A and then eluted with a

linear gradient from 30 to 500 mM imidazole in buffer A. Fractions containing recombinant His_6-MBP-CwlJ1 were pooled and stored at -80°C.

Fusion protein dialyzed in 20 mM Tris-HCl, 200 mM NaCl, and 1 mM EDTA (pH 7.4) (buffer B) was applied to 1 mL of amylose resin (New England Biolabs) in a 25 x 10 cm column and equilibrated with twelve column volumes of buffer B. The sample was eluted with a step-wise gradient of buffer B consisting of 2.5 mM, 5 mM, 7.5 mM, and 10 mM maltose. The fractions containing His_6-MBP-CwlJ1 were pooled, dialyzed in buffer A containing no imidazole (buffer C), and stored at -80°C.

His_6-MBP-CwlJ1 was next applied to a SP Sepharose™ HiTrap™ SP XL column (GE Healthcare) equilibrated with buffer C. The sample was eluted with a linear gradient from 50 to 500 mM NaCl in buffer C. The peak fractions containing His_6-MBP-CwlJ1 were pooled and dialyzed in buffer B. Aliquots were frozen and stored at -80°C.

Digestions with His_6-tagged TEV (S219V) protease (68) were carried out overnight with 1 mg of protease per 2-100 mg of fusion protein at 15°C.

Enzymatic activity assays. *Bacillus subtilis* strain 168 derivative PS832 was grown and sporulated in 2xSG medium at 37°C with shaking for three days. Spore harvesting and purification was performed as previously described (118). Spores were then inactivated and permeabilized as previously described (32) to generate spore sacculi for use as a cortex substrate. Briefly, spores were suspended at an OD_{600} of 30 in 1 mL of 50 mM Tris-HCl (pH 7.5), 1% sodium dodecyl sulfate (SDS), 50 mM dithiothreitol (DTT), boiled for 20 min, and then stored at 4°C after warm water washes had removed all detectable SDS (48).

Hydrolysis of spore sacculi by 34 nM His_6-MBP-CwlJ1 was assayed by monitoring OD_{600} as previously described except 1 mM DTT and 0.1% Triton X-100 were used in place of

sodium thioglycollate and $C_{12}E_9$ (86). Hydrolysis reactions were also observed with phase contrast microscopy at regular intervals in order to monitor the transition of substrate from phase-bright to phase-dark.

RESULTS

Structural features of CwlJ1, its overexpression, and purification. BAS5241 is transcribed during sporulation to produce CwlJ1 (51). CwlJ1 is a 140 amino acid protein that consists almost entirely of a putative enzymatic domain (pfam07486) (Fig. 5.1). Sequence similarity analysis indicates that this domain has 25% identity and 37% similarity to the C-terminal lytic transglycosylase domain of SleB.

CwlJ1 was overexpressed in *E. coli* as a protein fusion with a combined histidine and maltose-binding protein tag (His_6-MBP) on the amino terminus. In addition the C-terminus of the tag contained a TEV protease cleavage site, which after treatment with the protease will result in adding a single glycine residue to the N-terminus of the CwlJ1 protein. The fusion protein did not contain the CwlJ1 N-term methionine to account for likely N-terminal methionine excision (42). The cell lysate contained a protein corresponding to the predicted mass of His_6-MBP-CwlJ1 (59,262 Da) only when induced with IPTG (Fig. 5.2A and data not shown). A significant amount of the His_6-MBP-CwlJ1 protein fusion was insoluble after cell lysis (Fig. 5.2A lane 3); however, soluble fusion protein was partially purified from cell lysate with Ni-affinity. SDS-PAGE analysis of the eluent indicated that the fusion protein co-eluted with several other *E. coli* proteins (Fig. 5.2A lanes 7-12). A maltose binding protein-affinity purification was next carried out to separate the fusion protein from the undesired proteins. While this did improve the sample's purity somewhat, the eluent with His_6-MBP-CwlJ1 still contained a significant amount of unknown protein (data not shown). Anionic exchange chromatography was used to isolate His_6-MBP-CwlJ1 at 75% purity (Fig. 5.2B).

The solubility of His_6-MBP-CwlJ1 is improved with additives to the buffer. Earlier work in *B. subtilis* demonstrated that CwlJ had poor solubility when expressed in *E. coli*, and

was prone to covalently oligomerize (18). Similarly, our His_6-MBP-CwlJ1 protein fusion demonstrated a significant amount of insolubility at each stage of purification. In an effort to improve the protein's solubility prior to removing the His_6-MBP tag, a variety of buffer additives were tested (Table 5.1). Addition of a strong detergent, Triton X-100, which may prevent protein aggregation, had no effect on the fusion protein.

Modifications to the buffer components were next investigated on order to improve fusion protein solubility. It is widely known that ionic concentration often has a dramatic effect on protein solubility and previous work with other GSLEs indicated that enzymatic activity may likewise be affected (17, 86). Since the buffer used for cell lysis and the purification steps contained relatively low ionic strength (50 mM NaCl), we investigated an increase in ionic strength. What was observed was an obvious decrease in fusion protein solubility with increasing ionic strength. Another basic buffer component was glycerol, which at a concentration of 5%, was added to serve as a cryoprotectant. Increasing this concentration to 25% did result in a small improvement in His_6-MBP-CwlJ1 solubility.

We also tested whether Ca-DPA could improve the fusion protein's solubility, since previous work in our lab demonstrated that CwlJ1-facilitated cortex-lytic activity may be triggered solely with the presence of Ca-DPA (49). Unfortunately, the chelate was unable to clearly affect solubility, and the Ca-DPA itself rapidly precipitated as we had previously observed (49) (data not shown). The CwlJ1 protein contains four cysteine residues and as a result has the potential to create covalent interactions due to the formation of disulfide bonds. To investigate whether any covalent interactions were at fault, the reducing agents DTT and β-mercaptoethanol (BME) were added to the protein buffer. While the DTT had no obvious impact, 10 mM BME did improve His_6-MBP-CwlJ1 solubility. The most effective buffer

additive tested was the zwitterion 3-(1-Pyridinio) propanesulfonate (NDSB), which is a nondetergent sulfobetaine. NDSB has proven effective at preventing the aggregation of several proteins, including hydrolases, independent of protein size, fold, or origin (20). NDSB alone was capable of improving His_6-MBP-CwlJ1 solubility up to 90%. It was concluded from these tests that future attempts at purifying and manipulating the fusion protein should include 10 mM BME, 0.5 M NDSB, and an increase in glycerol to 25% in order to alleviate protein precipitation.

The His_6-MBP-CwlJ1 fusion protein is recalcitrant to TEV protease digestion. Early attempts at removing the His_6-MBP tag from the fusion protein did not produce ideal results. Firstly, TEV digestion was poor and varied from 50-75% efficiency (Fig. 5.3 and data not shown). Secondly, after TEV protease treatment only the His_6-MBP tag (43 kDA) was detected by SDS-PAGE; CwlJ1 (16 kDa) was not detected with either Comassie blue or Silver stains. It was initially expected that CwlJ1 may rapidly lose solubility after tag removal; however, the protein was not detected in insoluble fractions. Attempts at purifying CwlJ from *B. subtilis* suggested that the protein oligomerized even under denaturing conditions (18), but such an event was not observed with our *B. anthracis* protein.

In an effort to improve TEV protease digestion, several variables in the digestion reaction were altered including the protease to fusion protein ratio, reaction temperature, and the addition of buffer additives that previously improved the fusion protein solubility (Fig. 5.3 and data not shown). While NDSB, BME, and 25% glycerol were all individually capable of improving the solubility of protein fusion, removed tag, and sample contaminants, there was no obvious improvement in digestion efficiency, nor was CwlJ1 detected in any fraction. A ratio as high as 1 mg TEV protease per 2 mg His_6-MBP-CwlJ1 was required to achieve the most efficient

(~75%) removal of the His_6-MBP tag. The reaction efficiency was not noticeably improved with altered reaction temperatures.

Hydrolysis of cortex by His_6-MBP-CwlJ1 after TEV protease digestion. Although CwlJ1 appeared to experience an event after tag removal that resulted in its inability to be detected, it was postulated that the protein may be capable of activity shortly after TEV protease digestion. To test this possibility, TEV protease and His_6-MBP-CwlJ1 were added to an *in vitro* hydrolysis assay containing spore sacculi. The reaction was measured by two methods: the loss of OD_{600} by spore sacculi; and the transition of spore sacculi from phase bright to phase dark (Fig. 5.4). The spore substrate was stable and did not lose OD_{600} nor change phase when left untreated. Similarly, His_6-MBP-CwlJ1 and TEV protease, when added independently, did not cause any significant effects on the substrate. However, when decoated spores were incubated with both proteins a marked loss in OD_{600} and phase darkening was observed. This suggests that the His_6-MBP-CwlJ1 is capable of hydrolyzing cortex after interacting with TEV protease. This activity is likely due to untagged CwlJ1 since hydrolytic activity has never been attributed to the His_6-MBP tag.

Cloning and overexpression of an improved His_6-MBP-CwlJ1 protein fusion. TEV protease cleavage of the His_6-MBP tag from recombinant CwlJ1 was inefficient and problematic. However, despite poor protease performance, the detection of activity most likely attributed to CwlJ1 offered hope that further troubleshooting may provide improved results, and thus we sought out a way to improve the efficiency of tag removal. Earlier work with recombinant SleL, fused to the same His_6-MBP tag used in this work, demonstrated inefficient processing by TEV protease. This hurdle was crossed by introducing a glycine linker region between the TEV protease recognition sequence and the first amino acid of SleL (79). In addition, it is relatively

common to encounter a fusion protein that cannot be processed effectively by TEV protease because of steric hindrance at the cleavage site (69). For these reasons we sought to construct an improved His_6-MBP-CwlJ1 fusion protein that contained a glycine linker region to improve protease access to the recognition site.

This new construct was synthesized using the RF cloning method presented in Materials and Methods except the forward primer contained three codons for glycine between the TEV protease recognition site and Gly-2 from CwlJ1 (5'-GTGGAGAACCTGTACTTCCAGGGTGG AGGTGGAGGCGTTATCGCGTATAACGAAGCAG-3'). This new protein fusion was successfully cloned and its sequence was confirmed by DNA sequencing. It was successfully overexpressed in *E. coli* as described in Materials and Methods; future work will include lysing the cells with buffer containing 0.5 M NDSB, 10 mM BME, and 25% glycerol, purification with Ni-affinity and anion exchange chromatography, and tag removal with TEV protease. Proper tag removal from the improved His_6-MBP-CwlJ1 fusion protein is expected to yield recombinant CwlJ1 with three additional glycines at the N-terminus (Fig. 5.1).

DISCUSSION

In this study CwlJ1 was overexpressed as a fusion protein, His_6-MBP-CwlJ1, in *E. coli* and purified. The goal of this work was to produce recombinant untagged CwlJ1 that could be assayed for its activity on spore cortex *in vitro*. However, the fusion protein has demonstrated several characteristics that impede achieving this goal. This is not unexpected since the *B. subtilis* homolog, CwlJ, likewise proved intractable to purification (18).

Many coat derived proteins, including CwlJ, from *B. subtilis* are highly insoluble under typical protein extraction methods, and in the past have required the use of strong ionic detergents in order to achieve solubility (78). Unfortunately, this appears to also be the case with the *B. anthracis* homolog, because His_6-MBP-CwlJ1 is markedly insoluble once free from the cellular environment. This finding is most disconcerting because the His_6-MBP tag was chosen for this study due to its ability to greatly improve the solubility of many proteins and has been successful when fused to other GSLEs (Fig. 5.2) (70, 79, 122). It becomes logical then to assume that, once the tag is removed, CwlJ1 would become insoluble enough to prohibit further investigation. Experimentation with several buffer modifications has led to the conclusion that the fusion protein can achieve >95% solubility when the existing protein buffer contains 0.5 M NDSB, 10 mM BME, and an increased glycerol concentration to 25%.

Whether the modified buffer improves not only the fusion's stability but also that of the untagged protein is unclear, because CwlJ1 has not proven to be detectable after removal of the tag by TEV protease. There is no evidence for oligomer formation as was previously suggested with the *B. subtilis* homolog (18). This leaves degradation as a possible cause for the disappearance of CwlJ1. TEV protease recognizes a linear amino acid sequence of the general form E-X_{aa}-X_{aa}-Y-X_{aa}-Q-G/S (X can be any amino acid) with cleavage occurring between Q and

G or Q and S (111). The CwlJ1 protein has a similar sequence, E-G-E-G-Q-Q-G; however it does not contain the essential tyrosine residue at the P3 position. This makes it highly unlikely that TEV protease is cleaving the CwlJ1 protein, but that does not rule out the possibility of CwlJ1 degradation from some other source. One possible explanation is that one or more of the contaminating *E. coli* proteins that persist through purification are capable of degrading CwlJ1. Therefore it is concluded that future tests for tag removal should include various protease inhibitors such as (PMSF), aprotonin, and leupeptin, which are not inhibitory on TEV protease (28).

Another possible reason for the inability to locate CwlJ1 is TEV protease's poor efficiency of tag removal, which may result in too little stable untagged CwlJ1 being generated for detection. Despite this, there is evidence for hydrolysis of cortex by CwlJ1 after tag removal since His_6-MBP-CwlJ1 was able to cause a loss in OD_{600} and phase darkening of spore sacculi only after incubation with TEV protease. Additionally, it is promising that activity is measurable when the efficiency of tag cleavage was considered unsatisfactory. Due to these circumstances it was deemed appropriate to construct a new fusion protein with a glycine linker region between the TEV protease cleavage site and the first amino acid of recombinant CwlJ1.

It is likely that improved efficiency of tag removal due to a glycine linker combined with the augmented buffer to improve protein solubility will alleviate the challenges thus far experienced in an effort to overexpress and purify untagged recombinant CwlJ1 from *B. anthracis*. Future *in vitro* analyses will investigate whether hydrolysis by CwlJ1 is most effective on intact or partially hydrolyzed cortex by using spore sacculi and cortex fragments as substrate. In addition, any dependence on muramic-δ-lactam for hydrolysis will be explored by doing hydrolysis assays on cortex derived from a *cwlD* mutant strain that is unable to form

muramic-δ-lactam (118). The ability of CwlJ1 to bind peptidoglycan will be assessed using peptidoglycan binding assays against cortex fragments with and without muramic-δ-lactam. Of primary interest, however, would be to determine the precise nature of enzymatic activity carried out by CwlJ1. This will be investigated by collecting and separating muropeptides solubilized from cortex after incubation with CwlJ1, and identifying these products with combined RP-HPLC and mass spectrometry analyses (51). Since the exact enzymatic role of CwlJ1 and all known homologs are currently unknown, these experiments would greatly contribute to the understanding of cortex hydrolysis during spore germination.

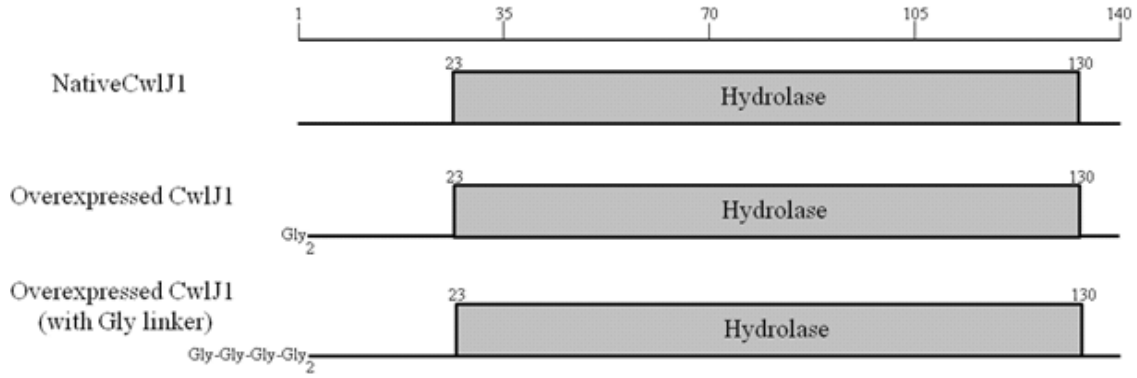

Figure 5.1. Domain architecture of CwlJ1 and overexpressed proteins. The scale at top indicates amino acid residues beginning with the amino-terminus of CwlJ1. The predicted hydrolase domain is illustrated as a gray box with residue numbers indicating the amino acids at either end of the putative domain. Overexpressed proteins were truncated from the native protein at amino acid Gly-2 for all constructs. CwlJ1 containing a Gly linker had another three Gly residues between the Gly resulting from TEV protease digestion and Gly-2.

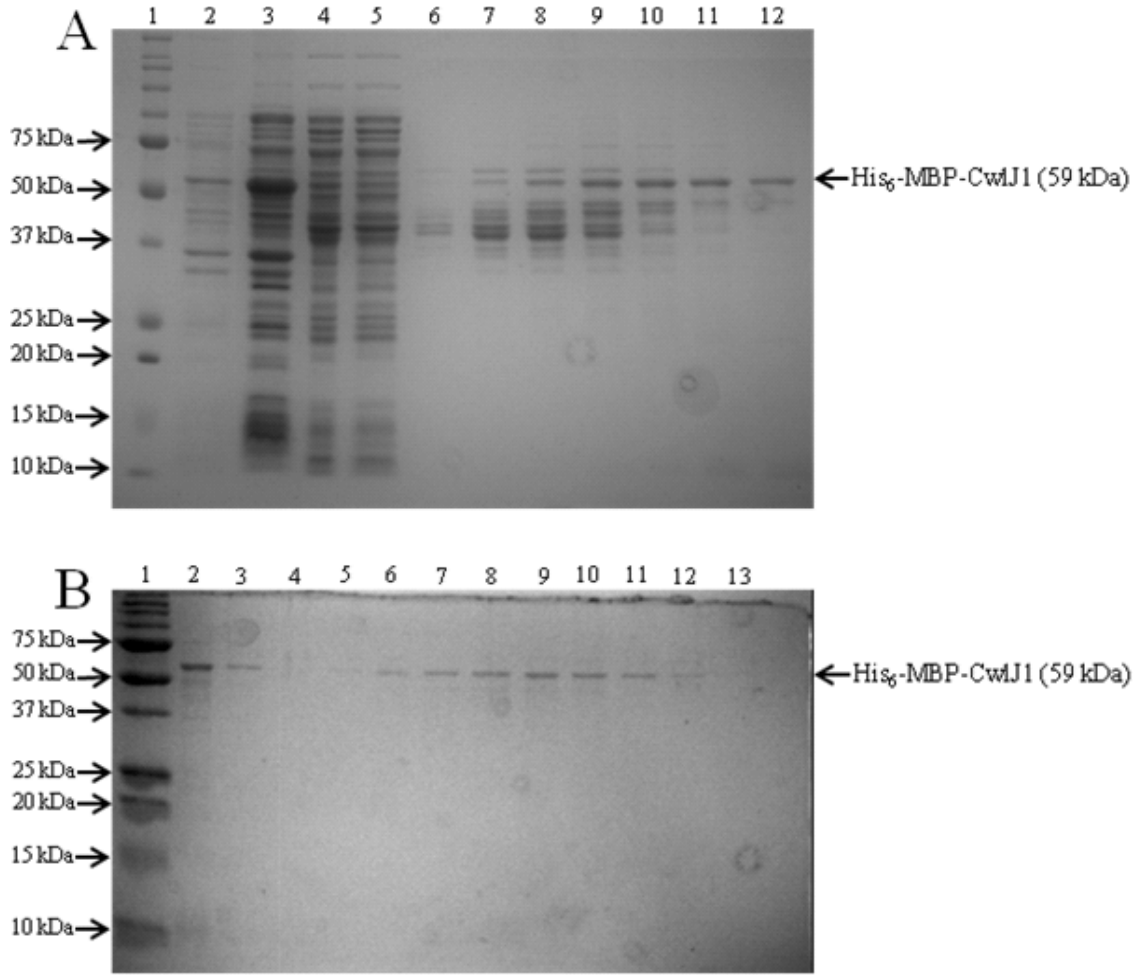

Figure 5.2. Purification of His_6-MBP-CwlJ1 fusion. (A) A 15% SDS-PAGE gel showing fractions of His_6-MBP-CwlJ1 Ni-affinity purification from cell lysate. Lanes: 1, protein markers; 2, cell lysate; 3, insoluble cell lysate post-centrifugation; 4, soluble cell lysate post-centrifugation; 5, Ni-affinity flowthrough; 6-12, Ni-affinity elution fractions. (B) A 15% SDS-PAGE gel showing fractions of His_6-MBP-CwlJ1 anion exchange purification following Ni-affinity purification and dialysis. Lanes: 1, protein markers; 2, lanes 8-11 from (A) pooled and dialyzed; 3, anion exchange flowthrough; anion exchange wash; 5-13, anion exchange elution fractions. The positions of molecular mass standards are shown on the left. The predicted masses of proteins are indicated at right.

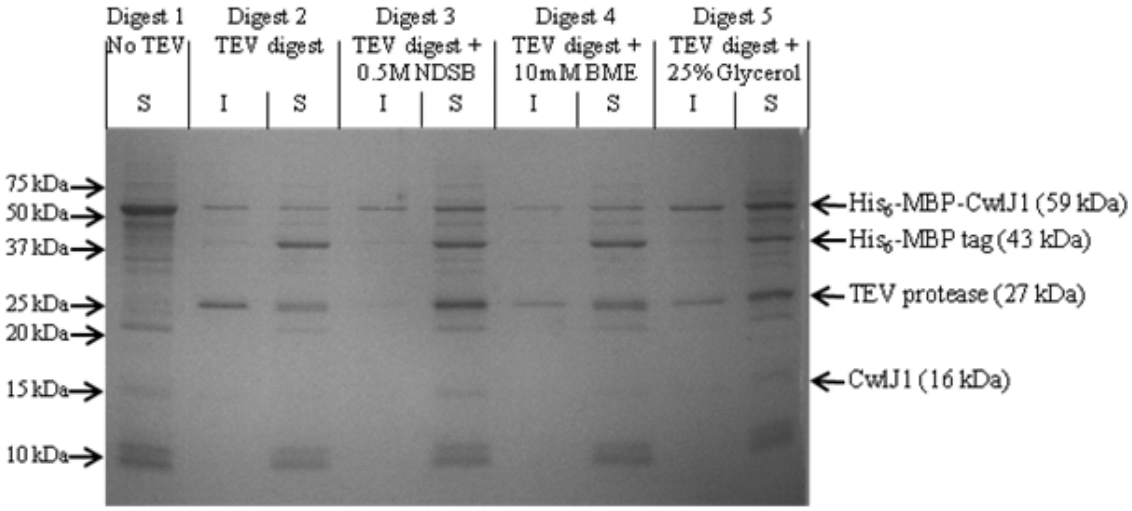

Figure 5.3. TEV protease digestions of CwlJ1 protein fusion. His_6-MBP-CwlJ1 was purified with Ni-affinity (Fig. 5.2A) and anion exchange (Fig. 5.2B) chromatography and digested with 1 mg TEV protease per 2 mg of protein fusion as described in Materials and Methods. Each digestion was separated into an insoluble (I) and soluble (S) fraction by centrifugation. Digest: 1, No TEV protease added; 2, TEV protease added; 3-5, TEV protease added plus indicated additive. Abbreviations: NDSB, 3-(1-Pyridinio) propanesulfonate; BME, β-mercaptoethanol. The positions of molecular mass standards are shown on the left. The predicted masses of proteins are indicated at right.

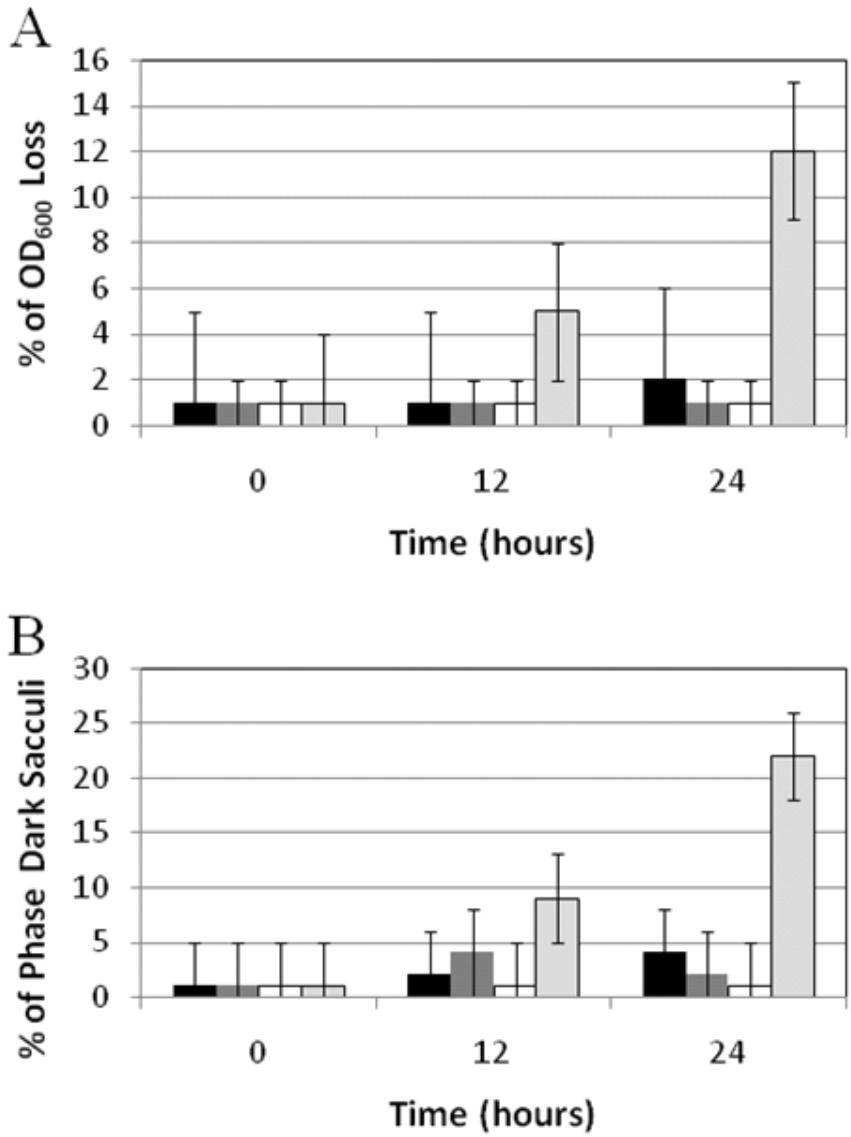

Figure 5.4. CwlJ1 activity on spore sacculi after TEV protease treatment. Spore sacculi were prepared from PS832 spores. These were then incubated at OD_{600} = 0.2 with either no protein (black bars), 70 nM TEV protease (dark gray bars), 34 nM His_6-MBP-CwlJ1 (white bars), or 34 nM His_6-MBP-CwlJ1and 70 nM TEV protease (light gray bars) at 25°C in a final volume of 1 mL 30 mM sodium phosphate buffer, pH 7.0, 1 mM EDTA, 1 mM DTT, and 0.1% Triton. OD_{600} (A) and microscopic observations (B) were made regularly with gentle mixing between measurements. Error bars represent 1 standard deviation of the mean of the results for two independent preparations. Only the 0, 12, and 24 hour time points are shown.

Table 5.1. His_6-MBP-CwlJ1 fusion protein solubility with various additives.

Additive[a]	Soluble Protein Fusion (%)[b]
None	77
1% Triton X-100	72
25% Glycerol	82
300 nM NaCl	76
500 nM NaCl	68
700 nM NaCl	65
900 nM NaCl	56
5 mM Ca-DPA	70
20 mM Ca-DPA	77
10 mM DTT	69
20 mM DTT	79
10 mM BME	90
20 mM BME	91
0.5 M NDSB	95

[a] 22.5 μg of His_6-MBP-CwlJ1 fusion protein was resuspended in water containing the additive indicated at 4°C for 2 hours.

[b] Band densities were calculated using the ImageQuant TL version 2005 software.

Abbreviations: Ca-DPA, calcium dipicolinic acid; NDSB, 3-(1-Pyridinio) propanesulfonate; BME, β-mercaptoethanol; DTT, dithiothreitol

ACKNOWLEDGEMENTS

This research was supported by Public Health Service grant AI060726 from the National Institute of Allergy and Infectious Disease. We thank F. Schubot for the gift of pDEST-HisMBP and His_6-tagged TEV (S219V) protease.

CHAPTER 6

Final Discussion

Sporulation, the mechanism whereby spores are formed from growing cells, is a well understood process that has been extensively studied in *B. subtilis* (113). Likewise, spore germination has been examined using *B. subtilis* as a model, but substantial gaps still persist in our current understanding of the process (134). Several of these questions focus on cortex degradation: How do GSLEs remain inactive during spore dormancy? How are GSLEs activated in response to germinants? How are GSLEs affecting the spore cortex? The findings detailed in this dissertation focus on addressing these questions using clinically relevant *B. anthracis* as a model. This work also creates a knowledge base for a more applied question: Can GSLEs be exploited to trigger premature and homogenous spore germination?

Chapters 2 and 3 utilize reverse genetics to show that CwlJ1, CwlJ2, SleB, and SleL in *B. anthracis* are all GSLEs. Of these four proteins CwlJ1 and SleB are the most critical for a spore to successfully degrade its cortex. This is true because both proteins can independently maintain spore viability, and secondly because in their absence CwlJ2 and SleL are ineffective at any detectable hydrolysis. That being said, these chapters also make it abundantly clear that the *B. anthracis* spore uses all four GSLEs, working in concert, to facilitate more efficient cortex depolymerization than is achievable with only one, two, or even three GSLEs present.

The canonical mechanism of spore germination is in response to nutritive germinants and consists of three main events: water uptake, ion release, and cortex degradation (95). Chapters 2 and 3 show that *B. anthracis* spores undergo partial rehydration and ion release first; however, the spores are not fully viable until the cortex PG is hydrolyzed in a 2-Stage process initiated by CwlJ1 and SleB (Fig. 6.1A).

CwlJ1 is responsible for the majority of hydrolysis during Stage 1 as indicated in Chapter 2 by NAM and Dpm release (Fig. 2.3). This conclusion is also supported by the fact that CwlJ1

is the most abundant GSLE, and that it is activated by Ca-DPA when the chelate is released during the preceding germination event. Location may also play a substantial role in CwlJ1's early prominence, because it is situated in or near the outermost cortex layers, which are the most highly cross-linked (90) and thus influential on cortical stability. It is unclear exactly what activity CwlJ1 is carrying out, but it is apparent from RP-HPLC analyses in Chapters 2 and 3 that most of the CwlJ1 products are large and can be further digested by other lytic enzymes. It is likely that CwlJ1 is a muramidase, because muropeptides from *cwlJ1* spores contain only muramidase products when treated with a known muramidase (Mutanolysin). If CwlJ1 carried out a different lytic activity than Mutanolysin, then one would expect a novel muropeptide product; no novel products have yet been observed in conjunction with CwlJ1.

SleB's contributions to early cortex degradation are far better understood due to the *in vitro* studies presented in Chapter 4. SleB is a lytic transglycosylase that generates anhydromuropeptides. Some of these products are small enough to be released from the spore without further hydrolysis, but the majority are large enough to be digested later. The PG-binding domain at SleB's N-terminus increases binding of the protein to its substrate, while the C-terminal hydrolytic domain is solely responsible for PG cleavage. In addition, the hydrolase domain is capable of differentiating cortex PG from germ cell wall by recognizing ML in the former. This recognition is without any help from the PG-binding domain, which interacts with PG regardless of ML. This also suggests that CwlJ1 and CwlJ2 have similar preferences for ML since they both consist solely of PG hydrolase domains that are homologous to that of SleB. The activation of SleB during germination remains an unresolved issue; but it is unlikely that SleB is stimulated by changes in PG stress as previously suggested (36), because it is clearly capable of hydrolyzing intact cortex in dormant spores, intact cortex in permeabilized rehydrated spore

sacculi, and fragmented cortex. Instead, it is probable that SleB is held inactive at the IFM by the YpeB homolog that is encoded immediately downstream in an apparent operon. YpeB has already been demonstrated to facilitate SleB localization in the *B. subtilis* spore and it apparently maintains this interaction throughout dormancy (18). The precise signal that terminates the relationship between these two proteins remains unidentified.

CwlJ2 carries out less digestion than any other GSLE in *B. anthracis*, and, even when given ample time, is unable to germinate spores independently. Nonetheless it is active during the nutritive germination response and likely performing the same functions as CwlJ1. This last conclusion is drawn because CwlJ2's effects can only be detected once CwlJ1 has been inactivated and because of their high level of homology.

SleL is an N-acetyl-glucosaminidase that can only recognize and degrade cortex fragments (80). It is responsible for nearly all of the cortex depolymerization occurring in Stage 2 (Fig. 6.1A). It is a very active GSLE that is capable of further hydrolyzing the large products from CwlJ1, CwlJ2, and SleB digestions. This role is not essential to spore viability, but it does permit the most rapid release of cortex from the spore integuments and shortens the time it takes the spore to reach outgrowth. SleL has a preference for lytic transglycosylase products over those from CwlJ1 or CwlJ2, which is why spores lacking SleB experience poor Stage 2 PG solubilization. It is also possible that SleB degrades some large fragments, but its role in this does not seem significant to the overall process. Ultimately, spores that germinate in response to nutritive germinants utilize all four GSLEs to rapidly depolymerize the cortex PG into a mixture of small and large muropeptides that are mostly soluble and easily released into the surrounding environment.

Chapter 3 demonstrates that *B. anthracis* spores can also germinate in response to the non-nutritive germinant Ca-DPA (Fig. 6.1B). During this response exogenous Ca-DPA is able to trigger CwlJ1 and CwlJ2 before any spore rehydration or ion release has occurred. SleL is active once CwlJ derived fragments are available as a substrate, and thus cortex PG is released from the spore. At some point in this process the spore eventually rehydrates and releases ions. SleB likely gets activated during non-nutritive germination, but it is definitely not involved in the initiation of this response.

Chapter 5 provides evidence that CwlJ1 can function *in vitro* without Ca-DPA present, providing hope for an analysis similar to that of SleB in Chapter 4. However, CwlJ1 has also proven to be refractory to purification, like its *B. subtilis* homolog (18) and many other coat-derived proteins (78). The enzymatic activity of CwlJ1 will be determined using the RP-HPLC method of analyzing muropeptides once sufficient CwlJ1 activity is achieved. This will be the first demonstration of any CwlJ homolog activity in any bacterial species known to carry it.

Future research on SleB will likely focus on how the protein is held inactive during spore dormancy and later activated during germination. As mentioned earlier, YpeB is likely involved in some fashion, but it should not be neglected that in *B. anthracis* the SleB operon contains a third gene, *ylaJ*, that encodes a putative lipoprotein. Reverse genetics-based analyses of these other two proteins may shed light on when, where, and how SleB is localized and stabilized during sporulation and spore dormancy. Locating the trigger for SleB during germination is a more challenging question. It may involve the germinant receptors in the IFM that detect nutritive signals (35), but currently very little is understood about what signals, if any, they pass on to initiate germination. Another option may lie in structural analysis of SleB. Its purity and high yield as indicated in Chapter 4 makes protein crystallization a possibility. Not only would

this be the first demonstration of a GSLE's structure, but it could reveal protein fold structures and binding sites that are better understood in other well-characterized enzymes, thus providing a knowledge base for potential molecules that may trigger SleB activity.

This current and future work is relevant because *B. anthracis* spores may be prepared in large quantities and used as a biological weapon to administer the disease anthrax. This is a significant challenge for the public health community, because bacterial spores are not easily inactivated prior to infection and may persist in a host long after antimicrobial treatments are terminated. Both of these issues may be alleviated if spores are induced to germinate prematurely and synchronously. This work demonstrates that GSLEs can provoke this desired premature germination response through multiple pathways, and that future testing to exploit GSLEs and their properties is a sound pursuit.

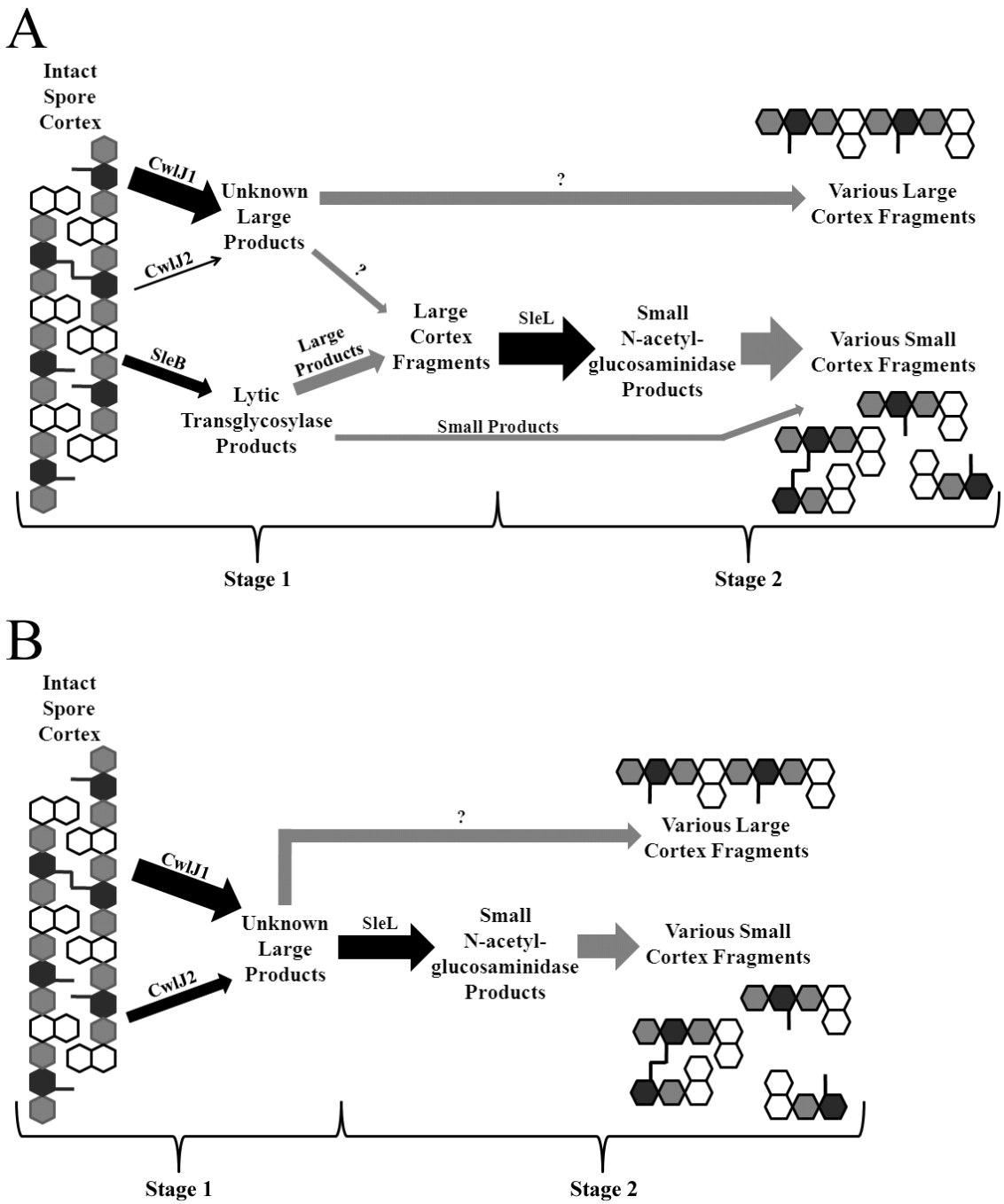

Figure 6.1. Cortex degradation during nutrient (A) and Ca-DPA (B) triggered germination. Black arrows indicate hydrolysis by the indicated GSLE. Gray arrows indicate pools of indicated muropeptide products. The relative thickness of arrows is relative to the activity of the indicated GSLE, or mass of the muropeptide pool. "?" indicates muropeptide pools that have not yet been determined experimentally.

REFERENCES

1. **Albrink, W. S.** 1961. Pathogenesis of inhalation anthrax. Bacteriol. Rev. **25:**268-273.
2. **Altschul, S. F., T. L. Madden, A. A. Schaffer, J. Zhang, Z. Zhang, W. Miller, and D. J. Lipman.** 1997. Gapped BLAST and PSI-BLAST: a new generation of protein database search programs. Nucleic Acids Res **25:**3389-402.
3. **Altschul, S. F., J. C. Wootton, E. M. Gertz, R. Agarwala, A. Morgulis, A. A. Schaffer, and Y. K. Yu.** 2005. Protein database searches using compositionally adjusted substitution matrices. FEBS J **272:**5101-9.
4. **Atrih, A., G. Bacher, G. Allmaier, M. P. Williamson, and S. J. Foster.** 1999. Analysis of peptidoglycan structure from vegetative cells of *Bacillus subtilis* 168 and role of PBP 5 in peptidoglycan maturation. J. Bacteriol. **181:**3956-3966.
5. **Atrih, A., and S. J. Foster.** 2001. In vivo roles of the germination-specific lytic enzymes of *Bacillus subtilis* 168. Microbiology **147:**2925-2932.
6. **Atrih, A., P. Zollner, G. Allmaier, and S. J. Foster.** 1996. Structural analysis of *Bacillus subtilis* 168 endospore peptidoglycan and its role during differentiation. J. Bacteriol. **178:**6173-6183.
7. **Atrih, A., P. Zollner, G. Allmaier, M. P. Williamson, and S. J. Foster.** 1998. Peptidoglycan structural dynamics during germination of *Bacillus subtilis* 168 endospores. J. Bacteriol. **180:**4603-4612.
8. **Bagyan, I., and P. Setlow.** 2002. Localization of the cortex lytic enzyme CwlJ in spores of *Bacillus subtilis*. J Bacteriol **184:**1219-24.
9. **Bagyan, I., and P. Setlow.** 2002. Localization of the cortex lytic enzyme CwlJ in spores of *Bacillus subtilis*. J. Bacteriol. **184:**1219-1224.
10. **Bales, M. E., A. L. Dannenberg, P. S. Brachman, A. F. Kaufmann, P. C. Klatsky, and D. A. Ashford.** 2002. Epidemiologic response to anthrax outbreaks: field investigations, 1950-2001. Emerg Infect Dis **8:**1163-74.
11. **Bendtsen, J. D., H. Nielsen, G. von Heijne, and S. Brunak.** 2004. Improved prediction of signal peptides: SignalP 3.0. J Mol Biol **340:**783-95.
12. **Bergman, N. H., E. C. Anderson, E. E. Swenson, M. M. Niemeyer, A. D. Miyoshi, and P. C. Hanna.** 2006. Transcriptional profiling of the *Bacillus anthracis* life cycle in vitro and an implied model for regulation of spore formation. J Bacteriol **188:**6092-100.
13. **Boland, F. M., A. Atrih, H. Chirakkal, S. J. Foster, and A. Moir.** 2000. Complete spore-cortex hydrolysis during germination of *Bacillus subtilis* 168 requires SleB and YpeB. Microbiology **146:**57-64.
14. **Brookmeyer, R., E. Johnson, and R. Bollinger.** 2003. Modeling the optimum duration of antibiotic prophylaxis in an anthrax outbreak. Proc Natl Acad Sci U S A **100:**10129-32.
15. **Brookmeyer, R., E. Johnson, and R. Bollinger.** 2004. Public health vaccination policies for containing an anthrax outbreak. Nature **432:**901-4.
16. **Chen, Y., S. Fukuoka, and S. Makino.** 2000. A novel spore peptidoglycan hydrolase of *Bacillus cereus*: biochemical characterization and nucleotide sequence of the corresponding gene, *sleL*. J. Bacteriol. **182:**1499-1506.
17. **Chen, Y., S. Miyata, S. Makino, and R. Moriyama.** 1997. Molecular characterization of a germination-specific muramidase from *Clostridium perfringens* S40 spores and nucleotide sequence of the corresponding gene. J. Bacteriol. **179:**3181-3187.

18. **Chirakkal, H., M. O'Rourke, A. Atrih, S. J. Foster, and A. Moir.** 2002. Analysis of spore cortex lytic enzymes and related proteins in *Bacillus subtilis* endospore germination. Microbiology **148:**2383-2392.
19. **Clements, M. O., and A. Moir.** 1998. Role of the gerI operon of Bacillus cereus 569 in the response of spores to germinants. J Bacteriol **180:**6729-6735.
20. **Collins, T., S. D'Amico, D. Georlette, J. C. Marx, A. L. Huston, and G. Feller.** 2006. A nondetergent sulfobetaine prevents protein aggregation in microcalorimetric studies. Anal Biochem **352:**299-301.
21. **Cortezzo, D. E., K. Koziol-Dube, B. Setlow, and P. Setlow.** 2004. Treatment with oxidizing agents damages the inner membrane of spores of Bacillus subtilis and sensitizes spores to subsequent stress. J Appl Microbiol **97:**838-52.
22. **Cortezzo, D. E., and P. Setlow.** 2005. Analysis of factors that influence the sensitivity of spores of Bacillus subtilis to DNA damaging chemicals. J Appl Microbiol **98:**606-17.
23. **Cowan, A. E., D. E. Koppel, B. Setlow, and P. Setlow.** 2003. A soluble protein is immobile in dormant spores of *Bacillus subtilis* but is mobile in germinated spores: implications for spore dormancy. Proc Natl Acad Sci U S A **100:**4209-4214.
24. **Cowan, A. E., E. M. Olivastro, D. E. Koppel, C. A. Loshon, B. Setlow, and P. Setlow.** 2004. Lipids in the inner membrane of dormant spores of Bacillus species are largely immobile. Proc Natl Acad Sci U S A **101:**7733-8.
25. **Cybulski, R. J., Jr., P. Sanz, F. Alem, S. Stibitz, R. L. Bull, and A. D. O'Brien.** 2009. Four superoxide dismutases contribute to Bacillus anthracis virulence and provide spores with redundant protection from oxidative stress. Infect Immun **77:**274-85.
26. **Daubenspeck, J. M., H. Zeng, P. Chen, S. Dong, C. T. Steichen, N. R. Krishna, D. G. Pritchard, and C. L. Turnbough, Jr.** 2004. Novel oligosaccharide side chains of the collagen-like region of BclA, the major glycoprotein of the Bacillus anthracis exosporium. J Biol Chem **279:**30945-53.
27. **Day, W. A., Jr., S. L. Rasmussen, B. M. Carpenter, S. N. Peterson, and A. M. Friedlander.** 2007. Microarray analysis of transposon insertion mutations in Bacillus anthracis: global identification of genes required for sporulation and germination. J Bacteriol **189:**3296-301.
28. **Dougherty, W. G., T. D. Parks, S. M. Cary, J. F. Bazan, and R. J. Fletterick.** 1989. Characterization of the catalytic residues of the tobacco etch virus 49-kDa proteinase. Virology **172:**302-10.
29. **Douki, T., B. Setlow, and P. Setlow.** 2005. Photosensitization of DNA by dipicolinic acid, a major component of spores of Bacillus species. Photochem Photobiol Sci **4:**591-7.
30. **Dowd, M. M., B. Orsburn, and D. L. Popham.** 2008. Cortex peptidoglycan lytic activity in germinating *Bacillus anthracis* spores. J Bacteriol.
31. **Dowd, M. M., B. Orsburn, and D. L. Popham.** 2008. Cortex peptidoglycan lytic activity in germinating *Bacillus anthracis* spores. J. Bacteriol. **190:**4541-4548.
32. **Dowd, M. M., B. Orsburn, and D. L. Popham.** 2008. Cortex peptidoglycan lytic activity in germinating *Bacillus anthracis* spores. J Bacteriol **190:**4541-4548.
33. **Driks, A.** 1999. *Bacillus subtilis* spore coat. Microbiol. Mol. Biol. Rev. **63:**1-20.
34. **Driks, A.** 2002. Maximum shields: the assembly and function of the bacterial spore coat. Trends Microbiol **10:**251-4.
35. **Fisher, N., and P. Hanna.** 2005. Characterization of *Bacillus anthracis* germinant receptors in vitro. J Bacteriol **187:**8055-62.

36. **Foster, S. J., and K. Johnstone.** 1987. Purification and properties of a germination-specific cortex-lytic enzyme from spores of *Bacillus megaterium* KM. Biochem. J. **242:**573-579.
37. **Frenkiel-Krispin, D., R. Sack, J. Englander, E. Shimoni, M. Eisenstein, E. Bullitt, R. Horowitz-Scherer, C. S. Hayes, P. Setlow, A. Minsky, and S. G. Wolf.** 2004. Structure of the DNA-SspC complex: implications for DNA packaging, protection, and repair in bacterial spores. J Bacteriol **186:**3525-30.
38. **Gerhardt, P., and R. E. Marquis.** 1989. Spore thermoresistance mechanisms, p. 43-63. *In* I. Smith, R. A. Slepecky, and P. Setlow (ed.), Regulation of Prokaryotic Development. American Society for Microbiology, Washington, D.C.
39. **Ghosh, S., and P. Setlow.** 2009. Isolation and characterization of superdormant spores of Bacillus species. J Bacteriol **191:**1787-97.
40. **Giebel, J. D., K. A. Carr, E. C. Anderson, and P. C. Hanna.** 2009. The germination-specific lytic enzymes SleB, CwlJ1, and CwlJ2 each contribute to Bacillus anthracis spore germination and virulence. J Bacteriol **191:**5569-76.
41. **Giebel, J. D., K. A. Carr, E. C. Anderson, and P. C. Hanna.** 2009. Germination-specific lytic enzymes SleB, CwlJ1, and CwlJ2 each contribute to *Bacillus anthracis* spore germination and virulence. J. Bacteriol. **191:**5569-5576.
42. **Giglione, C., A. Boularot, and T. Meinnel.** 2004. Protein N-terminal methionine excision. Cell Mol Life Sci **61:**1455-74.
43. **Gilmore, M. E., D. Bandyopadhyay, A. M. Dean, S. D. Linnstaedt, and D. L. Popham.** 2004. Production of muramic-d-lactam in *Bacillus subtilis* spore peptidoglycan. J Bacteriol **186:**80-89.
44. **Giorno, R., J. Bozue, C. Cote, T. Wenzel, K. S. Moody, M. Mallozzi, M. Ryan, R. Wang, R. Zielke, J. R. Maddock, A. Friedlander, S. Welkos, and A. Driks.** 2007. Morphogenesis of the *Bacillus anthracis* spore. J Bacteriol **189:**691-705.
45. **Guan, R., and R. A. Mariuzza.** 2007. Peptidoglycan recognition proteins of the innate immune system. Trends Microbiol **15:**127-34.
46. **Guidi-Rontani, C., Y. Pereira, S. Ruffie, J. C. Sirard, M. Weber-Levy, and M. Mock.** 1999. Identification and characterization of a germination operon on the virulence plasmid pXO1 of *Bacillus anthracis*. Mol Microbiol **33:**407-414.
47. **Hanna, P. C., and J. A. Ireland.** 1999. Understanding *Bacillus anthracis* pathogenesis. Trends Microbiol **7:**180-2.
48. **Hayashi, K.** 1975. A rapid determination of sodium dodecyl sulfate with methylene blue. Anal. Biochem. **67:**503-506.
49. **Heffron, J. D., E. A. Lambert, N. Sherry, and D. L. Popham.** 2010. Contributions of four cortex lytic enzymes to germination of Bacillus anthracis spores. J Bacteriol **192:**763-70.
50. **Heffron, J. D., B. Orsburn, and D. L. Popham.** 2009. Roles of germination-specific lytic enzymes CwlJ and SleB in *Bacillus anthracis*. J. Bacteriol. **191:**2237-2247.
51. **Heffron, J. D., B. Orsburn, and D. L. Popham.** 2009. Roles of germination-specific lytic enzymes CwlJ and SleB in *Bacillus anthracis*. J Bacteriol **191:**2237-47.
52. **Heine, H. S., J. Bassett, L. Miller, J. M. Hartings, B. E. Ivins, M. L. Pitt, D. Fritz, S. L. Norris, and W. R. Byrne.** 2007. Determination of antibiotic efficacy against Bacillus anthracis in a mouse aerosol challenge model. Antimicrob Agents Chemother **51:**1373-9.

53. **Helmann, J. D., and C. P. Moran, Jr.** 2001. RNA polymerase and sigma factors, p. 289-312. *In* A. L. Sonenshein, J. A. Hoch, and R. Losick (ed.), *Bacillus subtilis* and Its Close Relatives: From Genes to Cells. American Society for Microbiology, Washington, D.C.
54. **Henderson, D. W., S. Peacock, and F. C. Belton.** 1956. Observations on the prophylaxis of experimental pulmonary anthrax in the monkey. J Hyg (Lond) **54:**28-36.
55. **Henriques, A. O., and C. P. Moran, Jr.** 2000. Structure and assembly of the bacterial endospore coat. Methods **20:**95-110.
56. **Holtje, J. V., D. Mirelman, N. Sharon, and U. Schwarz.** 1975. Novel type of murein transglycosylase in *Escherichia coli*. J Bacteriol **124:**1067-76.
57. **Howell, A., S. Dubrac, K. K. Andersen, D. Noone, J. Fert, T. Msadek, and K. Devine.** 2003. Genes controlled by the essential YycG/YycF two-component system of Bacillus subtilis revealed through a novel hybrid regulator approach. Mol Microbiol **49:**1639-55.
58. **Hu, K., H. Yang, G. Liu, and H. Tan.** 2007. Cloning and identification of a gene encoding spore cortex-lytic enzyme in *Bacillus thuringiensis*. Curr. Microbiol. **54:**292-295.
59. **Hudson, K. D., B. M. Corfe, E. H. Kemp, I. M. Feavers, P. J. Coote, and A. Moir.** 2001. Localization of GerAA and GerAC germination proteins in the *Bacillus subtilis* spore. J Bacteriol **183:**4317-4322.
60. **Igarashi, T., and P. Setlow.** 2005. Interaction between individual protein components of the GerA and GerB nutrient receptors that trigger germination of Bacillus subtilis spores. J Bacteriol **187:**2513-8.
61. **Indest, K. J., W. G. Buchholz, J. R. Faeder, and P. Setlow.** 2009. Workshop report: modeling the molecular mechanism of bacterial spore germination and elucidating reasons for germination heterogeneity. J Food Sci **74:**R73-8.
62. **Inglesby, T. V., D. A. Henderson, J. G. Bartlett, M. S. Ascher, E. Eitzen, A. M. Friedlander, J. Hauer, J. McDade, M. T. Osterholm, T. O'Toole, G. Parker, T. M. Perl, P. K. Russell, and K. Tonat.** 1999. Anthrax as a biological weapon: medical and public health management. Working Group on Civilian Biodefense. JAMA **281:**1735-45.
63. **Ireland, J. A., and P. C. Hanna.** 2002. Amino acid- and purine ribonucleoside-induced germination of *Bacillus anthracis* DeltaSterne endospores: *gerS* mediates responses to aromatic ring structures. J Bacteriol **184:**1296-1303.
64. **Ishikawa, S., K. Yamane, and J. Sekiguchi.** 1998. Regulation and characterization of a newly deduced cell wall hydrolase gene (*cwlJ*) which affects germination of *Bacillus subtilis* spores. J. Bacteriol. **180:**1375-1380.
65. **Janes, B. K., and S. Stibitz.** 2006. Routine markerless gene replacement in *Bacillus anthracis*. Infect Immun **74:**1949-53.
66. **Janes, B. K., and S. Stibitz.** 2006. Routine markerless gene replacement in *Bacillus anthracis*. Infect. Immun. **74:**1949-1953.
67. **Kanneganti, T. D., M. Lamkanfi, and G. Nunez.** 2007. Intracellular NOD-like receptors in host defense and disease. Immunity **27:**549-59.
68. **Kapust, R. B., J. Tozser, J. D. Fox, D. E. Anderson, S. Cherry, T. D. Copeland, and D. S. Waugh.** 2001. Tobacco etch virus protease: mechanism of autolysis and rational design of stable mutants with wild-type catalytic proficiency. Protein Eng **14:**993-1000.

69. **Kapust, R. B., and D. S. Waugh.** 2000. Controlled intracellular processing of fusion proteins by TEV protease. Protein Expr Purif **19:**312-8.
70. **Kapust, R. B., and D. S. Waugh.** 1999. Escherichia coli maltose-binding protein is uncommonly effective at promoting the solubility of polypeptides to which it is fused. Protein Sci **8:**1668-74.
71. **Kau, J. H., D. S. Sun, H. H. Huang, M. S. Wong, H. C. Lin, and H. H. Chang.** 2009. Role of visible light-activated photocatalyst on the reduction of anthrax spore-induced mortality in mice. PLoS One **4:**e4167.
72. **Kim, H. U., and J. M. Goepfert.** 1974. A sporulation medium for *Bacillus anthracis*. J Appl Bacteriol **37:**265-7.
73. **Kim, H. U., and J. M. Goepfert.** 1974. A sporulation medium for *Bacillus anthracis*. J. Appl. Bacteriol. **37:**265-267.
74. **Klobutcher, L. A., K. Ragkousi, and P. Setlow.** 2006. The Bacillus subtilis spore coat provides "eat resistance" during phagocytic predation by the protozoan Tetrahymena thermophila. Proc Natl Acad Sci U S A **103:**165-70.
75. **Kodama, T., H. Takamatsu, K. Asai, K. Kobayashi, N. Ogasawara, and K. Watabe.** 1999. The Bacillus subtilis yaaH gene is transcribed by SigE RNA polymerase during sporulation, and its product is involved in germination of spores. J Bacteriol **181:**4584-91.
76. **Kodama, T., H. Takamatsu, K. Asai, K. Kobayashi, N. Ogasawara, and K. Watabe.** 1999. The *Bacillus subtilis yaaH* gene is transcribed by SigE RNA polymerase during sporulation, and its product is involved in germination of spores. J. Bacteriol. **181:**4584-4591.
77. **Kodama, T., H. Takamatsu, K. Asai, N. Ogasawara, Y. Sadaie, and K. Watabe.** 2000. Synthesis and characterization of the spore proteins of Bacillus subtilis YdhD, YkuD, and YkvP, which carry a motif conserved among cell wall binding proteins. J Biochem **128:**655-63.
78. **Lai, E. M., N. D. Phadke, M. T. Kachman, R. Giorno, S. Vazquez, J. A. Vazquez, J. R. Maddock, and A. Driks.** 2003. Proteomic analysis of the spore coats of *Bacillus subtilis* and *Bacillus anthracis*. J Bacteriol **185:**1443-54.
79. **Lambert, E. A.** 2009. Personal communication.
80. **Lambert, E. A., and D. L. Popham.** 2008. The Bacillus anthracis SleL (YaaH) Protein is an N-Acetylglucosaminidase Involved in Spore Cortex Depolymerization. J Bacteriol.
81. **Lambert, E. A., and D. L. Popham.** 2008. The *Bacillus anthracis* SleL (YaaH) protein is an N-acetylglucosaminidase involved in spore cortex depolymerization. J. Bacteriol. **190:**7601-7607.
82. **Liu, H., N. H. Bergman, B. Thomason, S. Shallom, A. Hazen, J. Crossno, D. A. Rasko, J. Ravel, T. D. Read, S. N. Peterson, J. Yates, 3rd, and P. C. Hanna.** 2004. Formation and composition of the *Bacillus anthracis* endospore. J. Bacteriol. **186:**164-178.
83. **Liu, H., N. H. Bergman, B. Thomason, S. Shallom, A. Hazen, J. Crossno, D. A. Rasko, J. Ravel, T. D. Read, S. N. Peterson, J. Yates, 3rd, and P. C. Hanna.** 2004. Formation and composition of the *Bacillus anthracis* endospore. J Bacteriol **186:**164-78.
84. **Mader, U., G. Homuth, C. Scharf, K. Buttner, R. Bode, and M. Hecker.** 2002. Transcriptome and proteome analysis of *Bacillus subtilis* gene expression modulated by amino acid availability. J Bacteriol **184:**4288-95.

85. **Magge, A., A. C. Granger, P. G. Wahome, B. Setlow, V. R. Vepachedu, C. A. Loshon, L. Peng, D. Chen, Y. Q. Li, and P. Setlow.** 2008. Role of dipicolinic acid in the germination, stability, and viability of spores of *Bacillus subtilis*. J Bacteriol **190:**4798-807.
86. **Makino, S., N. Ito, T. Inoue, S. Miyata, and R. Moriyama.** 1994. A spore-lytic enzyme released from *Bacillus cereus* spores during germination. Microbiology **140 (Pt 6):**1403-1410.
87. **Makino, S., and R. Moriyama.** 2002. Hydrolysis of cortex peptidoglycan during bacterial spore germination. Med Sci Monit **8:**RA119-127.
88. **Makino, S., and R. Moriyama.** 2002. Hydrolysis of cortex peptidoglycan during bacterial spore germination. Med. Sci. Monit. **8:**RA119-127.
89. **Masayama, A., H. Fukuoka, S. Kato, T. Yoshimura, M. Moriyama, and R. Moriyama.** 2006. Subcellular localization of a germination-specific cortex-lytic enzyme, SleB, of Bacilli during sporulation. Genes Genet Syst **81:**163-9.
90. **Meador-Parton, J., and D. L. Popham.** 2000. Structural analysis of *Bacillus subtilis* spore peptidoglycan during sporulation. J. Bacteriol. **182:**4491-4499.
91. **Miller, J. H.** 1972. Experiments in Molecular Genetics. Cold Spring Harbor Laboratories, Cold Spring Harbor, NY.
92. **Miyata, S., R. Moriyama, N. Miyahara, and S. Makino.** 1995. A gene (*sleC*) encoding a spore-cortex-lytic enzyme from *Clostridium perfringens* S40 spores; cloning, sequence analysis and molecular characterization. Microbiology **141 (Pt 10):**2643-2650.
93. **Mock, M., and A. Fouet.** 2001. Anthrax. Annu Rev Microbiol **55:**647-71.
94. **Mock, M., and A. Fouet.** 2001. Anthrax. Annu. Rev. Microbiol. **55:**647-671.
95. **Moir, A.** 2006. How do spores germinate? Journal of Applied Microbiology **101:**526-530.
96. **Moir, A., B. M. Corfe, and J. Behravan.** 2002. Spore germination. Cell Mol Life Sci **59:**403-409.
97. **Morgulis, A., G. Coulouris, Y. Raytselis, T. L. Madden, R. Agarwala, and A. A. Schaffer.** 2008. Database indexing for production MegaBLAST searches. Bioinformatics **24:**1757-64.
98. **Moriyama, R., H. Fukuoka, S. Miyata, S. Kudoh, A. Hattori, S. Kozuka, Y. Yasuda, K. Tochikubo, and S. Makino.** 1999. Expression of a germination-specific amidase, SleB, of Bacilli in the forespore compartment of sporulating cells and its localization on the exterior side of the cortex in dormant spores. J Bacteriol **181:**2373-2378.
99. **Moriyama, R., A. Hattori, S. Miyata, S. Kudoh, and S. Makino.** 1996. A gene (*sleB*) encoding a spore cortex-lytic enzyme from *Bacillus subtilis* and response of the enzyme to L-alanine-mediated germination. J Bacteriol **178:**6059-63.
100. **Moriyama, R., A. Hattori, S. Miyata, S. Kudoh, and S. Makino.** 1996. A gene (*sleB*) encoding a spore cortex-lytic enzyme from *Bacillus subtilis* and response of the enzyme to L-alanine-mediated germination. J. Bacteriol. **178:**6059-6063.
101. **Moriyama, R., S. Kudoh, S. Miyata, S. Nonobe, A. Hattori, and S. Makino.** 1996. A germination-specific spore cortex-lytic enzyme from *Bacillus cereus* spores: cloning and sequencing of the gene and molecular characterization of the enzyme. J Bacteriol **178:**5330-5332.

102. **Nicholson, W. L., N. Munakata, G. Horneck, H. J. Melosh, and P. Setlow.** 2000. Resistance of Bacillus endospores to extreme terrestrial and extraterrestrial environments. Microbiol Mol Biol Rev **64:**548-72.
103. **Nicholson, W. L., and P. Setlow.** 1990. Sporulation, germination, and outgrowth, p. 391-450. *In* C. R. Hartwood and S. M. Cutting (ed.), Molecular biological methods for *Bacillus*. John Wiley and Sons Ltd. , Chichester, England.
104. **Nicholson, W. L., and P. Setlow.** 1990. Sporulation, germination, and outgrowth., p. 391-450. *In* C. R. Harwood and S. M. Cutting (ed.), Molecular biological methods for *Bacillus*. John Wiley & Sons Ltd., Chichester, England.
105. **Orsburn, B., S. B. Melville, and D. L. Popham.** 2008. Factors contributing to heat resistance of *Clostridium perfringens* endospores. Appl Environ Microbiol **74:**3328-35.
106. **Paidhungat, M., K. Ragkousi, and P. Setlow.** 2001. Genetic requirements for induction of germination of spores of *Bacillus subtilis* by Ca(2+)-dipicolinate. J Bacteriol **183:**4886-4893.
107. **Paidhungat, M., B. Setlow, A. Driks, and P. Setlow.** 2000. Characterization of spores of *Bacillus subtilis* which lack dipicolinic acid. J Bacteriol **182:**5505-5512.
108. **Paidhungat, M., and P. Setlow.** 2000. Role of ger proteins in nutrient and nonnutrient triggering of spore germination in *Bacillus subtilis*. J Bacteriol **182:**2513-2519.
109. **Paidhungat, M., and P. Setlow.** 2002. Spore germination and outgrowth, p. 537-548. *In* J. A. Hoch, R. Losick, and A. L. Sonenshein (ed.), *Bacillus subtilis* and its relatives: from genes to cells. American Society for Microbiology, Washington, DC.
110. **Paredes-Sabja, D., P. Setlow, and M. R. Sarker.** 2009. SleC is essential for cortex peptidoglycan hydrolysis during germination of spores of the pathogenic bacterium *Clostridium perfringens*. J Bacteriol **191:**2711-2720.
111. **Parks, T. D., E. D. Howard, T. J. Wolpert, D. J. Arp, and W. G. Dougherty.** 1995. Expression and purification of a recombinant tobacco etch virus NIa proteinase: biochemical analyses of the full-length and a naturally occurring truncated proteinase form. Virology **210:**194-201.
112. **Peng, L., D. Chen, P. Setlow, and Y. Q. Li.** 2009. Elastic and inelastic light scattering from single bacterial spores in an optical trap allows the monitoring of spore germination dynamics. Anal Chem **81:**4035-4042.
113. **Piggot, P. J., and D. W. Hilbert.** 2004. Sporulation of Bacillus subtilis. Curr Opin Microbiol **7:**579-86.
114. **Popham, D. L.** 2002. Specialized peptidoglycan of the bacterial endospore: the inner wall of the lockbox. Cell Mol Life Sci **59:**426-433.
115. **Popham, D. L., M. E. Gilmore, and P. Setlow.** 1999. Roles of low-molecular-weight penicillin-binding proteins in *Bacillus subtilis* spore peptidoglycan synthesis and spore properties. J. Bacteriol. **181:**126-132.
116. **Popham, D. L., J. Helin, C. E. Costello, and P. Setlow.** 1996. Analysis of the peptidoglycan structure of *Bacillus subtilis* endospores. J. Bacteriol. **178:**6451-6458.
117. **Popham, D. L., J. Helin, C. E. Costello, and P. Setlow.** 1996. Analysis of the peptidoglycan structure of *Bacillus subtilis* endospores. J. Bacteriol. **178:**6451-6458.
118. **Popham, D. L., J. Helin, C. E. Costello, and P. Setlow.** 1996. Muramic lactam in peptidoglycan of *Bacillus subtilis* spores is required for spore outgrowth but not for spore dehydration or heat resistance. Proc. Natl. Acad. Sci. U S A **93:**15405-15410.

119. **Popham, D. L., J. Meador-Parton, C. E. Costello, and P. Setlow.** 1999. Spore peptidoglycan structure in a *cwlD dacB* double mutant of *Bacillus subtilis*. J. Bacteriol. **181:**6205-6209.
120. **Popham, D. L., S. Sengupta, and P. Setlow.** 1995. Heat, hydrogen peroxide, and UV resistance of *Bacillus subtilis* spores with increased core water content and with or without major DNA-binding proteins. Appl Environ Microbiol **61:**3633-3638.
121. **Popham, D. L., and P. Setlow.** 1993. The cortical peptidoglycan from spores of *Bacillus megaterium* and *Bacillus subtilis* is not highly cross-linked. J. Bacteriol. **175:**2767-2769.
122. **Pryor, K. D., and B. Leiting.** 1997. High-level expression of soluble protein in Escherichia coli using a His6-tag and maltose-binding-protein double-affinity fusion system. Protein Expr Purif **10:**309-19.
123. **Quinn, C. P., and B. N. Dancer.** 1990. Transformation of vegetative cells of *Bacillus anthracis* with plasmid DNA. J Gen Microbiol **136:**1211-5.
124. **Ragkousi, K., P. Eichenberger, C. van Ooij, and P. Setlow.** 2003. Identification of a new gene essential for germination of *Bacillus subtilis* spores with Ca2+-dipicolinate. J. Bacteriol. **185:**2315-2329.
125. **Redmond, C., L. W. Baillie, S. Hibbs, A. J. Moir, and A. Moir.** 2004. Identification of proteins in the exosporium of Bacillus anthracis. Microbiology **150:**355-63.
126. **Rubio, A., and K. Pogliano.** 2004. Septal localization of forespore membrane proteins during engulfment in Bacillus subtilis. EMBO J **23:**1636-46.
127. **Schleifer, K. H., and O. Kandler.** 1972. Peptidoglycan types of bacterial cell walls and their taxonomic implications. Bacteriol. Rev. **36:**407-477.
128. **Sekiguchi, J., K. Akeo, H. Yamamoto, F. K. Khasanov, J. C. Alonso, and A. Kuroda.** 1995. Nucleotide sequence and regulation of a new putative cell wall hydrolase gene, *cwlD*, which effects germination in *Bacillus subtilis*. J. Bacteriol. **177:**5582-5589.
129. **Setlow, B., E. Melly, and P. Setlow.** 2001. Properties of spores of *Bacillus subtilis* blocked at an intermediate stage in spore germination. J Bacteriol **183:**4894-4899.
130. **Setlow, B., L. Peng, C. A. Loshon, Y. Q. Li, G. Christie, and P. Setlow.** 2009. Characterization of the germination of *Bacillus megaterium* spores lacking enzymes that degrade the spore cortex. J. Appl. Microbiol. **107:**318-328.
131. **Setlow, P.** 2007. I will survive: DNA protection in bacterial spores. Trends Microbiol.
132. **Setlow, P.** 1995. Mechanisms for the prevention of damage to DNA in spores of Bacillus species. Annu Rev Microbiol **49:**29-54.
133. **Setlow, P.** 1994. Mechanisms which contribute to the long-term survival of spores of *Bacillus* species. J. Appl. Bacteriol. Sympos. Suppl. **76:**49S-60S.
134. **Setlow, P.** 2003. Spore germination. Curr Opin Microbiol **6:**550-6.
135. **Setlow, P.** 2006. Spores of *Bacillus subtilis*: their resistance to and killing by radiation, heat and chemicals. J Appl Microbiol **101:**514-25.
136. **Setlow, P., and E. A. Johnson.** 2007. Spores and their significance, p. 35-68. *In* M. P. Doyle and L. R. Beuchat (ed.), Food microbiology: fundamentals and frontiers. ASM Press, Washington, D.C.
137. **Shah, I. M., M. H. Laaberki, D. L. Popham, and J. Dworkin.** 2008. A eukaryotic-like Ser/Thr kinase signals bacteria to exit dormancy in response to peptidoglycan fragments. Cell **135:**486-96.

138. **Spotts Whitney, E. A., M. E. Beatty, T. H. Taylor, Jr., R. Weyant, J. Sobel, M. J. Arduino, and D. A. Ashford.** 2003. Inactivation of Bacillus anthracis spores. Emerg Infect Dis **9:**623-7.
139. **Thunnissen, A. M., N. W. Isaacs, and B. W. Dijkstra.** 1995. The catalytic domain of a bacterial lytic transglycosylase defines a novel class of lysozymes. Proteins **22:**245-258.
140. **Todd, S. J., A. J. Moir, M. J. Johnson, and A. Moir.** 2003. Genes of Bacillus cereus and Bacillus anthracis encoding proteins of the exosporium. J Bacteriol **185:**3373-8.
141. **van den Ent, F., and J. Lowe.** 2006. RF cloning: a restriction-free method for inserting target genes into plasmids. J Biochem Biophys Methods **67:**67-74.
142. **Vepachedu, V. R., and P. Setlow.** 2007. Role of SpoVA Proteins in Release of Dipicolinic Acid during Germination of Bacillus subtilis Spores Triggered by Dodecylamine or Lysozyme. J Bacteriol **189:**1565-72.
143. **Waller, L. N., N. Fox, K. F. Fox, A. Fox, and R. L. Price.** 2004. Ruthenium red staining for ultrastructural visualization of a glycoprotein layer surrounding the spore of Bacillus anthracis and Bacillus subtilis. J Microbiol Methods **58:**23-30.
144. **Warth, A. D., and J. L. Strominger.** 1972. Structure of the peptidoglycan from spores of *Bacillus subtilis*. Biochemistry **11:**1389-1396.
145. **Warth, A. D., and J. L. Strominger.** 1972. Structure of the peptidoglycan from spores of *Bacillus subtilis*. Biochemistry **11:**1389-1396.
146. **Warth, A. D., and J. L. Strominger.** 1969. Structure of the peptidoglycan of bacterial spores: occurrence of the lactam of muramic acid. Proc. Natl. Acad. Sci. USA **64:**528-535.
147. **Weiner, M. A., T. D. Read, and P. C. Hanna.** 2003. Identification and characterization of the *gerH* operon of *Bacillus anthracis* endospores: a differential role for purine nucleosides in germination. J Bacteriol **185:**1462-1464.
148. **Zhang, Z., S. Schwartz, L. Wagner, and W. Miller.** 2000. A greedy algorithm for aligning DNA sequences. J Comput Biol **7:**203-14.

APPENDIX A

Supplemental material for Chapter 2

Table A.1. Oligonucleotide primers for plasmid construction.

PCR product	Primer name	Sequence 5' to 3'[a]
cwlJ1 truncation	352	GGGGACAAGTTTGTACAAAAAAGCAGGCTAAAAGAGAGGTGACACATAATGG
	353	GGGGACCACTTTGTACAAGAAAGCTGGGTCCATAAGGCAAAATTTGCAGGCC
cwlJ2 truncation	348	GGGACAAGTTTGTACAAAAAAGCAGGCTCAGAAAGGTGGTATCACTATGCC
	349	GGGGACCACTTTGTACAAGAAAGCTGGGTCGAGCACGTTGATAAAAATATCCG
sleB truncation	350	GGGGACAAGTTTGTACAAAAAAGCAGGCTAAGGAGGGAAATTTATGCG
	351	GGGGACCACTTTGTACAAGAAAGCTGGGTCCATTTGGAACATTTGTCCC
cwlJ1 entire ORF	359	CGC*GCGGCCGC*TATGGTTTCTTAGACGGTAG
	362	CGC***GGATCC***GTACCGAGTGAGCTACCGCGCTC
cwlJ2 entire ORF	363	CGC*GCGGCCGC*CGAGGAGGAAAATGCATATG
	366	CGC***GGATCC***CGGTTCCAATCTAATTCTTGAAACGC
sleB entire ORF	288	CGC*GCGGCCGC*CTCGTCTTCTGGAACGACAC
	372	CGC*CTGCAG*TTCAAAACAAGATGTTGCAC
pBKJ236::*ΔcwlJ1*	360	**GCCCGCGCGGC**CAACGCCCATTATGTGTCACCTCTC
	361	G**GCCGCGCGGGC**GTATATTAAGGATTGATAATGAGGAGGG
pBKJ236::*ΔcwlJ2*	364	**GCCCGCGCGGC**CTCACGGTAGTAAAATTTGGAACGC
	365	G**GCCGCGCGGGC**AAGGGGCATAGTGATACCACC
pBKJ236::*ΔsleB*	289	**GCCCGCGCGGC**ACCTCCCTGCTATTTTAAAAATAGCTT
	290	GGGAGGT**GCCGCGCGGGC**AAGATCGGGAAACATATTTTC

[a] *att* sites for the Gateway system are underlined, *Not*I sites are underlined and italicized, *Bam*HI sites are italicized and in bold, *Pst*I sites are italicized, and *Bgl*I sites are in bold.
Abbreviations: ORF, open reading frame.